ADDIS ABABA UNIVERSITY

ADDIS ABABA INSTITUTE OF TECHNOLOGY

SCHOOL OF CIVIL & ENVIRONMENTAL ENGINEERING

TOWER CRANE LOCATION OPTIMIZATION FOR HIGH RISE BUILDINGS IN THE FINANCIAL DISTRICT OF ADDIS ABABA

by

ETSUB KETEMA TADESSE | GSR/3891/10

A thesis submitted to the School of Graduate Studies of Addis Ababa University in partial fulfillment of the requirements of the Degree of Master of Science in Civil Engineering in Construction Technology and Management

Advisor:

ABRAHAM ASSEFA TSEHAYAE (PhD)

ADDIS ABABA UNIVERSITY

ADDIS ABABA INSTITUTE OF TECHNOLOGY

SCHOOL OF CIVIL & ENVIRONMENTAL ENGINEERING

TOWER CRANE LOCATION OPTIMIZATION FOR HIGH RISE BUILDINGS IN THE FINANCIAL DISTRICT OF ADDIS ABABA

by

ETSUB KETEMA TADESSE | GSR/3891/10

Approved by the Board of Examiners

Abraham Assefa Tsehayae (PhD)	_____	_____
ADVISOR	SIGNATURE	DATE
Dereje Hailu (Dr-Ing)	_____	_____
INTERNAL EXAMINER	SIGNATURE	DATE
Asregedew Kassa (PhD)	_____	_____
EXTERNAL EXAMINER	SIGNATURE	DATE
_____	_____	_____
COMMITTEE CHAIRPERSON	SIGNATURE	DATE

DECLARATION

I certify that this research work titled "*Tower Crane Location Optimization for High Rise Buildings in Addis Ababa*" is my own work. The work has not been presented elsewhere for assessment. Where material has been used from other sources, it has been properly acknowledged/referred.

_____

ETSUB KETEMA TADESSE | GSR/3891/10

DATE:

EXECUTIVE SUMMARY

This thesis explores the Single Tower Crane Location Optimization problem for high-rise building construction projects in Addis Ababa. The optimal location for 6 case studies was found using Particle Swarm Optimization, a metaheuristic optimization technique. The proposed optimal location was then compared against the actual location on site to analyze the efficacy of traditional tower crane placement techniques.

Projects that used traditional placement techniques achieved results which were acceptably close to the theoretically optimal location. However the use of scientific placement techniques by China State Construction Engineering Corporation that considered the crane's lifting capacity, jib length and anchoring requirements resulted in the most accurate results.

This thesis recommends that contractors adopt scientific placement techniqeues, move unnecessary facilities off-site or use construction methodologies such as prefabrication and just-in-time construction to ease site congestion and if possible use mathematical optimization tools when determining the location of their tower cranes to guarantee that the tower crane is placed at an optimal location.

ABSTRACT

Tower cranes are an expensive investment for construction projects, and the appropriate selection of their location has a significant impact on the cost, efficiency, safety, and environmental impact of a construction project. In many cases, traditional techniques which simply ensure that the crane can reach all the supply and demand points while satisfying other site-specific constraints are used to find the location for the tower crane. However, this process doesn't necessarily mean the crane has been placed in the optimal location.

As construction sites become smaller, and the use of tower cranes becomes more prevalent, the role of Site Layout Planning, is becoming more critical. Tower Crane Location Planning Problem presented in this thesis is a subset of the larger Site Layout Planning problem. The problem is solved using a metaheuristic optimization technique known as Particle Swarm Optimization. The optimization integrates constraints such as temporary offices, plot limits, work information, and crane capacities to search for the optimal location based on the total travel time.

Six case studies of high-rise buildings in Addis Ababa were analyzed, with 5 of the projects located in the Financial District of Addis Ababa. In all cases, the optimal location was found to be acceptably close to the actual location on site, except for the Nile Insurance HQ Project.

The location selection techniques varied among the 5 contractors, with China State Construction Engineering Corporation using the most scientific technique which ensured that the crane could satisfy the demands of the project. Conversely, Rama Construction utilized the least scientific placement technique, which forced it to dismantle the first tower crane at great cost.

The primary recommendation of this thesis is that the contractors should ensure that the crane selected for the project should meet the demands of the projects in terms of capacity, lifting radius and anchoring requirements.

Key Words: *Particle Swarm Optimization; Site Layout Planning; Tower Crane Location Planning*

ACKNOWLEDGEMENT

I would like to thank all my instructors for their kind assistance throughout the past year. In particular, I would like to thank my advisor, Abraham Assefa Tsehayae (PhD) for his guidance. I would also like to thank my examiners, Asregedew Kassa (PhD) and Dereje Hailu (Dr-Ing) for their comments, which have allowed me to improve the research.

At the Commercial Bank of Ethiopia Head Quarters Project, I would like to thank Mr. Tesfaye Molla, Lead Office Engineer, AAiT Client Representative's Office for project, and Mr. Wu Bin, Design Manager for the China State Construction Engineering Corp. project team for their invaluable assistance in guiding the preparation of Chapter 4 and for spending their invaluable time in helping me understand the function of cranes for high-rise projects.

At Nile Insurance HQ, I would like to thank Mr. Behailu and Ms. Dename, Resident Engineer, and Deputy Resident Engineer respectively.

At Zemen Bank HQ, I would like to thank Mr. Eyobed Miriye, Zemen Bank's Client Representative for his input and assistance in contacting staff at the Nib International Bank HQ and Union Bank HQ projects.

Finally, I would like to thank my parents for their endless support and encouragement.

ABBREVIATIONS

A.A.	Addis Ababa
AACA	Addis Ababa City Administration
AAU	Addis Ababa University
AAU-SOC	Addis Ababa University – School of Commerce
CBE-HQP	Commercial Bank of Ethiopia – Headquarters Project
CSCEC	China State Construction and Engineering Corporation
CSLP	Construction Site Layout Problem
DB	Design Build
EPRDF	Ethiopian People's Revolutionary Democratic Front
ETB	Ethiopian Birr
F.D.R.E	Federal Democratic Republic of Ethiopia
GA	Genetic Algorithm
HCB	Hollow Concrete Blocks
JIT	Just-In-Time
NI-HQP	Nile Insurance – Headquarters Project
NIB-HQP	Nib International Bank – Headquarters Project
OLS	Ordinary Least Squares
OM	Optimization Module
PBA	Particle Bee Algorithm
PSO	Particle Swarm Optimization
SRCC	Steel Reinforced Concrete Column
TCLP	Tower Crane Location Problem
TTC	Travel Time Calculation
UB-HQP	United Bank – Headquarters Project
ZB-HQP	Zemen Bank – Headquarters Project

TABLE OF CONTENTS

LIST OF FIGURES

LIST OF TABLES

1. INTRODUCTION

In project implementation, it is a known fact that proper planning is critical in preventing poor performance and saving time and cost during project execution. This is especially true for construction projects that require plans for the 4M's: Money, Manpower, Machinery and Materials. Often, the planning of construction site layouts, known as Site Layout Planning (SLP) which deals with the optimization of the location of temporary facilities at construction sites is ignored [1].

A subset of SLP is the Tower Crane Layout Planning (TCLP). TCLP is the problem of mathematical optimization of the location of tower cranes on construction sites. High-rise buildings, which are defined as buildings with heights between 35 and 100 meters, or any building with 12 to 39 floors, are most reliant on tower cranes for their transportation needs, and the problems associated with misplaced tower cranes are felt more acutely on such projects [2].

In this thesis, the problem of site layout and tower crane location planning is explored, and the locations of tower cranes for selected high-rise projects in Addis Ababa, Ethiopia are compared against the theoretically optimal locations that is established using a stochastic optimization technique.

1.1. Background

Addis Ababa is one of the fastest growing cities in Africa. The booming economy has led to several high-rise building projects, which need tower cranes for construction. Simultaneously, plot sizes are decreasing, which is creating smaller and more congested sites. Due to the exorbitant land prices and congestion of construction sites, engineers treat each square-meter of land as a valuable and finite resource and attempt to plan for its use carefully. In addition, tower cranes are among the most expensive pieces of equipment on

construction sites, whether they are bought by the contractor or rented. They are also expensive to operate, and cranes that operate using diesel generators are major environmental pollutants.

1.1.1 Tower Cranes in Addis Ababa

Interviews conducted with various contractors and consultants working on construction projects throughout Addis Ababa have shown that tower cranes are becoming one of the most critical equipment, especially for high-rise building projects. The speed of horizontal and vertical transportation is drastically improved by tower cranes and on certain projects, the transportation of all materials is wholly dependent on tower cranes. Typically, cranes are used to transport reinforcement, formwork, scaffolding, hollow concrete blocks (HCB) and finishing materials. During interviews, all contractors indicated that the time-savings associated with tower cranes is the main reason behind their decision to use tower cranes.

High-rise buildings under construction in the new Financial District of Addis Ababa, located in Lideta Sub-City are among the tallest in Ethiopia, and all the projects use tower cranes. New projects such as the Amhara Credit and Savings Institution Headquarters Building Project in the area have installed tower cranes as well. However, the use of tower cranes in Addis Ababa is by no means limited to the Financial District or to high rise buildings.

Other projects which utilize tower crane's in the capital Black Lion Teaching Hospital's Cardiac Center Expansion Project, Ethiopian Standards Agency's Teaching and Training Center Project, and the Adey Abeba Stadium Project. The projects are being built by a mix of local and foreign contractors, with varying degrees of tower crane utilization. Unfortunately, neither the Federal Government nor the City Administration keeps a database of tower crane ownership or use, making it difficult for researchers to gauge the overall use of tower cranes in the city.

While engineers understand the enormous benefits of tower cranes, their methods for the selection of the location for tower cranes is often based on experience and simple techniques. The technique that all the interviewed contractors utilized was picking a location which they believed would allow the respective cranes to service the entire project periphery and, in some cases, imposing additional restrictions specific to their site conditions. These include:

- *Site congestion*: When a building under construction takes up a significant proportion of the site, the space available for the erection of the crane will decrease. For example, the new Ethiopian People's Revolutionary Democratic Front (EPRDF) HQ being constructed occupies approximately 85% of the space available. When coupled with public roads bordering the site, and the eventual dismantling operations which require ample space for the mobile crane limits the contractor's ability to freely find a location for the crane.

  A similar problem was faced by China Jiangsu for the Nib International Bank HQ and Union Bank HQ buildings, which occupy most of the available site area in heavily congested sites. In both cases, the contractor was forced to place the crane within the structure, with the base of the crane placed on the pile caps.

  For the Zemen Bank HQ and United Bank HQ projects, the space problem was so acute that the contractors had to lease land from an adjacent plot to accommodate the batching plant and offices for the contractor and consultant.

- *Consideration of dismantling operations*: As mentioned earlier, the contractor must consider the eventual process of dismantling the tower crane while looking for a suitable location. While the crane can be brought down using its own power, the final process of removing the jib requires a mobile crane, which requires access to the crane and open space to operate. The jib must also have enough horizontal clearance once it is jacked down to avoid collision with nearby structures. These constraints must be met before the tower crane is erected.

1.2. Statement of the Problem

The optimal location of tower cranes has been shown by various researchers to have a significant impact on the productivity of works and construction time [1] [3]. As the number of high-rise buildings in Addis Ababa increases, and the open space available decreases, the selection of optimal location will become of paramount importance to contractors.

The brief discussions held with engineers at various projects in Addis Ababa have shown that the location of tower cranes is often chosen using traditional techniques and that both local and foreign contractors approach the problem similarly. Such techniques rely primarily on the ability of the crane to service all locations on the construction site and the consideration of the erection, and eventual dismantling operations.

Improper tower crane placement can cause significant disruptions and losses. A particularly striking problem was that of the Addis Ababa University (AAU) Forum Building, a G+15 building located at Yekatit 12 Square in Arada Sub-City. The 56-meter tall project used a tower crane that the contractor placed too far from the building to be anchored. As shown in Figure 1, when the height of building exceeded the crane's maximum unanchored height, the crane was rendered useless as it was no longer able to rotate freely. For the remainder of the project, the crane sat idly on site at great cost to the contractor, until it was dismantled and moved to another site.

***Figure 1**: AAU Forum Building Crane (Courtesy of Yotek Construction)*

Such a turn of events is a waste of resources both in terms of the utilization of machinery and money. It also shows the lack of proper planning by the contractor during the pre-construction phase. If the contractor had appropriately positioned the crane from the outset, allowing it to be anchored to the building, it would have been able to properly use the crane throughout the duration of the project, possibly making it more efficient. Conversely, if it

had decided against using a tower crane during the planning stage of the project, it would have saved the thousands of ETB per day it lost by having its crane sit idle.

Due to the benefits of appropriately positioning the tower crane, the locations of tower cranes that are currently in use must be mathematically analyzed to find the optimal location. This study will show how accurate the traditional techniques that were discussed previously are compared to locations found by the Particle Swarm Optimization (PSO) and if it is possible for contractors to improve their decision-making process.

There are various optimization techniques which can be applied to the problem such as Genetic Algorithms, Particle Bee Optimization and exact techniques such as Mixed Integer Linear Programming. In this thesis, PSO was selected due to its relative simplicity when compared to other techniques, allowing the algorithms to be developed specifically for the problem at hand rather than being forced to use generic optimization tools and the ease with which people unfamiliar with the optimization technique can apply it.

1.3. Significance of the Research

Space for construction sites is becoming an expensive commodity in Addis Ababa. At the same time, the high-rise buildings that are being constructed which necessitate the use of tower cranes. The topic remains relatively unexplored throughout the developing world, with only two previous works found from Egypt and Iran [4] [5]. Therefore, the output of the research can positively impact various stakeholders in the construction industry both in Ethiopia and other developing countries.

Tower crane erection, dismantling and operation costs are high, therefore, placing the tower crane appropriately can reduce the time it is needed on site, which will reduce its operational costs. In addition, improperly placed tower cranes need to be dismantled and repositioned. Such costs can be avoided if the initial location is chosen carefully.

Other benefits associated with properly positioned tower cranes include increased productivity and improved safety of workers on site [6]. The appropriate placement of tower cranes can also significantly reduce environmental impacts associated with a project since according to Hasan et al. (2013). Cranes are a major source of environmental pollution, especially when they are powered by diesel generators, which emit copious amounts of smoke and sound [6]. Therefore, effective utilization of tower cranes can reduce the environmental impacts associated with construction projects.

1.4. Research Objective

1.4.1. General Objectives

- Determine the current site planning processes for high-rise building projects in Addis Ababa; and
- Identify the optimal tower crane location for tower cranes for the selected case studies.

1.4.2. Specific Objectives

The specific objectives of this thesis are:

- Develop a computer model with close-to-accurate depictions of real site conditions, including but not limited to: location and dimensions of objects, volumes of work and capacities of tower cranes;
- Calculate the theoretically optimal location for tower cranes on selected high-rise projects using Particle Swarm Optimization (PSO); and
- Compare the actual location with the theoretically optimal results.

1.5. Research Question

The research questions the thesis aims to address includes:

- What are the current tower crane location planning practices?
- Based on the total travel time required to transport materials, what is the mathematically optimal location for a tower crane?
- Compared to the mathematically optimal location, how well placed are the tower cranes used by the contractors in the case studies and do traditional techniques result in acceptable results?

1.6. Scope and Limitations

The research is limited to:

- High rise buildings in Addis Ababa that use single, top-slewing tower crane which services all locations on the site;
- The supply points for the activities are static; and
- All parameters and inputs have deterministic values.

1.7. Research Outline

The thesis is divided as follows:

Chapter 1 – Introduction: A general overview of the topic, background information, motivation and limitations are presented.

Chapter 2 – Literature Review: The theoretical background required to implement the research methodology and interpret the results is presented including tower cranes, site layout problems and particle swarm optimization

Chapter 3 – Research Methodology: The research instruments and methodologies that need to be implemented to answer the questions raised in the statement of the problem are reviewed and presented.

Chapter 4 – Trial Project: Commercial Bank of Ethiopia HQ: The algorithms and work methodologies that have been outlined in Chapter 3 will first be tested on the CBE HQ project, and refined as needed. The methodology will then be deployed on the remainder of the case studies included in Chapter Five.

Chapter 5 – Modelling and Optimization of Selected Sites: The methodologies discussed in Chapter Three and refined on the CBE-HQP project (Chapter 4) case study are implemented and theoretically optimal results shall be established for 4 case studies in the Financial District of Addis Ababa. The projects are: Nile Insurance HQ, Zemen Bank HQ, Nib International Bank HQ, and United Bank HQ.

Chapter 6 – Analysis and Discussion of Results: The outputs of the Particle Swarm Optimization are presented and compared against actual locations of tower cranes for the selected projects.

Chapter 7 – Conclusion and Recommendations: Based on the result of the research, this thesis will recommend possible courses of actions for the future, as well as possible avenues for further research.

2. LITERATURE REVIEW

The study of tower crane optimization problem draws upon knowledge from various fields. This literature review will present the theoretical background necessary to address the research questions by implementing the research instruments. The literature review will address the following core areas of knowledge:

- *Cranes and Vertical Transport for High Rise Projects* will present information on cranes, including types of tower cranes, transport mechanisms and terminology;
- *Site Layout Planning (SLP)* will deal with the positioning of temporary facilities on site as it relates to tower cranes will be addressed. It will also address the various tools at the disposal of construction engineers to find the best location of tower cranes;
- *Modelling of Site Layouts and Crane Transport Time* will discuss finding an optimal location on construction sites and the site layout will be modelled with Cartesian coordinates. By using Cartesian coordinates, the drawings provided by the contractor can be used without modification, simplifying the modelling. In addition, the equations developed by Zhang et al (1999) to model the time taken to transport objects will be introduced. These equations will form the objective function which will be minimized; and
- *Metaheuristics and Particle Swarm Optimization* will introduce the optimization technique to be used. There are several techniques that can be used to find the optimal tower crane location. These include exact techniques such Mixed Integer Linear Programming (MILP), as well as techniques which rely on stochastic optimization and metaheuristics such as Genetic Algorithm (GA) and Particle Swarm Optimization (PSO). PSO will be discussed specifically as it will be used to find the optimal location in this thesis.

2.1. Cranes and Vertical Transport for High Rise Projects

For high rise projects, cranes are an indispensable equipment that allow for the efficient vertical transport of a variety of materials and equipment. Due to a wide range of crane types available, engineers must select a variety of parameters as a basis to find the best crane for the project. A decision must also be made to either install a single crane or to install a group of cranes, depending on the loads and area to be serviced.

2.1.1. Tower Crane Varieties

Tower cranes come in a wide range of options, allowing engineers to choose a configuration that best fits their project's needs. The three common tower crane types are: a mobile crane with a special vertical boom attachment, a mobile crane superstructure mounted on top of a tower, and a vertical tower with a jib [7]. However, the most common type of tower crane is the vertical tower with a jib attachment and is the option that will be discussed further in the following section.

A vertical tower with a jib attachment can again be divided into two types: a top slewing (fixed-tower) or a bottom-slewing (slewing tower) type. A top slewing crane has a motor that is located at the top of the tower, allowing the jib to rotate independently from the tower, while for a bottom-slewing tower crane, the motor is located at the base of the crane, and the jib is unable to rotate independently, instead, the tower and jib rotate together [7].

The main difference that characterizes the two crane types is the maximum service height and the erection and dismantling speed. Bottom slewing cranes can erect themselves using their own motors in a matter of hours, while top-slewing cranes require the assistance of a mobile crane because the motor is one of the last elements to be installed, with installation times ranging from a day to a week. However, top-slewing cranes can reach much greater heights when compared to bottom-slewing variants since the tower can be anchored to the structure being constructed. Due to these benefits, the top-slewing options are more common on high rise building construction sites [7, 8].

2.1.2. Terminology of Tower Cranes

Since top-slewing cranes are the most common crane types for use in high-rise construction projects, the terminologies associated with it will be discussed briefly.

The hook block of a crane is where the loads to be transported are attached, while the hook block is attached to the trolley. The jib is the horizontal structure on to which the hook block, trolley and counterweights are attached. The section on to which the loads, hook block and trolley are attached is known as the saddle jib, while the section the counterweight is attached to is known as the counter jib.

The jib and counter jib are the horizontal components, and they are attached to a tower which is made up of sections that are added as the required height of the crane increases. As discussed previously, the tower cannot rotate, and when necessary, it is anchored to the structure being built to further increase the crane's height.

A top-slewing tower crane makes 3 distinct movements to transport a load from the demand to the supply point. The trolley and hook block arrangement can move back and forth along the saddle jib in a tangential movement known as trolleying. The hook block can also move vertically, in a hoisting movement. Finally, the entire jib can rotate about the fixed tower, which is known as slewing [7].

Figure 2 shows the parts of a top-slewing tower crane, and the 3 movements discussed above.

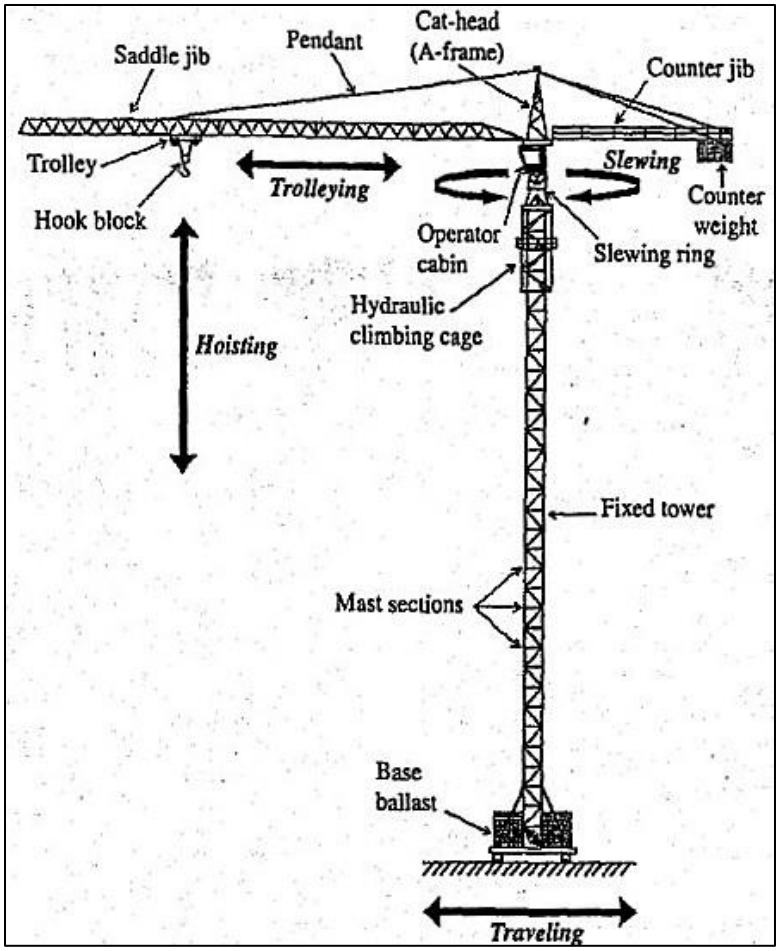

***Figure 2**: Top-Slewing Tower Crane* [7]

2.2. Site Layout Planning: Crane Location Optimization

All construction activities require prior planning and a critical part of this process is the creation of a site layout. According to Tommelein et al. (1992), site layout planning consists of "[…] identifying the facilities needed to support construction operations, determining their size and shape, and positioning them within the boundaries of the available on-site or remote areas." This includes offices, storage areas, first-aid areas, and tower cranes, to name a few. In general, such problems are referred to as Construction Site Layout Problems (CSLP).

According to Li and Love (1998), CSLP problems become difficult if "[…] a construction site is confined with available space or the site is very large in size where travelling between facilities can be considerably time consuming". The primary benefit to a properly planned construction site is the improvements in efficiency. RazaviAlavi and AbouRizk (2017) claim that the increases in efficiency due to efficient site layouts have a bearing on the construction site's productivity and safety, ultimately leading to more successful construction projects.

While there is significant interest in solving such optimization problems, the sheer number of variables and constraints has made it difficult for researchers to find exact solutions using techniques such as MILP. In recent years, the development of stochastic optimization algorithms and artificial intelligence tools has allowed for approximate solutions to be found to the problems in question.

CSLP can be divided into one of three categories:

- Layout Improvement, where an initial layout is improved through the relocation of some of the facilities;
- Partial Layout Problems, where some of the facilities are optimized with the locations for some facilities remaining unchanged; and
- Entire Site Layout Problems, where all the temporary facilities are placed according to a preset order until the best combination is found [9].

The Tower Crane Location Problem (TCLP) is a subset of the larger CSLP optimization problem which deals specifically with the positioning of tower cranes on the construction sites. All other facilities remain at a fixed position, making it a partial layout problem. This problem is an important one because for many construction sites, the tower crane is a key equipment on site that is required for the horizontal and vertical transport of materials and equipment [10].

According to RazaviAlavi and AbouRizk (2017) and Nadoushani et al. (2017), the complexity of the problem often forces engineers to rely on their intuition, experience and basic rules of thumb to find the best location for tower cranes. A good site layout must meet multiple objectives, including increased safety, productivity, minimize travel time and obstruct other movements on site [1]. The complexity of the objectives, and their effect on each other makes the optimization a difficult task. Over the past 30 years, mathematical optimization techniques, including metaheuristics are beginning to find favor among engineers to solve such problems. This process relies on the creation of mathematical models that can be used in the optimization process.

The appropriate choice for the location of a tower crane(s) has a wide-ranging impact on the project in terms of cost, completion time, safety and environmental impact. Tower cranes are one of the most expensive equipment to acquire on construction sites and are very expensive to operate. Therefore, reducing the time that a crane is needed on a given project can directly reduce the construction costs [10, 11].

Environmentally, cranes are considered by the United States' Environmental Protection Agency (EPA) to be a major source of air pollutants. Additionally, cranes which operate using diesel generators are often very loud and responsible for a significant portion of the sound pollution on construction sites. Again, reducing the length of time the crane is needed on site will reduce the associated environmental impact [6].

Due to the enormous benefits that good crane locations can bring to construction projects, it is logical for construction engineers to carefully plan the location of the crane and the supply points it needs to service. The main requirement for the location of the crane is determined by whether it can reach the supply and all the demand points on the construction site. This is affected by the capacity of the crane, because the maximum lift capacity is dependent on the load-radius curves which lead to decreased capacity at greater radii. The chosen location must also be able to service the project for the entire duration of the project since the erection and dismantling of cranes is an expensive and dangerous process.

2.3. Modelling of Site Layouts and Crane Transport Times

The data collected from various construction sites needs to be modelled in a way that is compatible with the chosen optimization technique. This process includes the creation of a model in Cartesian coordinate space, and the integration of equations which calculate the time taken for a crane to travel from supply point to the demand points. By integrating the site layout with the crane travel time equations and an optimization technique, an Optimization Module (OM) can be created that allows engineers to find an optimal crane location.

2.3.1. Site Layout Modelling

The modelling of a construction site focuses on three areas: the representation of elements on construction sites in Cartesian space with reference coordinates, assigning workloads to each work zone, and checking to avoid conflicts between objects.

The first step in modelling construction sites is the creation of a model in Cartesian coordinate space where the objects in construction sites are represented by equivalents in the computer model. When the objects have non-rectangular shapes, they must be simplified into rectangular or triangular objects with equivalent areas [12]. This simplification is necessary because equations that check for overlaps are based on rectangular objects. However, it doesn't lead to a significant reduction in the accuracy of the model.

For each floor that needs to be serviced by the crane, it must be divided into work zones, and a certain proportion of the total work load needs to be assigned to each work zone. This is a necessary part of the modelling because it accurately represents real life functions of the crane since the materials needed to complete a task are not transported all at once. The model creation process is essentially identical between different researchers except with regards to how the objects are referenced. Alkriz & Mangin (2005) and Abdelmegid

et al. (2015) used the coordinate of the centroid to refer to each object, while RazaviAlavi & AbouRizk (2017) use the top-left coordinate to refer to each object [4, 12, 11]. The difference in how objects are referred to is quite inconsequential because it has no effect on the accuracy of the results.

The other difference in site modelling is the use of gridlines by RazaviAlavi & AbouRizk (2017). The gridlines are used to divide the entire site into cells and the top-left coordinate of each object must lie at an intersection of gridlines. When searching for candidate locations for objects, the intersections are all treated as candidate locations. With this approach, the change in the number of gridlines affects the efficiency and accuracy of the model. As the number of gridlines and cells increases, the number of candidate solutions will increase. This leads to an increase in the computational power needed but will result to a more accurate solution. The effect also occurs in reverse if the number of gridlines and cells is decreased [11]. By comparison, Alkriz & Mangin (2005) avoid this problem by not using gridlines to divide the site. This makes all locations available to the optimization algorithm.

Finally, the locations of the objects represented on the site model must be checked to ensure that there are no overlaps or violations of any constraints that have been imposed. The main categories of constraints are being inside all site boundaries, avoiding any overlaps between facilities, and crane locations, satisfaction of any given minimum/maximum distances between facilities and inclusion/exclusion of facilities from certain areas [11]. These constraints are all modelled as inequalities, which must be satisfied. The effect of using the coordinate of the centroid or the top-left corner manifests in the equations used to check the overlaps. While the equations by RazaviAlavi & AbouRizk (2017) differ from those used by Alkriz & Mangin (2005), they are equivalent to each other, and can be transformed with slight modifications.

The first check that must be performed is if the crane's jib can reach all supply and demand points. This check is perhaps the most important because, it would be a waste to proceed any further if the crane is unable to service all locations. This check is performed with the inequality presented below:

$$\max(D_j, D_i) \geq l_{cr} \ (EQ.\ 1)$$

where:

D_j & D_i *are the distance from the crane's location to any demand or supply point respectivley*
$l_{cr} = length\ of\ the\ crane's\ jib$

This requirement can also be checked manually by drawing circles with the radius equal to the crane's jib length from the centroid of each supply and demand point. Any proposed location for the tower crane must lie at the intersection of all the circles. This check can be performed on the final proposed location to ensure that it can serve all the locations on site. Next, the positions of objects on site must be checked to avoid conflicts and overlaps. To avoid such an overlap, the base of the structure is modelled as either a single rectangle, or the smallest number rectangles possible. Figure 3 illustrates the variables and the coordinate system used to check for any violations of the overlap constraints.

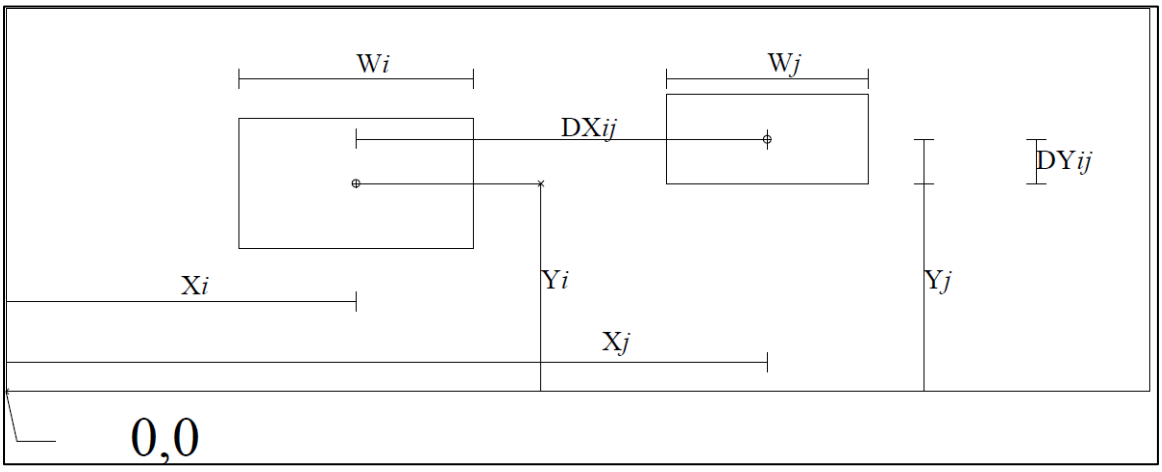

***Figure 3**: Coordinate System to Check for Object Overlap*

Then the following inequality is checked:

$$\max\left[\begin{matrix}\left(dX_{ij}-\frac{W_j+W_i}{2}\right)\times\left(dX_{ij}+\frac{W_j+W_i}{2}\right),\\ \left(dY_{ij}-\frac{A_j}{2W_j}-\frac{A_i}{2W_i}\right)\times\left(dY_{ij}+\frac{A_j}{2W_j}+\frac{A_i}{2W_i}\right)\end{matrix}\right]\geq 0\ (EQ\ .2)$$

$$dX_{ij}=X_j-X_i\ \&\ dY_{ij}=Y_j-Y_i\ (EQ.\ 3)$$

$$X,Y=centroid\ coordinates\ for\ the\ objects$$
$$W=width\ of\ the\ objects$$
$$A=Area\ of\ the\ objects$$
$$Note\text{: }H_j=Height\ of\ Object={A_j}/{2W_j}$$

The first equation checks for overlaps in the *x* direction, while the second checks in the *y* direction. When checking in the *y* direction, the area of the object is used instead of the height of the object. However, this is of no consequence because the length can be found by dividing the area with the width. The area is used for other calculations, thereby reducing the number of variables introduced.

When needed to check proposed locations of the tower crane, the base of the tower crane is modelled as a rectangle, which is then treated as any other object in the model. A simple proof of Equation 2 is provided in the Appendix 1. Finally, any proposed location for a crane must be checked to make sure that it is located entirely within the construction site. This can again be done using the same coordinates that have been used so far using Equations 4 and 5 [12]. Figure 4 visualizes the coordinate system and variables used by the equations.

$$X_j\in\left[X_i+\frac{W_j-W_i}{2},X_i+\frac{W_i-W_j}{2}\right]\ (EQ.\ 4)$$

$$Y_j\in\left[Y_i+\left(\frac{A_j}{2W_j}-\frac{A_i}{2W_i}\right),Y_i+\left(\frac{A_i}{2W_i}-\frac{A_j}{2W_j}\right)\right]\ (EQ.\ 5)$$

$where$:
$i=the\ site's\ centroid$
$j=\ the\ crane's\ centroid$

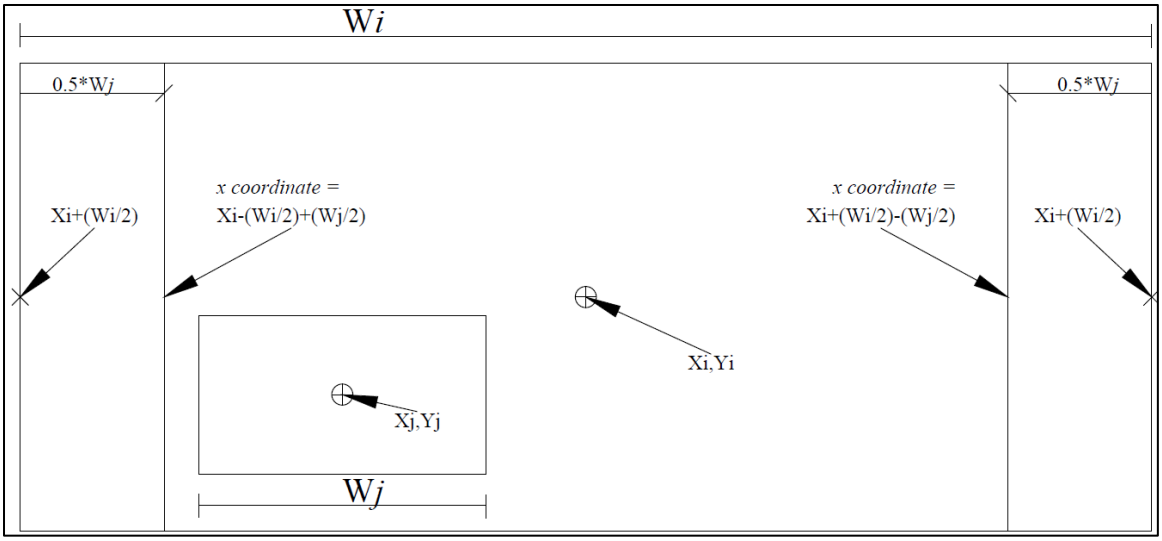

***Figure 4**: System for Checking if an Object Lies Within Site Boundaries*

2.3.2. Factors Influencing Crane Travel Time

Before the introduction of the crane travel time equations, it is important to study what factors are most influential in determining the travel time. In this section, a brief review of these factors is presented.

Despite research into the hoisting time and equations which can calculate the hoisting times, the factors with the greatest influence on the hoisting times are not well known [3]. Leung and Tam (1999) use regression models to determine the variables that affect the total travel time during the construction of residential towers in Hong Kong. The researchers explored 22 variables they believe can explain the hoisting times. The authors performed the regression for the supply and return journeys and their research found that the hoisting height is the variable that has the greatest explanatory power for both parts of the journey.

Another variable which explains the travel time significantly is what the researchers called “simultaneous movement”. This is the ability of the crane operator to simultaneously perform the hoisting and trolleying [3]. This is dependent on the experience of the crane operator, site conditions and weather. Zhang et al. (1995) incorporate both factors in their equations that model the travel time.

During the travel from the supply to the demand points, the length of the object is a variable which greatly influences the hoisting times [3]. This is a logical effect since a larger object is more difficult to maneuver and more vulnerable to the effects of wind. Unfortunately, it is difficult to include the effects of the object dimension into the crane travel time equations.

2.3.2. Crane Travel Time Calculation

The goal of the PSO algorithm is to minimize the travel time equations as developed by Zhang et al. (1999) in "Location Optimization for a Group of Tower Cranes", which is based on the paper "Single Crane Location Optimization" by Rodriguez-Ramos & Francis (1983). Zhang et al.'s (1999) seminal paper integrates a variety of variables that influence the travel time, including those found by Leung & Tam (1999) to accurately predict how long it takes a load to travel from the supply to the demand point. Their work remains the basis of much of the research in this area, often with minimal modification.

The equations are based on the 3 distinct movements made by a crane when transporting a load as discussed in Section 2.2. The total travel time is simply a sum of the three components. To replicate real site conditions, the travel time equations use the work zones that were created to model the site. The loads are transported from the supply point to each of the work zones, and the time taken for the entire floor is the summation of the time taken for each work zone [13].

For a crane located at *x*, *y* the travel time equations as developed by Zhang et al. 1999) are as follows:

$$\rho(S_j) = \sqrt{(XS_j - x)^2 + (YS_j - y)^2} \; (EQ.\ 6)$$

$$\rho(D_j) = \sqrt{(XD_j - x)^2 - (YD_j - y)^2} \; (EQ.\ 7)$$

$$l_j = \sqrt{(XD_j - XS_j)^2 + (YS_j - YD_j)^2} \; (EQ.8)$$

$$\theta = \frac{l_j^2 - \rho(D_i)^2 - \rho(S_j)^2}{2 * \rho(D_i) * \rho(S_j)} \; (EQ.9)$$

$$0 \leq \arccos(\theta) \leq \pi$$

$$Trolleying\ (Angular\ Travel\ )\ Time = T_a = \frac{|\rho(D_j) - \rho(S_j)|}{V_a} \; (EQ.10)$$

$$V_a = Trolleying\ Speed\ (m/min)$$

$$Slewing\ (Angular\ Travel)\ Time = T_\omega = \frac{1}{\omega} * \arccos\theta \; \; (EQ.11)$$

$$\omega = Slewing\ Speed\ (rad/min)$$

$$Hoisting\ Time = T_v = \frac{|ZS_i - ZD_i|}{V_h} \; (EQ.12)$$

$$V_h = Hoisting\ Speed$$

$$Horizontal\ Travel\ Time = T_h = \max(T_a, T_\omega) + \alpha \min(T_a, T_\omega) \; \; (EQ.13)$$

$$Total\ Travel\ Time = T = \max(T_h, T_v) + \beta \min(T_h, T_v) \; \; (EQ.14)$$

$$\alpha, \beta \in [0,1]$$

Figure 5 shows a graphical representation of the equations and variables used by Zhang et al. (1999) to model the movements of a tower crane.

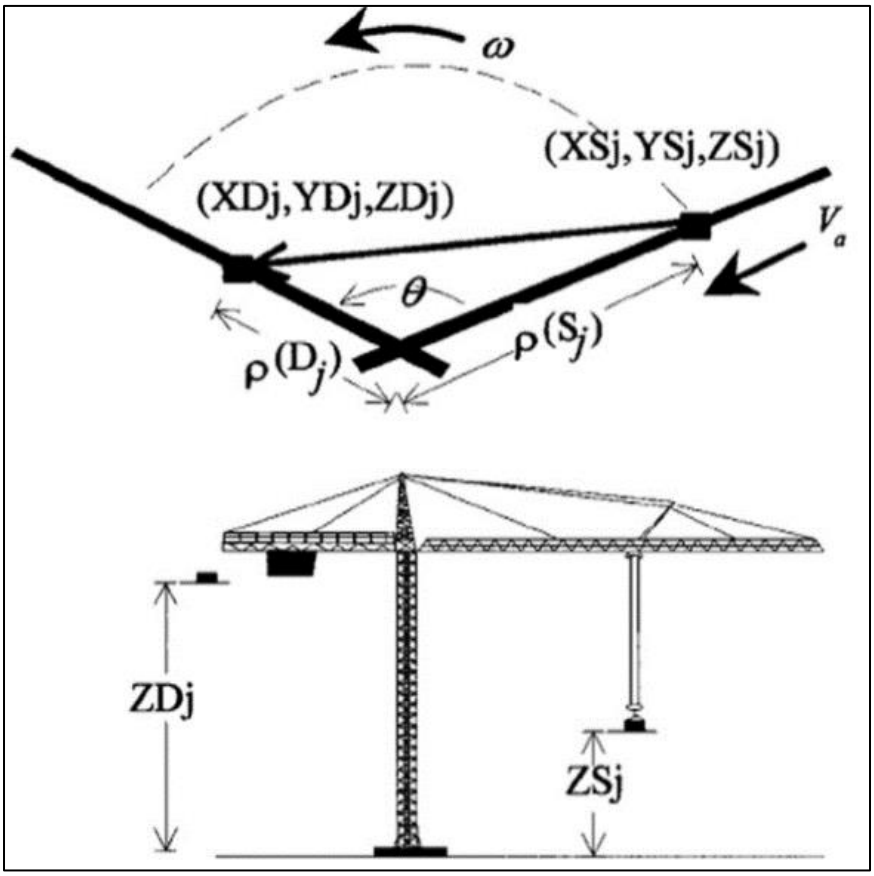

***Figure 5**: Hook Travel Time (Adopted from Zhang et al. (1999))*

The accuracy of the equations lies in their ability to capture real life conditions and the variables that Leung & Tam (1999) listed as the most influential on the speed of operations. For example, it has been established that simultaneous movements have a significant impact on the hoisting times [3]. Zhang et al. (1999) incorporate this effect with two parameters α and β. The choice of values for the parameters is at the discretion of the researchers and dependent on the site conditions, experience of the operator and other factors. α represents the degree of coordination between "[…] hook movement in the radial and tangential directions in the horizontal plane […]" [13].

As $\alpha \rightarrow 1$, the slewing and trolleying motions are performed sequentially. α has been estimated empirically by researchers who observed crane operators at work. It was found that experienced operators can make simultaneous movements 76% of the time, so α can be assumed to have the value 0.25 [14]. However, this parameter is highly dependent on the experience of the crane operator and specific site conditions such as the weather which can affect the degree of coordinate between movements. For example, of the operator's view of the object being lifted is obstructed by the structure, he must rely on his assistant, and the degree of simultaneous movement decreases.

β represents the degree of coordination in the "[…] vertical and horizontal planes […]" according to Zhang et al. (1999). The value of β is dependent on the height of the building and as the working height increases, the value of β does as well [13]. Based on this assumption, Tam et al. (2001) assume that for high rise projects, it is impossible to combine the horizontal and vertical movements because the object being lifted must first have vertical clearance from the structure before any horizontal movement can occur. Based on this logic, they set β to be 1.

The equations developed by Zhang et al. (1999) have been widely adopted; however, researchers have made modifications to some parts to address possible shortcomings. Abdelmegid et al. (2015), note that Zhang et al. (1999) don't account for the return travel time in their equations. If the number of trips between all supply and demand points is limited to 1, this is not a problem, since for any proposed location, the total length of the return journey would be identical. However, if there are multiple journeys, affected by the crane's load-radius curve, which in turn is affected by the location of the crane, then the total length of the return journey will vary depending on the chosen location. An easy rectification to this problem is to assume the crane can make the return journey either at or close to the maximum speeds found in the owner's manual [4].

While some parameters are chosen at the discretion of the researchers, others are determined by the crane and its capacity. The vertical lift speed (V_h) is dependent on the weight of the load, and as the weight of the load approaches the maximum rated capacity

of the crane, the speed at which it can be lifted will decrease. The hoisting speed data for a Liebherr 630 EC-H 40 (Figure 6) crane illustrates how as the weight of the object increases, the maximum hoisting speed decreases.

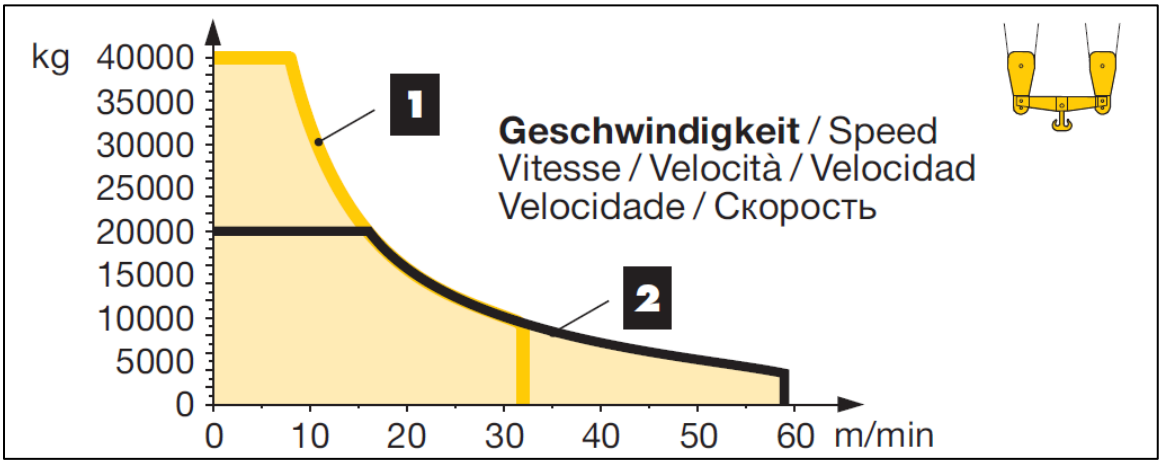

***Figure 6**: Hoisting Speed-Load Curves for Liebherr 630 EC-H 40 Cranes [15]*

The maximum hoisting speed of the crane in question is 60 m/min; however, it can only achieve this speed at weights lower than 4,500 kg. If the weight being lifted increases, then the maximum speed that the hoisting motor can achieve decreases as the graph shows.

A second effect which needs to be incorporated is the location along the crane's saddle jib the object hangs. As an object moves further away from the tower, the laws of mechanics reduce the maximum lift capacity of the crane as dictated by the load-radius curves of the crane as shown in Figure 7 [16, 7].

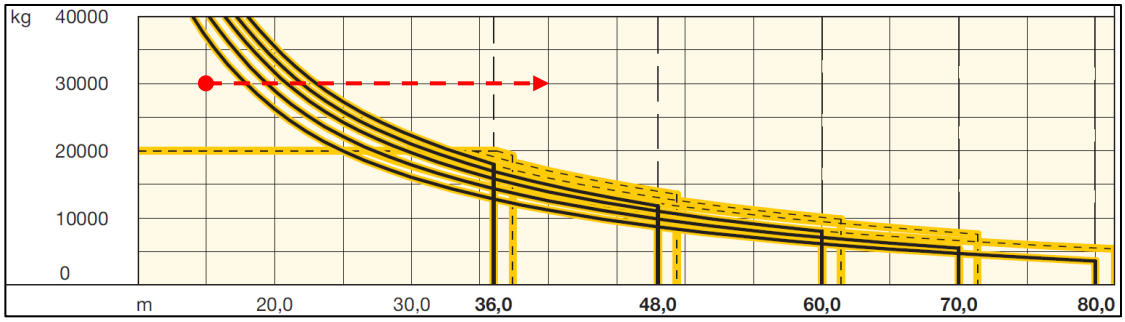

***Figure 7**: Load-Radius Curves for Liebherr 630 EC-H 40 [15]*

While the crane might be able to lift the object from the supply point, the crane's lift capacity limit might be exceeded as the object is moved away from the tower [4]. This problem means the maximum lift capacity of the crane is limited by the following equation:

$$weight_{max} = \min(capcity\ at\ supply\ point, capcity\ at\ demand\ point) \quad (EQ.15)$$

This effect can be graphically represented using the load-radius curves supplied for a Liebherr 630 EC-H 40 crane. If an object is lifted at a radius of 10m, it can weigh up to 30,000 kg. However, since the theoretical demand point is located 40m from the tower, the highest possible lift capacity is approximately 15,000 kg. This means, even if the object can safely lift from the supply point, it cannot be delivered at the demand point. Therefore, for a load to be delivered at 40m, the maximum possible weight is 15,000 kg, regardless of the maximum load the crane can pick up at the supply point [15].

Another key assumption that needs to be made is with regards to the divisibility of the item being transported. If the load is divisible, it means that even if the weight exceeds the maximum rating of the crane, it can lift the load in smaller portions to complete the task. Otherwise, it means for a given candidate location, the crane cannot complete the lift, making that candidate location infeasible. For example, if the item being lifted is reinforcement, then the total load can be divided but if the load is a heavy machinery required at the top, then it is difficult to break it up into smaller loads. The Nib International Bank Head Quarters Project (NIB-HQP) faced this problem when attempting to lift a

cooling tower, which weighed above the cranes limit. This forced the contractor to instead use smaller cooling tower's that were within the crane's capacity.

In the case of a divisible load, Abdelmegid et al (2015) added an equation which allows for the calculation of the number of trips between two points, i and j. N_{ij}, the total number of trips is based on the weight of the load (Q_{ij}) and the crane's lift capacity (C_j).

$$N_{ij} = \frac{Q_{ij}}{C_j} \ (EQ.16)$$

2.4. Metaheuristics and Particle Swarm Optimization

As previously stated, SLP is essentially an optimization problem and a suitable optimization technique must be chosen to find the optimal location. The tools that researchers have previously used can be divided into 2 types. The first group includes tools such as MILP that yield exact solutions, while the second group includes tools such as Genetic Algorithms (GA), Particle Bee Algorithm (PBA) and Particle Swarm Optimization (PSO). The latter are metaheuristic techniques that are also known as stochastic optimization techniques, and they don't necessarily guarantee an optimal solution [12, 5, 10, 11]. As new techniques become available, they are being applied to the TCLP to find ever more accurate solutions efficiently.

2.4.1. Stochastic Optimization / Metaheuristics

Stochastic optimization techniques and metaheuristics have been used extensively in finding the optimal tower crane locations owing to their efficiency and ease of application. Metaheuristics are techniques which randomly sample large solution spaces and while they don't guarantee an exact solution, they are generally found to be more efficient than traditional techniques. Some techniques such as GA and PSO mimic behaviors in nature to

find efficient solutions. In the case of GA, it takes inspiration from the process of evolution and natural selection in nature whereby good genes can survive and reproduce, while PSO mimics the behavior of swarms such as flocks of birds or schools of fish in their attempt to find an optimal food source.

Since GA and PSO both require a large number of candidate solutions, they are also classified as population-based techniques, and PSO is further classified as a swarm intelligence technique because it mimics the behavior of natural swarms.

PSO is a technique that was developed by Kennedy & Eberhart (1995). A population of particles searches the solution space and works both individually and in cooperation with the other particles in the swarm to find the optimal solution. Over several iterations, the particles will converge to an optimal solution. The exact algorithm will be discussed in Section 2.4.2.

However, like all metaheuristic techniques, there is no guarantee that the solution will be the optimal one. The main advantage of techniques such as GA and PSO is that the objective function need not be differentiable, since both techniques rely on generating many candidate solutions and comparing their values. The number of candidate solutions generated is simply the product of the number of particles and the number of iterations. The cause of the wide adoption of metaheuristics is due to their ability to solve problems that are as complex as site layout problems efficiently.

2.4.2. Theory of Particle Swarm Optimization and Integration with Crane Travel Times

PSO is one of the easiest metaheuristics to apply to problems and is easily adopted which explains why it is used widely. According to Shi (2004), the PSO algorithm works as follows:

1. Initialize *n* particles, that are randomly scatters throughout the search space. This is done by randomly assigning x and y coordinates using a uniform random generator so that $x_i \in [x_{min}, x_{max}]$ and $y_i \in [y_{min}, y_{max}]$.
2. For each particle, calculate the fitness value using the specified objective function.
3. Find the personal best (*pbest)*, the position at which the highest value achieved by each particle and global best (*gbest)*, where the highest value among all the particles was achieved.
4. Calculate the next candidate location for each particle using the following formula:

$$V_{id,t+1} = \omega V_{id,t} + [c_1 * U[0,1] * (p_{id} - x_{id})] + [c_2 * U[0,1] * (p_{gd} - x_{id})] \ (EQ.17)$$

$where$:
$V_{id} = velocity\ vector$
$\omega = inertia\ factor$
$c_1, c_2 = factors\ which\ allow\ for\ priority\ of\ local\ or\ global\ search;$
$p_{id} = pbest; p_{gd} = gbest; x_{id} = current\ fitness\ value$

5. Repeat steps 2-4 until the stopping criteria is met.

To compute the candidate solutions in the next iterations, PSO relies on the information gathered by individual particles and the common information that each particle has access to. In nature, birds and fish are attracted to the area with the biggest food source, and as members of the swarm move towards the source, the remaining members of the swarm will also move in that direction. This behavior occurs in the PSO algorithm because areas with near optimal values will attract the other particles.

Figure 8 shows how the location of the next candidate location is dependent on the locations of the current personal and global best locations. If the vector *w* has a high value, then it will have greater influence on the next velocity, pulling the particle towards the area around the global best, and vice versa. This is determined by the value of c_1 and c_2, which are set by the user. As the number of iterations increases, the current positions will be close to the global best, and as *pbest* → *gbest,* the value of the velocity vector will decrease, and the search will be limited to an area around the current position. This can be a disadvantage since the particles can be stuck searching a suboptimal area and leading to a premature convergence.

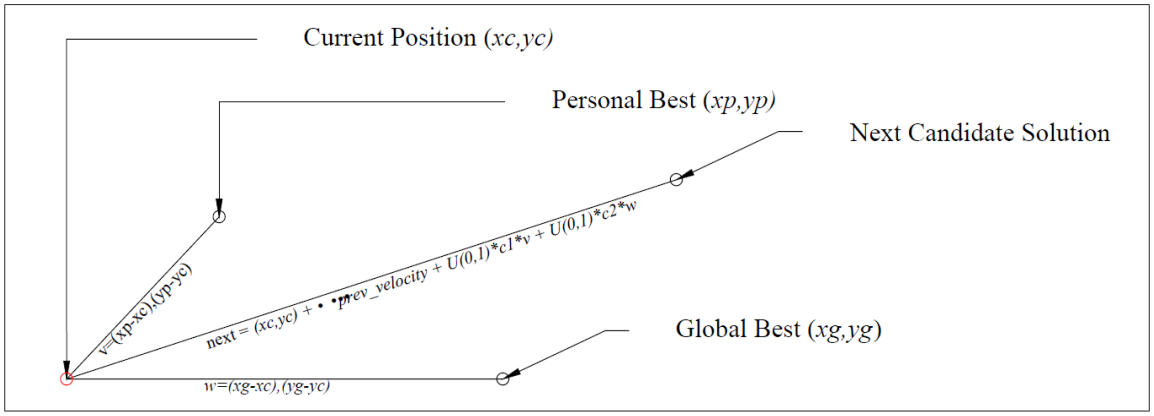

***Figure 8**: PSO Process for Calculation of Next Candidate Locations (Not to scale)*

According to Tian & Shi (2017), the pseudocode to implement the PSO algorithm is as follows:

```
Randomly initialize n particles throughout the search space
While (stopping criteria isn't met):
     Evaluate the objective function
          For all n particles:
               Find local_best, global_best
                    For all d dimensions, and n particles:
                         Update the velocity
                         Update the position
          Update the inertial weights
```

***Figure 9**: Pseudocode for PSO*

Based on the simple algorithm described above, many variants of PSO have been developed to tackle different optimization problems, including constrained optimization, combinatorial problems, and min-max problems [17]. Since the parameters included in the equations above have a significant impact on the efficiency of the PSO algorithm, they are each discussed below:

- U [0,1] is a uniform random number between 0 and 1. This acts as a scaling factor which introduces randomness into the search. Without this random number, the next candidate solution would simply be determined using deterministic values and the algorithm would lose its ability to randomly explore parts of the solution space;
- ω is an inertia value which determines the influence that the previous velocity has on the next velocity. This factor wasn't part of the initial algorithm as introduced by Kennedy & Eberhart. Without this factor, the algorithm tends to "explode", and the particles may never converge. There are 2 approaches to set the value of ω. The first is to simply select a value between 0 and 1. The second uses functions that decrease the value of ω as the number of iterations increased. The second approach guarantees that as the particles start to converge, their velocity will decrease and will start to focus on candidate solutions near the higher values;
- $c_1 \; and \; c_2$ are factors which determine whether local or global search have a priority. They are alternatively known as the cognitive and social parameters. If $c_1 > c_2$, then local search is prioritized, and the particles historically best experiences will have a greater priority. When $c_2 > c_1$, the historically best experiences of the swarm will have more influence on the candidate locations. Setting the value of either parameter to a high value allows the particles to explore distant areas of the space, biasing them towards a global search, however, this has the potential to lead to a divergence of the particles [18].

The final component of the PSO algorithm is the number of particles to initialize. As their numbers increase, more candidate solutions are created and compared. However, this also increases the computational power needed since more calculations need to be done per

iteration. Their number needs to be fine-tuned just like the other parameters to ensure an efficient search.

The stopping criteria is dependent on the on the nature of the optimization problem at hand. Two of the available approaches are either setting a maximum number of iterations or terminating the algorithm when the optimal value reaches a certain level [19, 17]. Both approaches have their own advantages and disadvantages, and the choice of a stopping criterion depends on experiments and knowledge regarding the optimization problem.

If a maximum number of iterations is set as the stopping criterion, there are two possible drawbacks. The first is that the algorithm terminates before an optimal value is reached, or it keeps iterating after reaching the optimal value. The former leads to a sub-optimal result, while the latter wastes computing power and time. One possible approach to prevent such problems is to check the convergence of the objective function to find how many iterations are needed before the optimum value generated stabilizes. Using a predetermined value of the objective function relies on having prior knowledge of the optimization problem. While this approach is efficient in terms of time and computing power, it cannot be employed to problems where no prior knowledge is available.

2.4.3. Comparison of PSO with GA

PSO is an extremely versatile optimization techniques, especially when compared to other optimization algorithms such as GA. While GA has been the more common metaheuristic applied to solve the tower crane location problem, it should be noted that PSO has been proven to perform at least as well as GA in optimization problems. While the performance of PSO and GA is comparable, PSO requires less computational power and is very simple to implement, requiring few lines of code. When tuned properly, PSO converges towards the global optima quickly.

The main similarity of the two algorithms is that they both require finetuning so that they can solve the problem at hand. For a GA, poor tuning affects the mutation and natural selection process that it's trying to mimic from nature, and if PSO is untuned, the risk of "explosions" increases.

Both GA and PSO have an advantage over other techniques such as MILP because they can search large spaces efficiently. MILP, an exact technique can only optimize based on a discrete set of locations that researchers much choose beforehand. There is a risk that such locations can be sub-optimal.

2.4.4. Parameter Tuning

Before using the PSO algorithm to optimize a function, it is important to tune the parameters to ensure convergence, efficiency and to guarantee the lowest possible value is found. The importance of tuning can be illustrated by testing the PSO algorithm on a set of benchmark functions that were created for this purpose.

Setting the values of $c_1 \; and \; c_2$ has a significant impact on the accuracy and convergence of the particles as discussed previously. Kennedy & Eberhart (1995) initially had a single weighting parameter, *c* but a separate parameter was assigned to both the local and global search in later versions. In this original version by the authors, $c_1 = c_2 = c = 0$. In later versions of the PSO algorithm, $c_1 \; and \; c_2$ were assigned values in the [0,4] range, with a general rule that $c_1 + c_2 \leq 4$ [18].

2.4.5. Refinements to the Basic PSO Algorithm

It is also possible to refine the basic PSO algorithm to solve some of its drawbacks. A focus of many refinements is the velocity update mechanism. The update mechanism determines which areas of the solution space are searched next, directly influencing the convergence

and accuracy. The two variants of PSO discussed below affect the velocity of the particles via two changes to the update mechanism and are often combined by researchers. The first imposes a maximum velocity on all the particles, while the second gradually decreases the value of ω.

One variation of the PSO algorithm imposes a maximum velocity on all the particles. If the particles velocity exceeds a given maximum, the velocity will be restricted to a given $\pm vmax$. This prevents particles from flying past good candidate locations especially during the first iterations when the fitness values of individual particles are much smaller than the globally best fitness values, leading to high velocities during the next iteration [17].

Another variation sets the value of ω dynamically, rather than fixing it to a given number. This approach gradually reduces the influence that previous velocities have on the next velocity, which forces the particles to focus their search on a smaller area of the solution space as the number of iterations increases. Alternatively, this can be thought of as decreasing the memories of the particles as the number of iterations increases [17, 18].

2.5. Summary of Literature Review

The literature review for this thesis was divided into 4 basic areas of knowledge whose understanding was deemed to be critical before proceeding further with the research. In the first section, the three basic types of cranes: mobile, bottom-slewing and top-slewing were discussed. The similarities and differences, as well as the advantages and disadvantages of the different crane types was analyzed. The terminology and functions of a top-slewing tower crane was discussed in depth because of its prevalence in Addis Ababa, and the fact that it's the only anchorable type of crane, making it the sole option for high-rise projects such as those analyzed in the case studies. Part of the discussion was also dedicated to factors which influence the travel time of tower cranes. As shown by Leung & Tam (1999), the ability to perform simultaneous movements was the factor with the most influence on

the total travel time. This was incorporated into travel time equations that were developed by Zhang et al. (1999) through the use of parameters α and β.

The second area of discussion was that of Site Layout Planning, and Tower Crane Location Problem, which is a subset of the larger CSLP problem. CSLP involves the positioning of all temporary facilities on construction sites in a manner which increases efficiency. TCLP, being a subset of SLP, deals specifically with the positioning of tower crane(s) on construction sites. TCLP encompasses the optimization of single tower cranes, which is the focus of this thesis, as well as that of multiple tower cranes. It was found that the appropriate placement of a tower crane has significant implications with regards to the environmental impact, safety and efficiency of a construction project.

Next, the techniques involved in modelling site layouts and crane transportation times were discussed. In modelling site layouts, the two competing approaches of Alkriz & Mangin (2005) and RazaviAlavi & AbouRizk (2017) were discussed in terms of their advantages and disadvantages. The former approach allows for the exploration of the entire feasible area, while the latter limits the search space to within vertices of a predefined grid. In fact, the approach by Alkriz and Mangin (2005) is a generalization of the RazaviAlavi & AbouRizk (2017) approach where the number of vertices approaches infinity. The travel time calculations were based on the seminal work by Zhang et al. (1999) in "Location Optimization for a Group of Tower Cranes". Minor refinements made to their equations by Abdelmegid et al. (2015) which accounted for the return to the ground of the hook block were discussed.

The final area of knowledge focuses on the optimization of the tower crane's location based on the equations introduced in Section 2.3. A range of optimization techniques that could be applied to the problem were discussed, with an emphasis on metaheuristic techniques such as Genetic Algorithms and Particle Swarm Optimization. Both techniques were found to be well suited to the problem, with the PSO algorithm being easier to implement and having a lesser computational demand.

2.6. Gap Analysis

The literature review has identified several gaps in knowledge in previous research. Three areas which remain unexplored are:

- Finding a solution to the TCLP for high-rise buildings: In general, previous research has focused on cranes which haven't exceeded their freestanding height, which allows the crane to be placed at any location on the construction site as long as lifting capacity of the crane isn't exceeded.

  For high-rise buildings, anchoring becomes a critical requirement, restricting the crane's position to an area surrounding the building which allows the crane to be anchored since the freestanding height of the crane is usually exceed in such projects.
- Optimization tower crane locations for small construction sites: Both CSLP and TSLP are of paramount important on small and congested construction sites as discussed by Li and Love (1998). Previous research hasn't taken the effects of small sites with plot limits that are close to the permanent structure into account.
- Checking the performance of traditional crane placement techniques: Most of the research surveyed has focused on finding the optimal location, without comparison to the actual location on site and how the contractor's placement technique has fared. Such comparison can allow for either the acceptance or rejection of traditional placement techniques.

3. RESEARCH METHODOLOGY

The methodology employed by this thesis will bring together various fields that have been discussed previously in the literature review to answer the research questions that have been posed. Broadly, the methodology section of this thesis employs the following research instruments:

- Data collection;
- Site layout modelling; and
- Optimization and comparison with actual location on site.

The first two instruments are part of the inputs for the OM, which enables engineers to input site-specific data in order to get the optimal location of a tower crane.

As illustrated in Figure 10, the 4 major information categories for the computer model are the Site Layout Information, Tower Crane Capacities, Total Quantity of Work and Interviews. This information is used in the construction of the computer model, which is performed in Python 3.6, which ensures its compatibility with the algorithms in the OM, which is coded in Python 3.6 as well. These inputs are discussed in Sections 3.1 and 3.2.

The computer model serves as an input for the OM, which is made up of the PSO module, which attempts to minimize the objective function as calculated by the Travel Time Calculation (TTC) module. Upon completion of the optimization, the OM will yield an optimal location. This location is then compared against the actual location on the construction site. This step is discussed in Section 3.3.

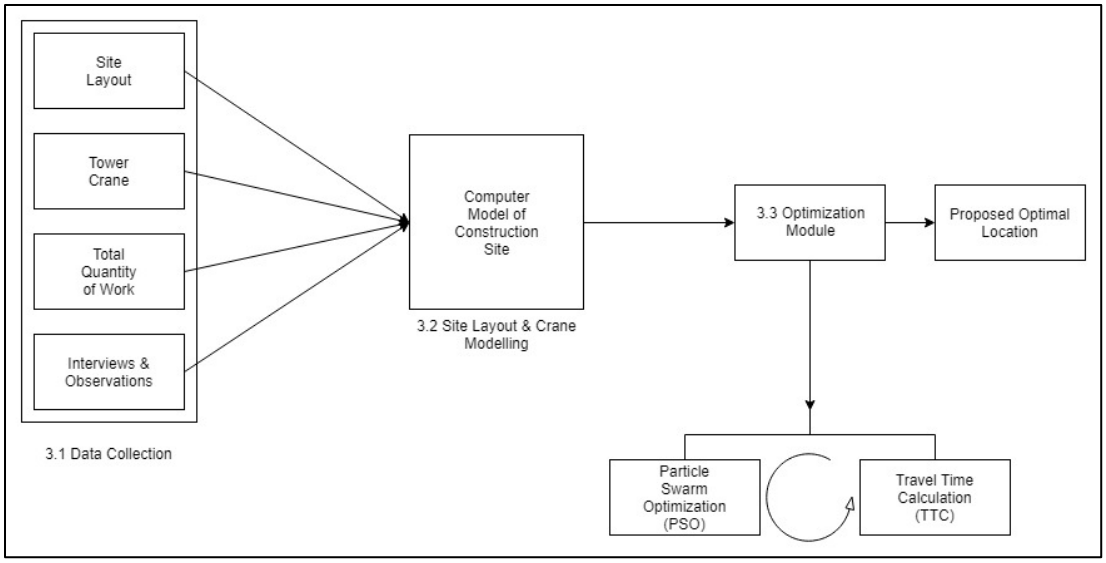

***Figure 10**: Flow Chart of Research Instruments and Methodologies Applied*

3.1. Data Collection

The primary input for the OM is the site model which accurately depicts the real site conditions. This information will be collected from various construction sites throughout Addis Ababa that meet a set of criteria that will be discussed in section 3.1.1. According to Emporis, a high-rise structure is defined as "[…] a structure whose architectural height is between 35 and 100 meters." Any building with 12 to 39 floors, whose height is unknown is also referred to as a high-rise building [2]. This definition of high-rise buildings is adopted in the selection process.

The following information is collected from the construction sites:

- Location of temporary and permanent structures on site;
- Entry and exit points;
- Site layout drawings;
- Current location of the tower crane and the tower crane model and information included in the owner's manual such as: Hoisting/Slewing/Trolleying speeds, load-radius curves and jib length; and
- Construction schedules and volumes of work.

Table 1 summarizes the various types of data required for the thesis, their importance to the work, and the collection method.

***Table 1**: Summary of Data Sources*

SOURCE	DESCRIPTION	PURPOSE	COLLECTION
Contractors and/or consultants	▪ Crane type, location ▪ Work breakdown & sequencing ▪ Site layouts	▪ Data input for simulation.	▪ Collected by researcher, entered manually into model.
	▪ Previous experience on the location of cranes	▪ To understand current practices	▪ Collected using interviews and analyzed
Tower crane manufacturers, rental/sales offices	▪ Tower crane capacities and operations manuals	▪ Input into the travel time calculation equations	▪ From the manufacturer's websites ▪ Personal collection from offices
Tower Crane Operators	▪ Preferred operation methodology (sequence) and timing	▪ To understand the problem from the viewpoint of the operators.	▪ Survey & interview of operators on site.

3.1.1. Site Selection

There are numerous construction sites in Addis Ababa that use a tower crane, and it would be impossible to survey all of them due to resource limitations. Instead, purposive sampling is used to select a set of representative case studies within the Financial District of Addis Ababa. A major problem in this process is the lack of a central database with information on sites that utilize tower cranes. The F.D.R.E. Ministry of Construction, which oversees the registration of construction equipment doesn't keep a record of where the equipment is used and cannot force owners to register their equipment.

In selection of the construction projects for the case studies, the primary requirement is that the site is serviced by one tower crane only. However, there are a range of other selection criteria that ensure a wide range of projects are explored. This includes:

- Building height: A range of building heights are modelled, with the Emporis definition of a high-rise building adopted;
- Anchoring: Cranes that are both freestanding and anchored are modelled; and
- As per the scope and limitation of this thesis, the sites are limited to Addis Ababa.

Crane use in Addis Ababa is largely restricted to high-rise building projects such as the Commercial Bank of Ethiopia HQ, large-scale construction projects such as Adey Abeba Stadium Project or smaller projects being undertaken by contractors that understand the benefits of tower cranes can bring to smaller projects such as the Black Lion Teaching Hospital's Cardiac Center Expansion Project.

Purposive sampling is used to select the case studies because the unique requirements of the thesis. In addition to the criteria discussed above, the willingness of the contractor to participate by allowing access to the site and project information makes it impossible to randomly select construction sites. Based on these requirements, the 6 construction sites summarized in Table 2 are selected. With the exception of the Marriott Hotel project, all the case studies are located in the Financial District. The Marriott Hotel case study is presented separately in Appendix 6.

***Table 2**: Summary of Participants*

PROJECT NAME	LOCATION	CONTRACTOR	HEIGHT (m)
Commercial Bank of Ethiopia HQ	Ambassador, Lideta Sub-City	CSCEC	198
Marriott Hotel	Bole Medhanialem, Bole Sub-City	Sunshine Construction	67.5
Nib International Bank HQ (NIB-HQP)	Beherawi, Lideta Sub-City	China Jiangsu	122
Nile Insurance HQ Project (NI-HQP)	Beherawi, Lideta Sub-City	Rama Construction	87.5
Union Bank HQ (UB-HQP)	Beherawi, Lideta Sub-City	China Jiangsu	133
Zemen Bank HQ (ZB-HQP)	Beherawi, Lideta Sub-City	China Wu Yi	130

3.1.2. Site Layout and Work Data Collection

Following the selection of the projects to serve as case studies, the information summarized in Figure 10 and Table 1 is collected from participants. The unique layouts of each site and the location of all structures, boundaries and entry/exit points are required to model the site. This information is extracted from the site layout drawings produced either by the contractor or the consultant. The current location of the tower crane, and the dimensions of its base is recorded for the model and used during the comparison of the actual and theoretical locations.

The second component of the information that needs to be collected from the construction sites is the work schedule. A construction project is composed of many different activities, and the degree to which each activity utilizes the crane differs. The group of activities that use the crane most intensively must be selected for inclusion in the model. The contractor's staff are an alternative source of information about the crane utilization, and interviews are used to gather the information.

The methodology selected by the contractor has a significant impact on what the crane is used for. For example, the Marriot Hotel project, in which the contractor chose not to use a concrete pump relies entirely on the tower crane for the transport of all the concrete, while Nib and Union Bank HQ projects that use a concrete pump don't need to use the crane for concrete transport except for vertical elements. Compared to the reinforcement transported using the crane, it means the concrete transported isn't as significant for the latter, while it's the heaviest material transported cumulatively for the Marriot Hotel project. When selecting the activities to be modelled, such variations need to be considered based on the information collected from the contractors. Once the activities are selected, the total volume of work per floor must be divided up among the work zones. The demand points for concrete for vertical elements and indivisible items such as steel columns are based on the structural drawings.

3.1.3. Crane Information Collection

Each crane is unique, and its capacity is dependent on its design. One of the inputs for the model is the crane's capacity information that is provided by the manufacturer of the crane. In addition, the dimension of the base of the crane must be included in the information collected regarding the crane. The easiest source of information on its capacities is the owner's manual provided by the crane's manufacturer. Additional information can also be sought online by using the crane's model number. The data generated through the combination of both approaches is used to find the information needed to complete the model.

3.2. Site Layout and Crane Modelling

AutoCAD drawings of the construction site layout and each of the floors that contain a demand point to be included in the model are used to create a Python 3.6 model of the site. The centroid coordinates are added to the files, which completes the model. The model's attributes can then be exported from AutoCAD using the "DATAEXTRACTION" function

that's included in AutoCAD. This information can then be imported into the OM and is compatible with the PSO and Travel Time Calculation (TTC) modules which are will be discussed in Section 3.3. Following the approach by Alkriz & Mangin (2005), the objects in the model are referred to using the coordinate of the centroid, each object is given a unique name.

Part of the modelling process is concerned with the tower crane and its functions. For any given load weight, the model must be able to calculate the associated slewing, hoisting and trolleying speeds, and this requires the replication of the capacity graphs that were discussed in Section 2.3.2. The data points on the load-radius curves can be extracted, and a curve can be fitted using linear regression to find the equations. The function takes a length as an input and returns the corresponding maximum possible lift weight. Figure 11 shows a replication of the load-radius curve of a Liebherr 630 EC-H 40, after a polynomial function was fitted to a set of data points extracted from Figure 6.

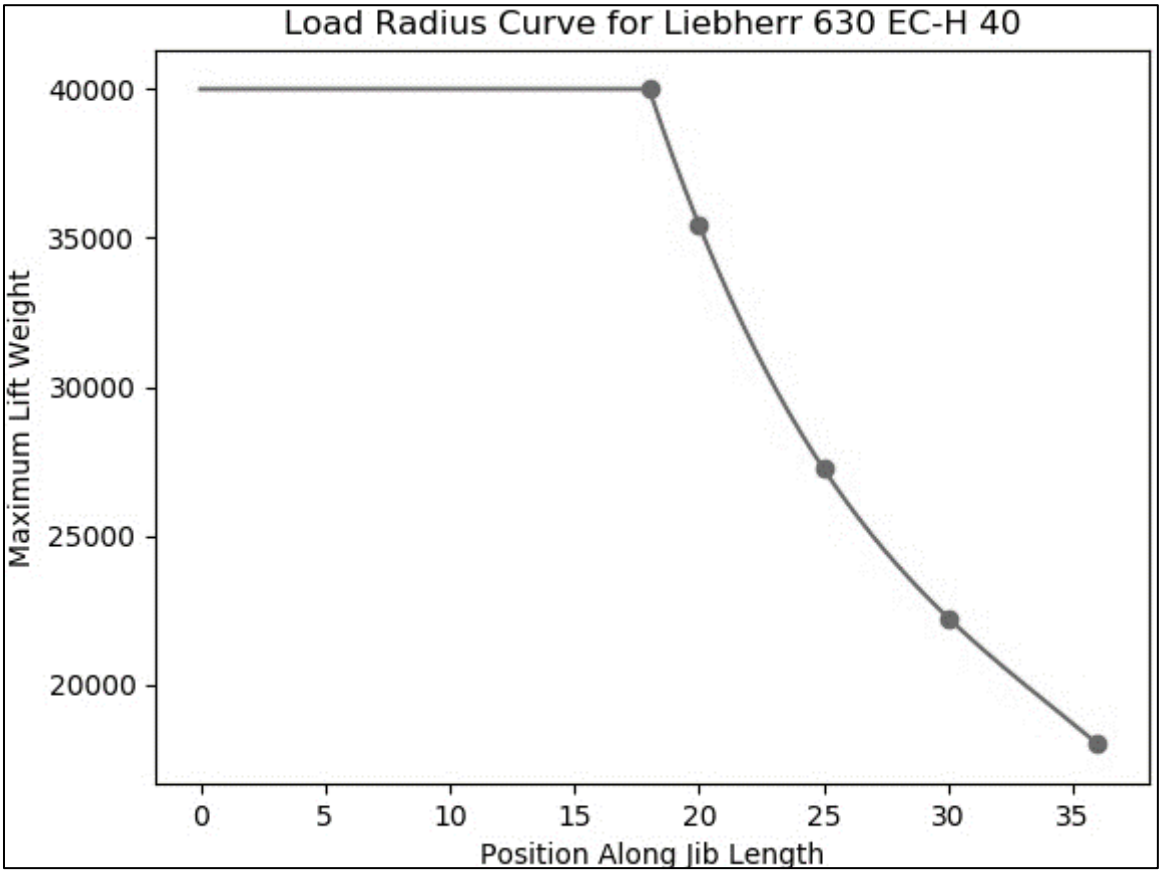

***Figure 11**: Replication of the Load-Radius Curve for a Liebherr 630 EC-H 40*

The 3rd degree polynomial which was found using linear regression in statsmodels had a R^2 of 1, indicating a perfect fit. The process to find the line of best fit is described in detail in Appendix 3.

The process of site modelling can be summarized in the following 5 steps:

1. Collection of information from construction sites;
2. Calculation of centroid coordinates and other parameters in AutoCAD;
3. Modelling of the crane's capacity as functions in Python after the equations are found using Ordinary Least Squares (OLS) regression;
4. Division and assignment of total volume of work among the work zones; and
5. Importing of the information into Python.

3.3. Optimization Module

So far, the methodology has focused on the collection and processing of the various inputs that the model needs to produce an optimal location. Once the steps outlined previously are completed, they are introduced to the OM which optimizes the location of the tower crane based on the total travel time. The OM has two modules working in unison to find the best locations for tower cranes.

The PSO module generates random locations for which the travel time calculation (TTC) module estimates the travel times. This fitness value is used to evaluate the current locations and generate the next candidate solutions. The process repeats until a maximum number of iterations is reached. The TTC model is composed of the equations developed by Zhang et al. (1999) and the modifications that were introduced by Abdelmegid et al. (2015).

The process of integrating PSO with the crane travel time equations discussed previously is a straightforward step. The output of the travel time equations is the value of the objective function that the PSO algorithm optimizes, and that value is used to judge the fitness of each candidate solution. This step is a simplified adoption of the process used by

RazaviAlavi & AbouRizk (2017) where they used a simulation to determine the construction time, and used this output as the fitness value for the GA. The integration of the two is as shown in Figure 12.

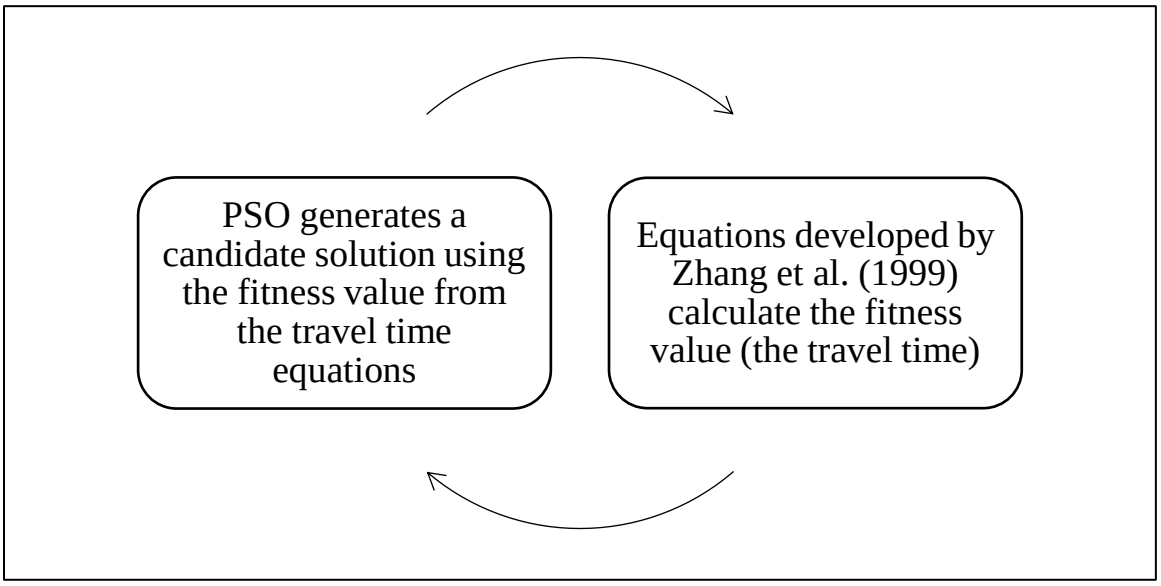

***Figure 12**: PSO and Crane Travel Time Integration in the Decision Support System*

3.3.1. PSO Module

A basic form of PSO, with minor changes to the update mechanism is used to optimize the objective function. The constraints that were discussed in Section 2.3.1 are built into the PSO module so that all candidate locations satisfy the requirements before the TTC module is used. This approach can save computational power and time, because the TTC module is used only on the locations which satisfy all constraints.

At every iteration, the locations of the candidate locations are checked to make sure that none of the constraints are being violated that have been previously discussed. If they are violated, a penalty is imposed, and in the next iteration of the algorithm, the particles will avoid that area. Since the problem is one of minimization, the objective function's value initial value is set to a high value as a penalty. For many high-rise structures, it is necessary to anchor the crane to the structure being built. This means that the feasible locations are

further restricted to a ring around the structure, while much be within the maximum permissible anchoring length. Again, this can be enforced by penalizing the locations which violate this requirement.

The number of particles and iterations are tuned on one of the projects and checked continually to ensure convergence. Literature has shown that the number of particles can range from 12 to 60 but in this case, the restricted search space allows for a smaller number of particles to be used. The convergence rate is used to determine the number of iterations that the algorithm goes through before termination. The pseudocode for the algorithm is shown in Figure 13:

```
Randomly initialize n particles throughout the search space

While (stopping criteria isn't met):
   Use TTC module to calculate the travel time
          For all n particles:
                If any constraints are violated:
                      Impose a high travel time
                Else
                      continue

          For all n particles:
                Find local_best, global_best
                      For x and y dimensions:
                            Update the velocity of the particles
                            Update the position of the particles

                            For all n particles:
                                  If any constraints are violated:
                                        Impose a high travel time
                                  Else
                                        continue

          Update the inertial weights
```

***Figure 13**: Pseudocode for PSO for Implementation in Thesis*

The effect of such restrictions on the feasible region can be illustrated using the Ackley function (Figure 14), which was developed to test the efficiency of optimization algorithms. The global optimum of the Ackley Function is at (0,0) but the feasible region has been restricted to the black triangles and rectangles. In addition, a green triangle located within Rectangle-A imposes a further restriction that no candidate location can be within

it. As shown on Figure 14, the feasible locations (in shades of red) are all located within the rectangles, while all other points (in shades of green) are infeasible. Additionally, the points in the green rectangle within Rectangle-A are infeasible.

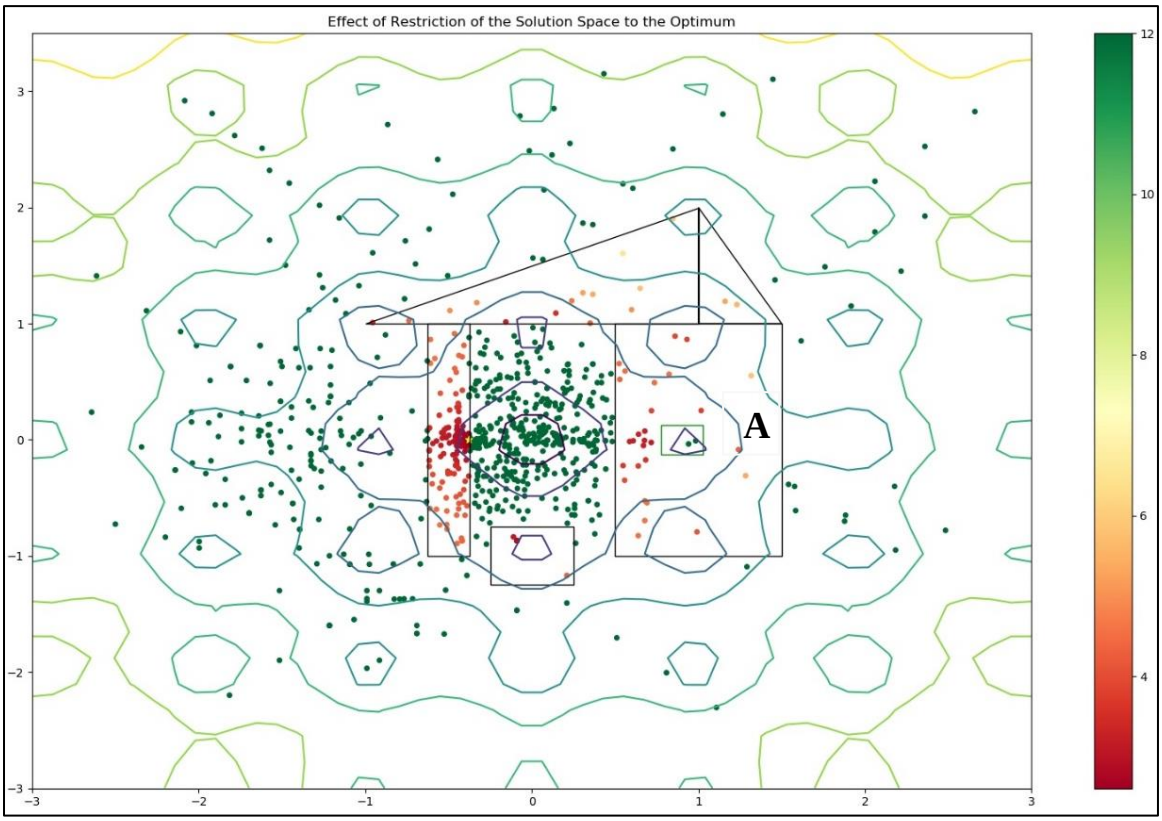

***Figure 14**: Effect of the Restriction of the Feasible Solution Space*

As Figure 14 shows, the new optimum value occurs at $(-.2525, -6.583 \times 10^{-5})$, which satisfies the constraints defined previously. This approach is used during the optimization to eliminate the candidate locations that don't satisfy any given constraint. This process is applied to ensure all locations are on the given site and if the crane is anchored to the structure, to check if it is within the maximum permissible anchoring distance.

3.3.2. TTC Module and the Objective Function

The second component of the OM is the objective function. The objective function in this thesis takes the form described by Zhang et al (1999) and Abdelmegid (2015). There are multiple approaches that have been taken in defining the objective function such as using the costs or environmental impacts as the objective function [6, 20]. There is no practical difference in results because both approaches are based on the total travel time. In this research, the travel time is minimized directly. For each proposed location, and all supply/demand points, the TTC function will be used to calculate the total travel time.

The TTC module will be composed of various functions, whose tasks are described below:

- *Maximum Load Calculator*: Based on the crane's load-radius curves, this function calculates the maximum lift weight for the supply and demand points;
- *Trip Number Calculator*: Following the approach by Abdelmegid et al. (2015), if the load is divisible, and it exceeds the maximum capacity of the crane, the number of trips necessary to complete the task is calculated. If it is impossible to divide the load, it means the proposed location of the tower crane is infeasible, and the TTC module automatically returns a high value;
- *Speed Calculations*: Given the weight of the load, and other variables this function calculates the hoisting, slewing and trolleying speeds of the crane; and
- *Travel Time Calculations*: Finally, the outputs of the previous functions are combined to calculate the travel time between each supply and demand point for the proposed crane location.

Abdelmegid et al. (2015) made one important modification to the equations developed by Zhang et al (1999). The study added the time taken for the hook to return to the supply point, and this approach has been adopted. This ensures a more realistic representation of real-life conditions because the proposed location of the tower crane affects the maximum capacity of the crane which in turn affects the number of trips that need to be made from any pair of supply and demand points.

The overall procedure that the TTC follows is as follows:

1. Calculate the number of trips;
2. Calculate the speeds for each load;
3. Calculate the journey time for each work zone;
4. Repeat steps 1 through 3 for all work zones, on all floors; and
5. Aggregate the travel time for each work zone to find the travel time for a floor and sum the travel time for each floor to calculate the total travel time.

Appendix 9 provides a summary of the mathematical optimization problem described in this section.

3.4. Comparison with Actual Location on Site

The final objective of this thesis is to compare the theoretically optimal location of the crane as generated by the OM against the actual location on site. Once the model generates a theoretically optimal location, it can be compared against the actual location of the tower crane on site. Concerned project managers are asked to comment on the generated location and the total transport time of the theoretically optimal location. The actual location can then be compared to find the time savings for the selected activity.

4. COMMERCIAL BANK OF ETHIOPIA NEW HQ PROJECT

The Commercial Bank of Ethiopia New Headquarters Project (CBE-HQP) is a major building construction project which is composed of a main office tower, a commercial center and a conference center. The G+48 tower is the tallest building in Ethiopia and East Africa, and the second tallest on the continent, with a height of 198 meters [21] [22]. The Design-Build project is being undertaken by the China State Construction Engineering Corporation (CSCEC), the biggest contractor in China by revenue and is being supervised by the Addis Ababa Institute of Technology (AAiT) as a Client's Representative [23]. As of November 2018, the major structural works have all been completed.

This first case study serves a dual purpose. As with the case studies in Chapter 5 the results are used to answer the research question. However, it is also be used to test and define the algorithms to be used in the thesis. In addition, the PSO algorithm requires tuning to ensure efficiency and convergence. The second purpose of this chapter is to accomplish the testing, development and tuning before a wider deployment on other selected projects. The procedures outlined below are repeated for the other projects with minor modifications only.

4.1 Background Information

The project is located in the Ambassador area of Lideta Sub-City, Addis Ababa on a 18,275 m^2 plot of land, close to other high-rise buildings in the Financial District of the Addis Ababa City. The cost of the project is approximately 6.23 billion ETB (298.5 million USD). Compared to other projects in the area, the project has a larger plot area and unlike other high-rise projects in the vicinity, the proportion of the area taken up by buildings is small, which has allowed the contractor a greater amount of freedom with regards to site planning.

4.2 Design and Construction Methodology

Since the design of the structure, and the work methodology selected by the contractor affects how the crane is used, both factors are discussed. As previously mentioned, the CBE-HQP project is divided into 3 major structures: the office tower block (198 m), the conference center (46 m), and the commercial center (45.5 m). The three structures are each serviced by their own tower crane.

The structures are built using reinforced concrete, and the columns up to the 30^{th} floor are made of composite steel columns. Unlike other items transported by the crane, the structural steel composite columns are transported to the exact location and welded since it is impossible to move them using any other tool.

The concrete for the structural elements is produced at an offsite location and transported using dedicated concrete pumps for each of the 3 buildings that make up the project. No concrete is lifted using the cranes because of the significant differences in efficiency between a crane and bucket lift and a concrete pump.

The main use of the tower cranes is to transport reinforcement, structural steel and formworks [24]. The convention center and the commercial building blocks each have one construction elevator, while the main tower has 2 construction elevators. These elevators are used for the transport of other materials such as HCB and pieces of the curtain wall to the desired location. Small quantities of mortar used for the construction of the partition walls are also transported using the construction elevators.

4.3 Site Information

The CBE-HQP site has an area of 18,275 m^2 and is bordered by Ras Abebe Damtew Road to the West, Ras Desta Damtew Road to the East and Yohannes Road to the North. The southern side of the plot is also bounded by a service road.

The absence of nearby buildings has allowed the cranes to operate freely and allowed the contractor to freely position its entry and exit points. Due to the entire site being surrounded by roads, the contractor has built several entries and exit points that lead to either Ras Abebe or Ras Desta Damtew roads.

As shown in Figure 15, the gates serve specific purposes such as two gates on Ras Abebe Aregay Street for concrete delivery and staff and visitor entrance, and a gate on Ras Desta Damtew Street for reinforcement delivery. The material entry gates are both located close to where the material is eventually used, with the reinforcement gate adjacent to the reinforcement working area, and the concrete delivery point close to the pump for the main tower.

There are also several facilities such as the contractor's offices in the north-eastern corner, a residential block on the north-western side and a reinforcement workshop on the eastern side of the plot which is a common resource for all 3 buildings.

Figure 15 shows the location of both temporary and permanent structures on the site, including the locations of the 3 tower cranes and the various supply points included in the computer model.

The drawings presented below are courtesy of the Commercial Bank of Ethiopia and the Addis Ababa Institute of Technology Client Representative's Office.

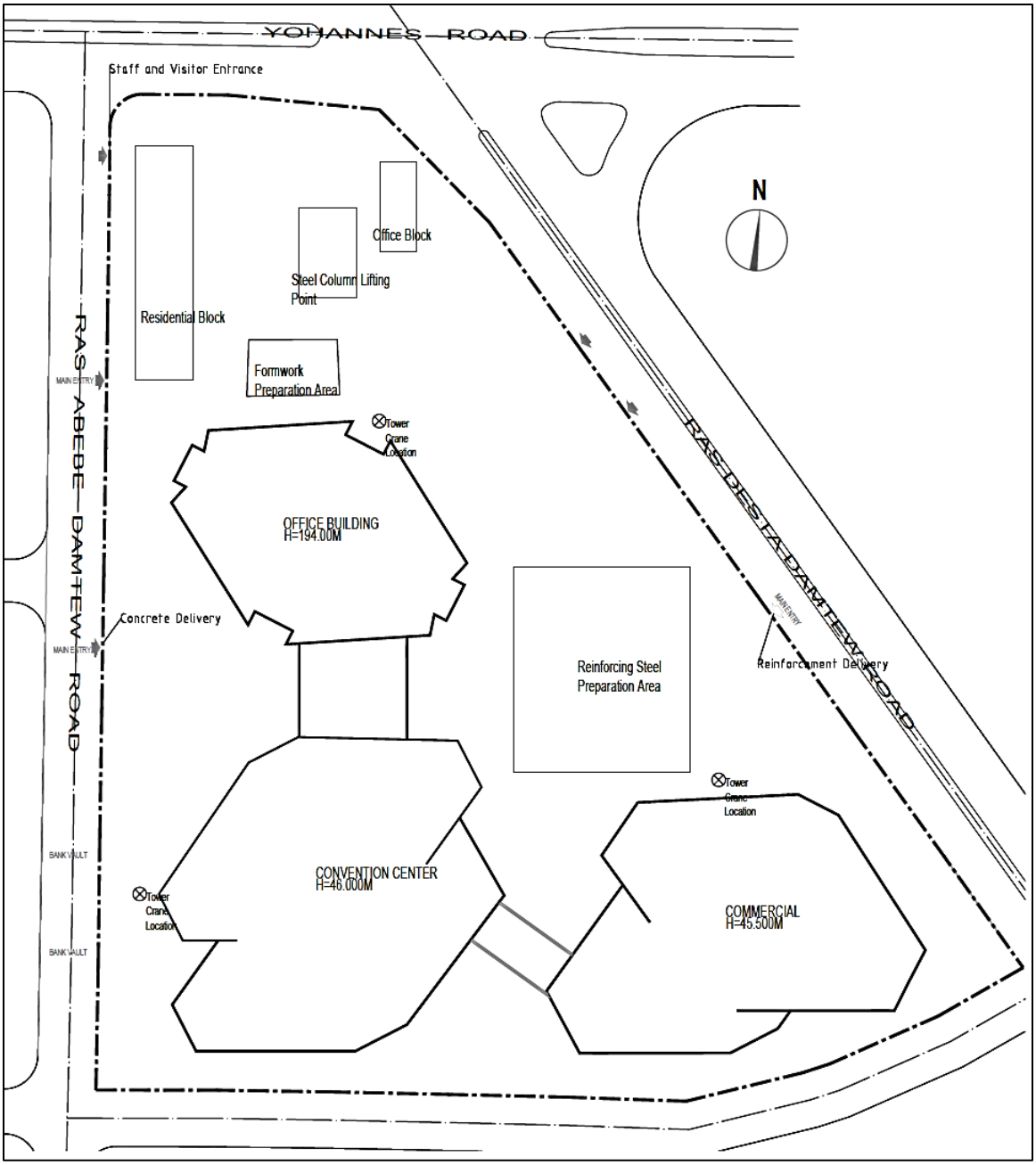

***Figure 15**: Site Plan of CBE-HQP Project (Courtesy of CBE and CSCEC)*

One of the benefits of a construction site on a large plot of land is the freedom to move the supply points as desired. While the formwork and reinforcing steel are transported from predetermined locations, the steel columns were lifted from 3 separate locations, depending on the location where they were needed. However, most of the columns were lifted from the location included in Figure 15 which is treated as the single supply point.

4.4 Crane Information and Modelling

The office tower is serviced by a Shenyang Sanyo R75/25 crane, with a jib length of 60m, maximum capacity of 18 tons and maximum capacity of 4.3 tons at the tip. The recommended base of the crane is 3mx2.2m. The maximum service height of the crane is 240m, which exceeds the height of the CBE tower.

The base of the tower crane is located on a pile on the bottom floor of the basement. The pile and concrete used around the base of the crane has been made stronger using a higher class of concrete to ensure that it can handle the extra load. This means the decision regarding the location of the tower crane was made prior to the construction of the foundation. Figure 16 shows the Load-Radius table extracted from the owner's manual.

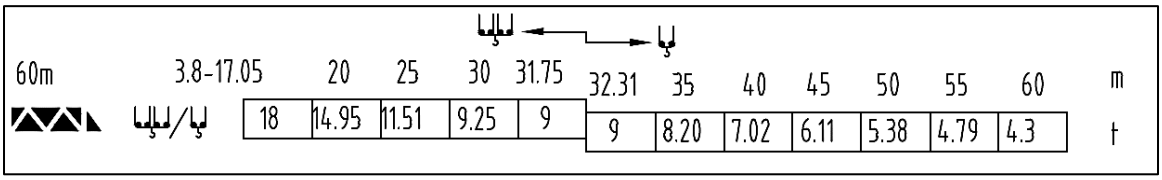

***Figure 16**: Load-Radius Table of ShenyangSanyo R75/25 Tower Crane [25]*

The crane's capacity is modelled using the process outlined previously in Section 3.1.2 using OLS regression. The crane's maximum capacity at varying points along the jig are modelled as follows, where *x* is measured in mm:

$$Maximum\ Load\ (kg)\ (EQ.18)$$

$$= \begin{cases} 18000, & x \in [0,17050] \\ 5.919602 * 10^{-9} * x^3 - 3.238021 * 10^{-4} * x^2 - 4.855701 * x + 7.250718 * 10^{-4}, & x \in (17050,25000] \\ 2.396823 * 10^{-9} * x^3 - 1.622386 * 10^{-4} * x^2 - 3.018352 * x + 3.160848 * 10^{-4}, & x \in (25000,32100] \\ 6.109950 * 10^{-10} * x^3 - 5.758177 * 10^{-5} * x^2 + 1.501179 * x - 1.117783 * 10^{-4}, & x \in (32310,40000] \\ 2.309889 * 10^{-10} * x^3 - 2.757000 * 10^{-5} * x^2 + 0.9088778 * x + 5.447695 * 10^{-5}, & x \in (40000,50000] \\ 1.016970 * 10^{-10} * x^3 - 1.478 * 10^{-5} * x^2 - .5923576 * x + 3.348602 * 10^{-5}, & x \in (45000,60000] \end{cases}$$

Similarly, the radius-load curves, which dictate the crane's lifting radius for various positions on the jib have been developed using linear regression, where *x* is measured in kilograms.

$$Maximum\ Location\ on\ Jib\ (mm)\ [EQ.19]$$

$$= \begin{cases} 60000, & x \in [0,4300] \\ 0.001601 * x^2 - 24.760752 * x + 136861.460215, & x \in (4300,5380] \\ 0.000826 * x^2 - 16.341243 * x + 114004.820772, & x \in (5380,7020] \\ 0.000442 * x^2 - 10.961670 * x + 95178.2396, & x \in (7020,9000] \\ 0.000825 * x^2 - 19.823146 * x + 143932.625976, & x \in (9000,11510] \\ 0.00007493 * x^2 - 3.436053 * x + 54622.651435, & x \in (9250,18000] \end{cases}$$

According to the manufacturer's manual, the crane has a maximum hoisting speed of 20 m/min when carrying a maximum load of 18,000 kg. The maximum speed increases to 30 m/min when the load is decreased to 9,000 kg and to 40 m/min when the load is decreased to 4,500 kg. This information is modelled using a logarithmic function fitted using OLS regression. The resulting equations, where *x* is the weight of the load in kg are:

$$Hoisting\ Speed\ \left(\frac{mm}{min}\right)\ [EQ.20] = \begin{cases} 40, & x < 4500 \\ -14.427 * \ln(x) + 161.357, & x \in [4500,18000] \end{cases}$$

Figures 17 and 18 show the replications of the 3 curves.

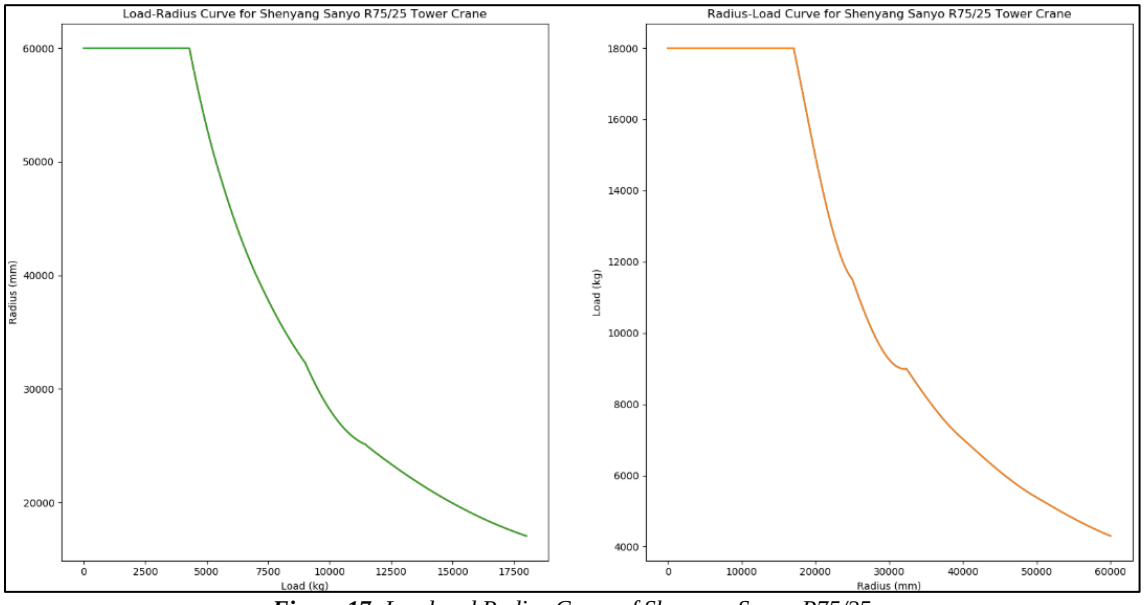

***Figure 17**: Load and Radius Curve of ShenyangSanyo R75/25*

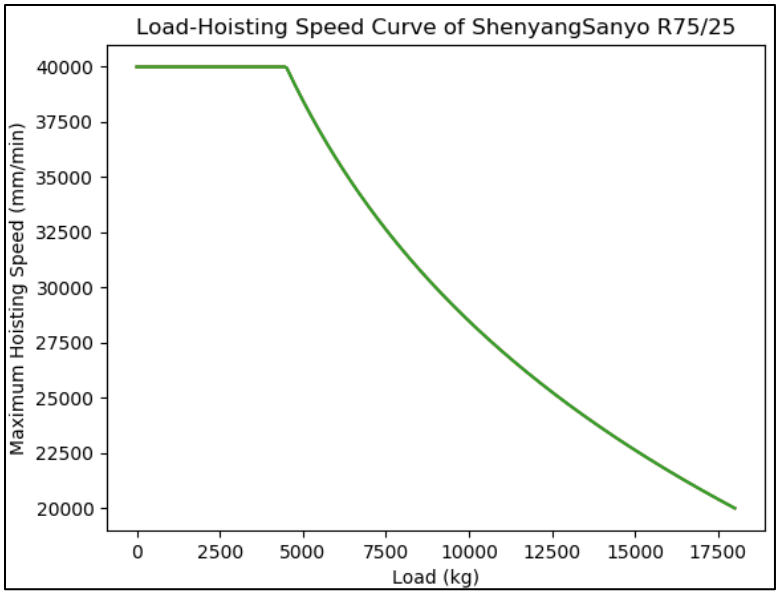

***Figure 18**: Load Hoisting Speed Curve of ShenyangSanyo R75/25*

The trolleying speed of the hook block ranges from 0 to 65 m/min. However, the crane operator has indicated that it never exceeds 60 m/min. This speed is unaffected by the weight of the load. The trolleying speed is only affected by the proximity of the object being lifted to the buildings, or other objects on site. An average of 30 m/min is used for the modelling.

The last crane parameter to be included in the model is the slewing speed of the tower crane. The crane has a maximum slewing speed of 0.8 rad/min, which is used during all operations since according to the crane operator, the speed is unaffected by the weight of the object being transported.

4.5 Site Model

Despite the presence of 3 cranes on the construction site, their position allows them to operate independently without any interference. Therefore, each crane is dedicated to one of the structures under construction. However, the convention center and the commercial blocks don't meet the requirements to be classified as high-rise buildings and are not included in the research. Due to the project being undertaken with a DB contract, the Bill of Quantity was only available to the contractor's team. Therefore, the quantities needed to build the model are extracted from the structural drawings.

4.5.1 Office Tower Model

The biggest and most resource intensive portion of the project is the main office tower which has G+48 floors. Each one of the 48 floors are divided into 4 work zones, as per the recommendation of the contractor and the consultant. A central location of each work zone is used to calculate the transport times. The structural steel is transported directly to 16 column locations which correspond to the location of the columns.

There are 3 types of formwork that have been utilized for the construction: steel formwork is used for the vertical members (columns and shear walls) while plywood formwork is used for the beams and slabs, and plastic formwork was used for the columns. Both the plastic and plywood formworks were light, especially when compared to the steel formworks. Due to the significant disparities in weight between the steel and other formwork materials, only the steel formworks are modelled [24].

The steel formworks are first washed and lubricated on the ground, before being lifted directly to the desired location. Like the steel columns, they are too heavy to be maneuvered without the tower crane. Once they are used, they are again brought back to the ground. This is unique because other materials such as reinforcement are transported to the desired location and don't return to the ground. The travel time is independent of the direction of

movement; therefore, the time take to lift the formwork to the top is simply doubled to find the total travel time for the two-way journey.

Compared to Ras Abebe Damtew St. which bounds the site from the west side, the main tower lies at a 27.18º angle. To simplify the creation of the Cartesian coordinate space, the building has been rotated by a similar amount counterclockwise.

The location of each of the materials to be transported using the tower crane is as follows:

***Table 3**: Location of Material Supply Points*

SUPPLY POINT	X LOCATION (mm)	Y LOCATION (mm)	Z LOCATION (mm)
Steel Columns	20830	80184	0
Reinforcing Steel	97834	36623	0
Formwork	24635	59247	0

The contractor hasn't imposed a minimum allowable distance between the crane and the building, but various operational guides state that the positioning must be such that the risk of collision is minimized. The Hong Kong Code of Practice for Safe Use of Tower Cranes imposes a 3-meter minimum clearance between the crane and the structure under construction [26]. This restriction has been placed on the CBE-HQP model.

In addition to a minimum 3-meter exclusion zone surrounding the building, there are several areas that are off-limits to the crane for a variety of reasons. These are:

- Two areas where the construction elevators have been installed;
- The bridge which connects the main tower to the convention center; and

The residential and office blocks have been omitted from the model because they are too far from the tower to act as constraints. The pictures of the CBE-HQP Main Tower below (see Figure 19 and 20) show the main constraints which affect the optimization result. The bridge which connects the office tower with the convention center, the exclusion zone that surrounds the building and the construction elevator are all visible.

***Figure 19**: CBE-HQP Main Tower, Crane and Construction Elevator Visible*

***Figure 20**: CBE-HQP Main Tower, Pedestrian Bridge, Elevator and Tower Crane Visible*

It isn't practical to transport the entirety of the reinforcing steel at once. In addition to safety concerns, the process of laying out the reinforcement happens in groups. For example, the bottom bars needed for a slab may be transported first, followed by the side bars, stirrups and top bars. In addition, each group of reinforcement is further divided into 2 batches. However, the formwork and structural steel are indivisible, and their weights have a significant impact in determining the location of the crane. The constraining effects of heavy indivisible loads such as the steel composite columns is discussed along with the other results.

4.6 Summary of Model

Based on the information requirements and flow charts outlined in Section 3.1, Sections 4.3, 4.4 and 4.5 have presented the information outlined in Section 3.1 which are necessary for the optimization process. The information has been reproduced in .csv files which are summarized in the following table:

***Table 4**: Summary of CBE-HQP Tower Inputs*

INFORMATION	PURPOSE	FILE NAME
Site Boundaries	Describes the boundaries of the construction site. It was unused because of the location of the tower in relation to the site's boundaries.	Test.csv
Off-limit Areas	Includes the location and size of areas which are infeasible as described in Section 4.5.1	OffLimitAreas.csv
Demand Points	The x and y coordinates of the demand points along with the required loads	NewWZ.csv
Supply Location	The points on the ground from where the loads are lifted.	Supply.csv
Floor Heights	The z coordinates of each floor are listed.	FloorHeights.csv

The files outlined in the table above are imported into Python to create the computer model which accurately represents the site conditions. The model in Python created by the above inputs is shown in Figure 21:

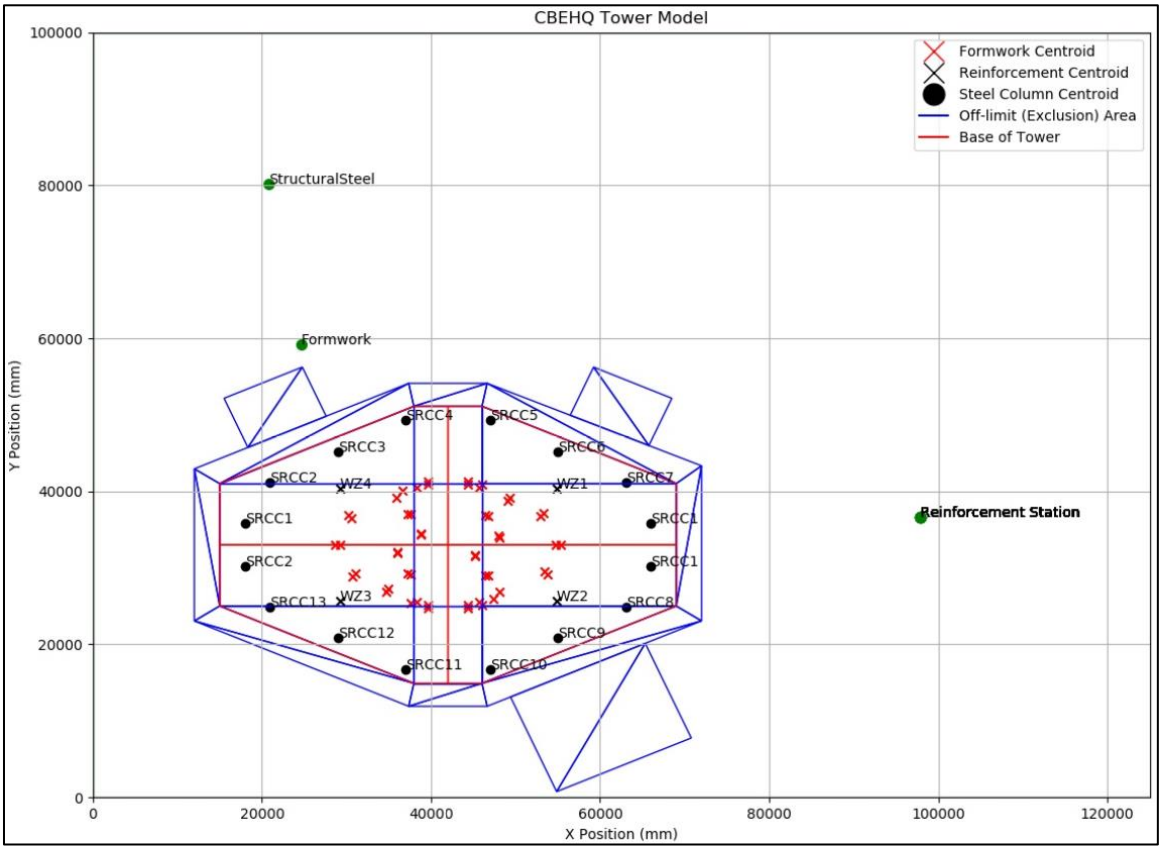

***Figure 21**: CBE-HQP Tower Model*

4.7 Optimization and Results

The first half of this section deals with the tuning of the parameters for the PSO algorithm. The number of particles, number of iterations, local and global weights are tuned to ensure convergence and efficiency. Following this process, the results of the optimization are presented.

4.7.1 Parameter Tuning

The accuracy of the result and the convergence was tested for different values of the number of particles, maximum number of iterations, maximum velocity, local weight, global weight and omega. The algorithm initially creates 50 particles which satisfy the constraints that have been previously defined. By beginning the search within the feasible region, the algorithm saves computational power and time. As discussed in the literature review, a maximum of 60 particles is recommended, but such an increase didn't produce any improvement in results, and instead increased the computational load. Table 5 summarizes the parameters to be used by the PSO algorithm.

***Table 5**: PSO Algorithm Parameters*

NUMBER OF PARTICLES	50
MAXIMUM NO. OF ITERATIONS	30
LOCAL WEIGHT	2.1
GLOBAL WEIGHT	1.8
MAXIMUM VELOCITY	5000
ω	0.6

Using the above parameters, a reasonable degree of accuracy was achieved with regards to the results which are presented below. This approach will be employed on the other projects presented in Chapter 5.

4.7.2 Optimization Results

The results below have been quoted to the nearest tenth of a millimeter, which is of sufficient accuracy for the site planning purposes. Similarly, the travel time has been quoted to the nearest tenth of a minute. Tables 6 and 7 present the optimal location without inclusion of an anchoring requirement. While Tables 8 and 9 present the results when an anchoring requirement has been imposed.

Without an anchoring requirement, the optimal location was found to be at (47495.3, 55623.5) where the travel time was calculated to be 287797.108 minutes. When the anchoring requirement is imposed, the optimal location shifted to the left, with the optimal location found at (42167.1,56942.3) and the travel time increased to 298036.644 minutes. This is an increase of 10239.536 minutes.

Figures 22 and 23 shows a graphical representation of the results presented in Tables 6,7,8 and 9. For all the case studies presented, the results of 10 optimization runs are used to ensure that the PSO module is able to converge towards the optimal location. The mean, standard deviation and coefficient of variation of the 10 optimization runs is calculated to verify that the algorithm performed as designed with minimal variations between runs. Lower coefficients of variation indicate greater stability and confirm that the tuning of the PSO algorithm was successful. However, it should be noted that as a stochastic optimization technique, it is impossible for the results to be identical between runs.

For the CBE-HQP case study, the results were stable, and the only exception was Run 7 on Figure 22 and Run 5 on Figure 23. In both cases the travel time was higher than other runs, as shown by the spike in the graph. The increase is associated with changes in the *x* and *y* position of the optimal location, which indicates that the algorithm converged towards a local rather than a global minima.

Tables 7 and 9 show the effects that small changes in distance have on the travel time. The most extreme example is under the no anchoring requirement scenario. Table 9 shows that a change in distance of 51.9 mm in the x direction resulted in a 96-minute change in the total travel time. In practice, such small changes are immaterial during site planning.

***Table 6**: CBE-HQP Tower Results, No Anchoring Constraint*

RUN NO.	1	2	3	4	5	6	7	8	9	**10***	μ	σ	μ/σ (%)
X (MM)	47492.4	47473.6	47494.5	47477.4	47497.1	47490.0	47488.1	47413.4	47459.7	**47495.3**	47478.152	24.317	.051
Y (MM)	55625.9	55628.9	55623.6	55627.9	55622.0	55625.8	55629.6	55684.6	55653.6	**55623.5**	55634.552	18.757	.034
TIME (MIN)	287801.335	287843.392	287798.964	287835.391	287794.585	287807.249	287807.378	287923.323	287847.775	**287797.108**	287825.650	37.68	.013

* *Optimal Result*

***Table 7**: Summary of Results, CBE-HQP, No Anchoring Constraint*

MIN X LOCATION (mm)	47413.4	**MIN Y LOCATION (mm)**	55622.0	**MIN TRAVEL TIME (min)**	287797.108
MAX X LOCATION (mm)	47497.1	**MAX Y LOCATION (mm)**	55684.6	**MAX TRAVEL TIME (min)**	287923.323
Δ X LOCATION (mm)	83.7	**Δ Y LOCATION (mm)**	62.6	**Δ TRAVEL TIME (mm)**	126.215

***Table 8**: CBE-HQP Tower Results, No Anchoring Constraint*

RUN NO.	1	2	**3***	4	5	6	7	8	9	10	μ	σ	μ / σ (%)
X (MM)	42165.8	42154.5	**42167.1**	42167.0	42167.1	42153.2	42115.2	42166.5	42165.8	42166.9	42158.9	16.257	0.039%
Y (MM)	56942.1	56944.5	**56942.3**	56936.0	56941.7	56949.5	56942.0	56925.3	56940.0	56937.1	56940.1	6.390	0.011%
TIME (MIN)	298039.545	298059.378	**298036.644**	298044.544	298037.438	298061.694	298132.740	298038.254	298060.171	298039.086	298055.027	29.130	0.010%

* *Optimal Result*

***Table 9**: Summary of Results, CBE-HQP, No Anchoring Constraint*

MIN X LOCATION (mm)	42167.1	**MIN Y LOCATION (mm)**	56942.3	**MIN TRAVEL TIME (min)**	298036.644
MAX X LOCATION (mm)	42115.2	**MAX Y LOCATION (mm)**	56942.0	**MAX TRAVEL TIME (min)**	298132.740
Δ X LOCATION (mm)	51.9	**Δ Y LOCATION (mm)**	0.3	**Δ TRAVEL TIME (mm)**	96.096

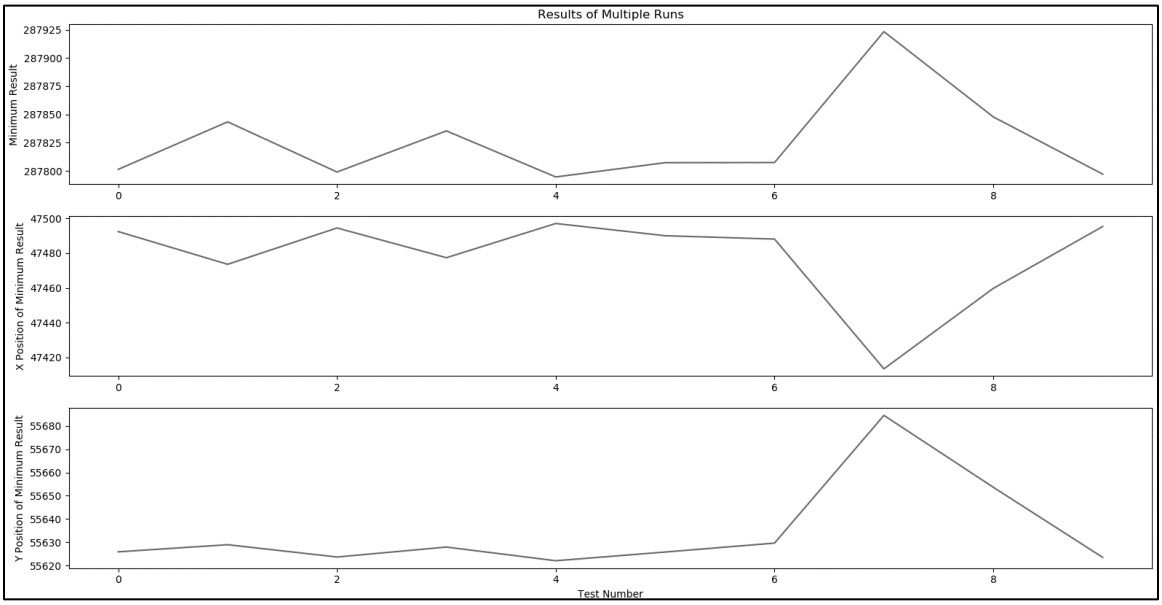

***Figure 22**: CBE-HQP Optimization Results, No Anchoring Requirement*

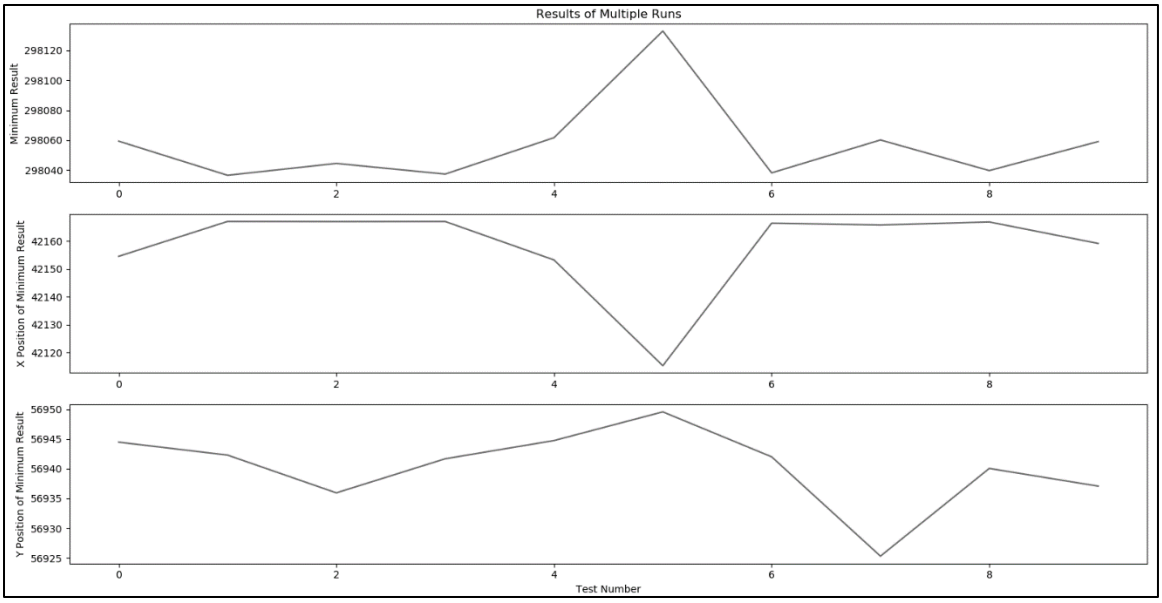

***Figure 23**: CBE-HQP Optimization, With Anchoring Requirement*

For the run without an anchoring requirement, the results appear to have great variations, but the coefficients of variation show otherwise. The coefficients of variation for the positions and the travel time are .051%, .034%, and .013% respectively, which shows the results are stable.

The clustering of multiple local minima in the feasible region means that small changes in position (< 100 mm) lead to changes in the value of the objective function by 120 minutes. Similar effects were seen when the anchoring requirement was imposed. However, the anchoring requirement has reduced the variation of the results. This shows that the PSO algorithm has succeeded in finding the optimal location repeatedly, and that the selected parameters have been proven correct.

Figure 24 provides visual evidence of the results generated using the OM as both optimal locations are within the intersection of the circles representing the maximum lifting radius for the steel columns, reinforcement and steel formworks.

The lifting radii for the reinforcement and the formwork have been omitted to improve the clarity of the drawing. The reinforcement is a divisible load, which allows it to utilize the 60m jib in its entirety and need not be shown. The heaviest piece of formwork is 2924.1 kg, and the maximum radius for this load is also 60m.

The drawing illustrates the shift in the optimal location upon imposition of an anchoring constraint. The crane’s location shifts towards a position that closely approximates the actual location of the crane on the construction site.

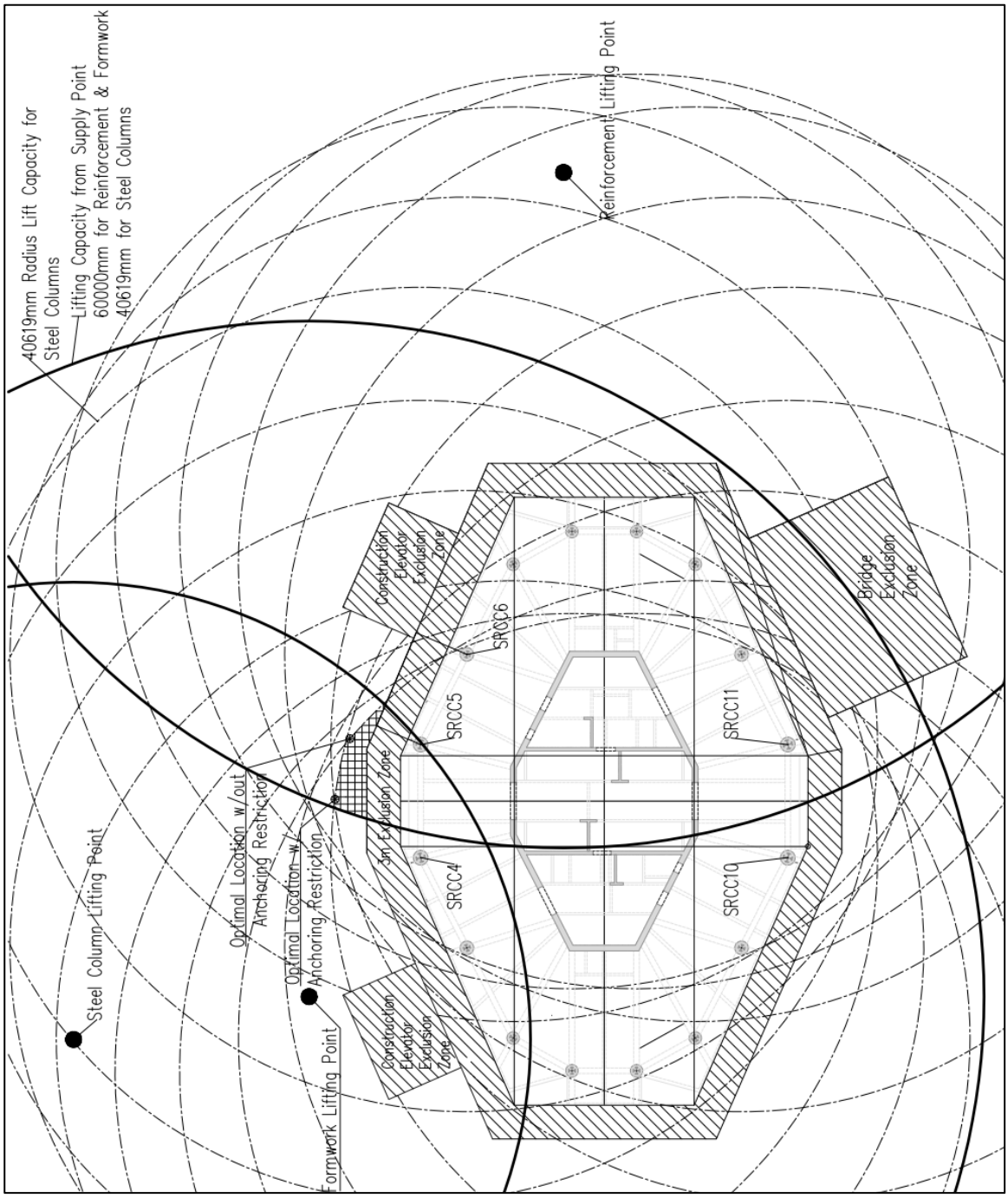

***Figure 24**: CBE-HQP Tower Optimization Results, With and Without Anchoring*

4.8 Analysis and Discussion

During an early introductory visit to the CBE-HQP site, the contractor indicated that their chosen location for the main tower crane is the only feasible location and that the results of this thesis could not be any different. As the contractor predicted, the results of the optimization have validated the assertions made by the contractor that the chosen location is optimal.

The simple technique used in Figure 24 to visualize the feasible region was used by the CSCEC engineers to determine the feasible region and place their crane. Since the crane is anchored to the columns, there is no possible location for the tower crane other than the location chosen by the contractor.

The first set of results, which don't include the anchoring requirement resulted in the optimal location being close to Steel Reinforced Concrete Column 5 (SRCC5). But this point would have been infeasible in practice since it is impossible to anchor it to 2 columns as required. With slight modification which restricted the feasible region only to locations which are equidistant from 2 columns, the result approximates the actual location on the construction site.

As Figure 24 shows, the crane could have also been anchored between SRCC10 and SRCC11, but the feasible region is restricted further by the circles drawn from the supply points, making that area infeasible. The shape of the structure also makes other locations infeasible because along the x-axis, the structure is 60m wide when including the exclusion zone, compared to 42.2 meters along the y axis. When taking all the factors into consideration, the only feasible region is the dotted area on the upper region. Both locations that were found using the PSO algorithm are found within this region.

While the anchoring requirement had a significant impact on the results of the optimization, another factor which greatly affected the location was the weight of the steel columns. The combination of the heavy steel columns, which could only be moved to 40619 mm along the crane's jib, and the distance between the supply point for the steel columns and reinforcement severely restricted the feasible region.

If a crane with a higher capacity in terms of both maximum load and jib length was used instead of the Shenyang-Sanyo R75/25, it would have been possible to enlarge the feasible region, allowing the contractor to anchor the crane between another pair of columns. For example, for the crane that the contractor used, its lift radius for a 6.898-ton object was only 40619 mm, even though the crane has a capacity of 60000 mm. This represents only 67.7% of the total capacity of the crane.

On the other hand, if the Liebherr 630 EC-H 40 crane introduced in Chapter 3 was used for the project, the radius for the same load would be 47259 mm, which is 78.77% of the crane's total capacity. Even though the crane has the same physical jib length, the extra lifting capacity would have allowed the distance the steel column can be moved along the jib to increase.

This would have given the contractor a greater degree of freedom when positioning the crane when compared to the chosen tower crane. As Figure 25 shows, the use of the Liebherr 630 EC-H 40 has expanded the feasible region allowing for the inclusion of locations which allow anchoring to columns SRCC5 and SRCC6. For comparison, the original feasible region is shown in the crosshatch.

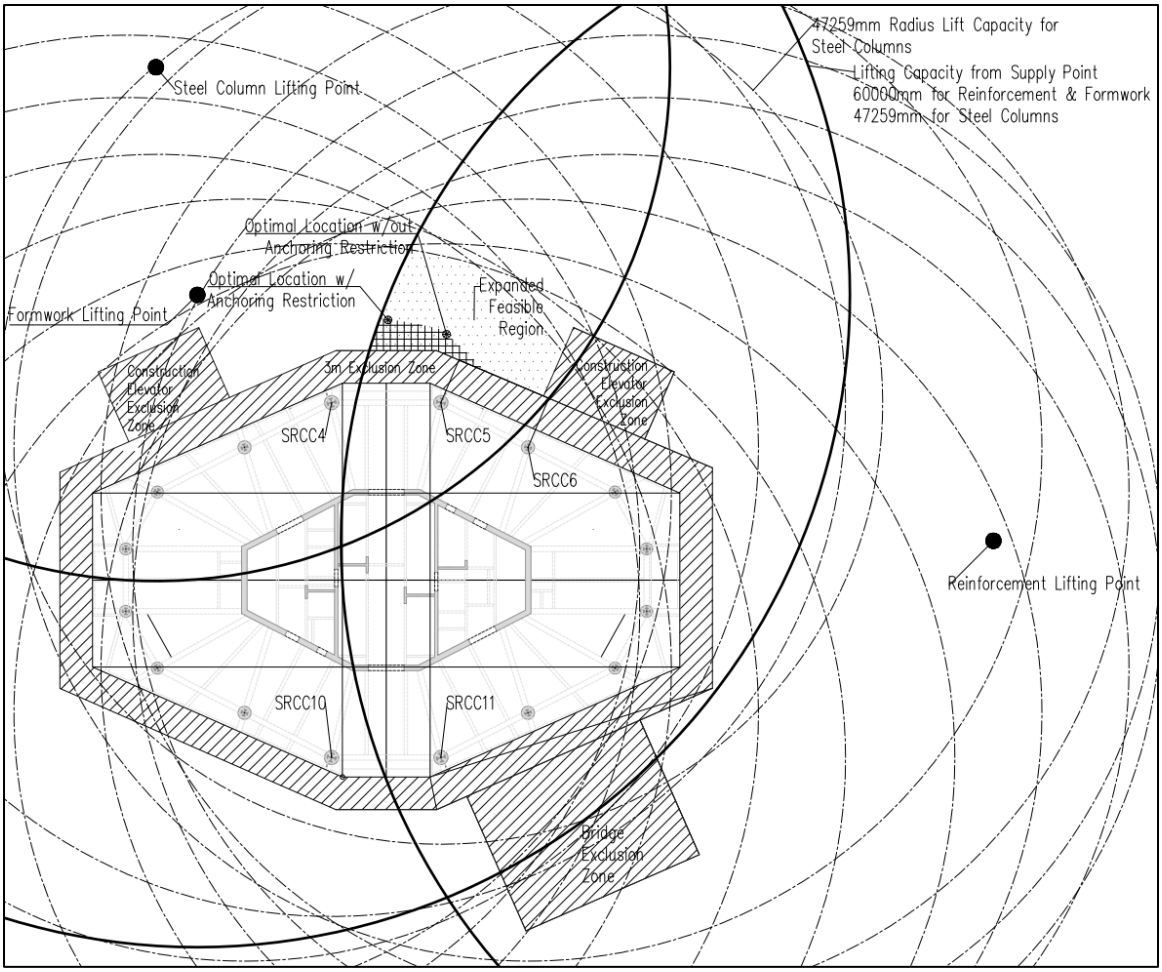

***Figure 25**: CBE-HQP Tower Feasible Regions Based on Liebherr 630 EC-H 40*

In conclusion, the suitability of the location chosen by the contractor for the tower crane has been verified by the optimization, given the currently available crane. However, the crane's maximum capacity was close to the demands of the project, which limits the ability of the contractor to freely place the tower crane. Instead, if as shown by Figure 25, a higher capacity crane is used, the area of the feasible region could be expanded along with the options available to satisfy the anchoring requirement.

The second aim of the chapter has also been met. The PSO algorithm and the other supporting functions have functions as expected, and the parameters of the PSO algorithm have been found.

5. MODELLING AND OPTIMIZATION OF SELECTED SITES

While the number of projects which use tower cranes in Addis Ababa is relatively small, time limitations do not allow the inclusion of all of them. Therefore, a group of projects have been selected for the optimization based on the criteria that have been discussed previously. The processes outlined in Chapter 4 is applied on the selected projects to calculate the optimal location of tower cranes.

In addition, some of the projects have been selected for their unique features. For example, the ZB-HQP building has a changing cross-sectional area, while NIB-HQP and UB-HQP both feature elliptical floors. Some of the projects also utilized unique construction techniques which affected the crane's utilization such as NI-HQP, NIB-HQP, ZB-HQP and UB-HQP, which used their cranes to transport concrete for their columns. On the other hand, Marriott Hotel, used the tower crane for transportation of all its concrete.

The contractors featured in this chapter are also a mix of local and foreign firms. NI-HQP is being built by an Ethiopian contractor, while the remaining projects are being were built by Chinese contractors. Apart from Marriott Hotel, the other projects are all located within the new Financial District in Lideta Sub-City and will serve as the headquarters for some of Ethiopia's financial institutions.

One common theme among all the projects is the use of reinforced concrete and the requirement necessitate that the cranes be anchored to the structure under construction and since the cranes have all exceeded their maximum unanchored height, requiring anchoring to either beams/slabs or columns.

The final 2 projects to be analyzed feature unique elliptically shaped floors. Modelling curved objects requires a large number of triangles, and this leads to an increase in the computational power necessary to produce an output.

The projects summarized in Table 10 have been selected as case studies:

***Table 10**: Summary of Selected Projects*

	PROJECT NAME	BUILDING HEIGHT (m)	SLEWING TYPE	CRANE TYPE	ANCHORING	MATERIALS LIFTED
1	Nib Intl. Bank HQ	122	Top Slewing	Zoomlion T7015-10E	Slab	Concrete, Reinforcement
2	Nile Insurance S.C. HQ	97.4		Zoomlion TC5013B-6	Column	Concrete, Reinforcement
3	United Bank HQ	133		Zoomlion TC5013B-6	Slab	Concrete, Reinforcement, Cooling Towers
4	Zemen Bank HQ	130		Zoomlion TC6513	Beam or Slab	Concrete, Reinforcement
5	Marriott Hotel*	67.5		Soima 6015TL	Slab	Concrete, Reinforcement

** The Marriott Hotel project is located away from the Financial District; the results are presented separately in Appendix 6.*

5.1 Nile Insurance S.C. Headquarters Project

Located in the Financial District, along with other Ethiopian financial institutions, the Nile Insurance Headquarters Project (NI-HQP) project is a G+25 building with a height of 97.4 meters and a total cost of approximately 1 billion ETB. The contractor for the project is Rama Construction PLC, a local Grade 1 contractor. making it one of the only high-rise structures in the area being constructed by an Ethiopian contractor. The consultant for the project is Wossen Architects PLC. As of January 2019, all the structural works have been completed, and the contractor has begun finishing works.

5.1.1 Background and Model Information

The project is composed of 2 parts: A G+25 tower (Block A) which will serve as the Nile Insurance S.C. HQ and a G+5 commercial wing (Block B). The tower crane is expected to serve both wings; therefore, the commercial block must also be included in the optimization process even though it doesn't meet the requirements for a high-rise building. However, it has been rendered off-limits to the crane's base because it cannot be anchored to it.

The first part of the model is the site boundaries. The actual site, as shown in the drawings is small, and the building occupies a significant proportion of the space available on site. This forced the contractor to obtain permission from the city administration to temporarily expand the site to allow for the construction of temporary facilities. Even with the extra space available, the area available for the placement of the tower crane is small. The placement of the offices, storage sheds and material storage areas further reduce the space available and limits the areas where a tower crane can be placed in terms of safety, noise and other considerations.

Due to the severe restrictions on available space, the site boundaries can affect the optimal location unlike the CBE-HQP model where the boundaries of the site are too far away from the edges for them to have any impact. There are also several areas which are off-limits to

the tower crane such as the offices for the contractor and the consultant, as well as the storage sheds that have been included in the model.

The project has been served using 2 cranes. The crane initially brought to service the structure couldn't meet the requirements of the project due to capacity limitations and was replaced after the completion of Block B. The second crane brought in was a Zoomlion TC5013B-6, which has a maximum capacity of 6 tons and 1.3 tons at the tip of the jib with a 50-meter jib length configuration.

As with the previous model for the CBE-HQP, this model contains 5 parts. The site layout drawing on the following page (Figure 26) shows the current and future site boundaries, with the building and the temporary facilities present.

The drawings and BOQ presented in Figure 26 are courtesy of Wossen Architects PLC.

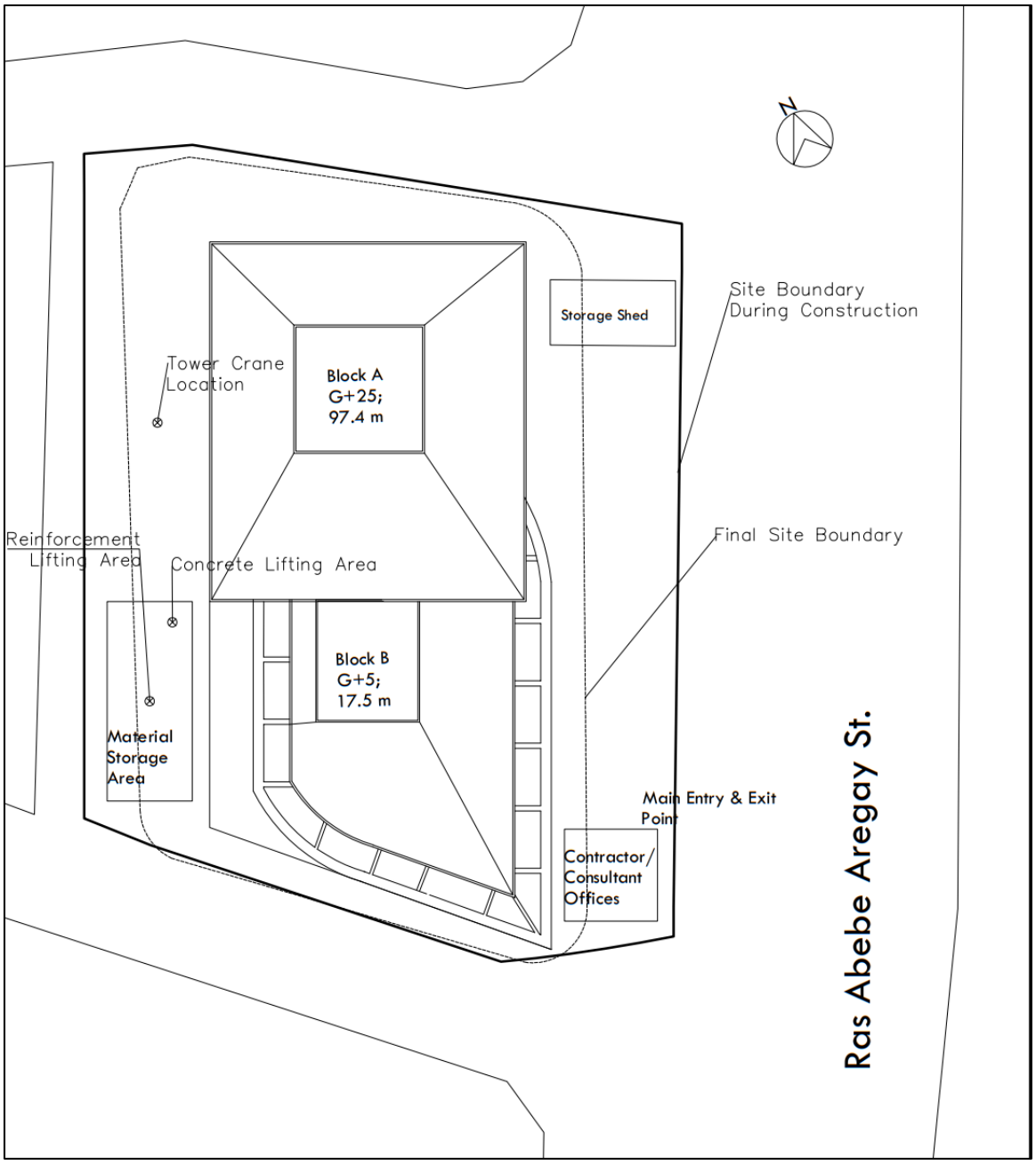

***Figure 26**: NI-HQP Site Plan*

5.1.2 Crane Utilization

The contractor indicated that the tower crane was used for the transport of the concrete and reinforcement only. The formwork was never brought to the ground for cleaning and was instead moved by the daily laborers from each floor to the next.

The reinforcement requirement is based on the information provided by the consultant. The BOQ provided included the total reinforcement requirement for the construction of the super-structure. Based on this quantity and the total floor space of the building, the average quantity of steel in terms of $\frac{kg}{m^3}$ is calculated. The reinforcement allocated to each floor is based on the average quantity of steel and the floor area.

Block A is divided into 4 work zones, while Block B is composed of 3 working zones, and the required reinforcement is delivered to the centroid of each zone. This mimics the methodology employed by the contractor whereby the reinforcement is transported in batches that are then arranged before the next batch is transported up. On the other hand, the concrete must be transported to the exact location where it is needed. This requires 16 demand points on each floor.

The NI-HQP building has a total floor area of 28747.4 m^2. According to the BOQ, the total reinforcement used in the construction of the superstructure is 1,087,888.35 kg [27]. Based on this information, the average quantity of steel is found to be 37.84 $\frac{kg}{m^2}$. Each floor in Block A has an area of 979.95 m^2, while each floor in Block B has an area of 849.73 m^2. Using this information, and the floor area of the building, the total quantity of steel required for the construction of each floor is calculated. The quantity of steel is calculated to be as follows (Table 11):

***Table 11**: Reinforcement Requirements*

BLOCK	FLOOR AREA (m^2)	QTY. OF REINFORCEMENT PER FLOOR (kg)	NO. OF FLOORS	TOTAL (kg)
Block A	979.95	37081.31	25	927032.75
Block B	849.73	32153.78	5	160768.92

The concrete requirement was calculated based on the dimensions of the columns. The concrete used for the columns was produced on site and transported using a 0.5 m^3 capacity bucket. The concrete used was normal weight C40 concrete with a density of 2400 $\frac{kg}{m^3}$. The empty bucket weighs 100 kg.

According to the structural drawings, there are 3 different column types used, 2 of the columns have rectangular cross-sections and 1 has a circular cross-section. However, the column height is constant at 3.5 meters. Table 12 summarizes the concrete requirements and the number of trips that need to be made to fulfil them.

***Table 12**: Summary of Columns Used for NI-HQP*

COLUMN NAME	CROSS-SECTION	LOCATION	DIMENSIONS (mm X mm) or (mm)	VOLUME OF CONCRETE (m^3)	NUMBER OF TRIPS
C1	Square	Block B	500 x 500	0.875	2
C2	Circle	Block B	Radius = 400	1.8	4
C3	Rectangle	Block A	800 x 1000	2.8	6

Figure 27 shows the transportation of concrete using the tower crane and a bucket to cast columns for the 18th floor of Block A.

***Figure 27**: NI-HQP Concrete Transportation with Crane and Bucket*

5.1.3 Summary of Model

As with the CBE-HQP model, the information required is imported into the OM using 5 csv files.

In addition to the off-limits areas that correspond to objects on the site, an area labelled Crane_Exclusion_Zone is added to the off-limit areas. This prevents the optimal location from being close to Block B which would make it unanchorable since the building is only 17.5 meters tall while the crane requires anchoring every 17.5 meters once it exceeds its free-standing height of 49 meters. The exclusion zone also prevents the crane from being located next to the entry/exit point.

For the site boundaries, the irregular shape of the site meant that it had to be divided into 5 triangles to ensure it conformed to the requirements of the algorithms used to check for inclusion and exclusion of points. The demand information discussed in Section 5.1.2 is combined with the exact coordinates at which the materials are required and entered into the model using a csv file.

The material storage area in the top-left corner is an open-air storage location where aggregates, water tankers, steel, waste and other materials are stored. The contractor also produces the concrete on site in the area labelled Material Storage due to its proximity to the raw materials required for concrete production. Both supply points are located within the material storage area and the area has been made into an exclusion zone since the crane cannot be placed within the storage and concrete production area.

The floor-to-floor height of the building is 3.5 meters, and this height is used for the entirety of Block A and B. The FloorHeights.csv file contains the names and heights of each of the 25 floors that make up the building. As with the CBE-HQP model, a 3-meter exclusion zone is included, and the base of the crane is assumed to have a dimension of 3 meters by 3 meters.

Table 13 summarizes the information used in the creation of the NI-HQP model.

***Table 13**: Summary of NI-HQP Model*

INFORMATION	PURPOSE	FILE NAME
Site Boundaries	The boundaries of the NI-HQP sites are used to ensure the location is within the site. The site has been broken down into a series of triangles.	NI-HQP_SITE_BOUNDS.csv
Off-limit Areas	Includes the location and size of areas which are infeasible including offices, sheds, material storage areas and impractical areas for crane placement. A second file allows for the inclusion of the skylight within the feasible region.	OffLimitAreas_NI-HQP_NoSkyLight.csv
Demand Points	The x and y coordinates of the demand points along with the required loads.	WorkInfo_NI-HQP.csv
Supply Location	The points on the ground from where the loads are lifted.	Supply.csv
Floor Heights	The z coordinates for each floor is listed.	FloorHeights.csv

Based on the information presented in the table above, the Python model shown in Figure 28 has been created. This model is based on OffLimitAreas_NI-HQP_NoSkyLight.csv, and doesn't include the skylight within the feasible region.

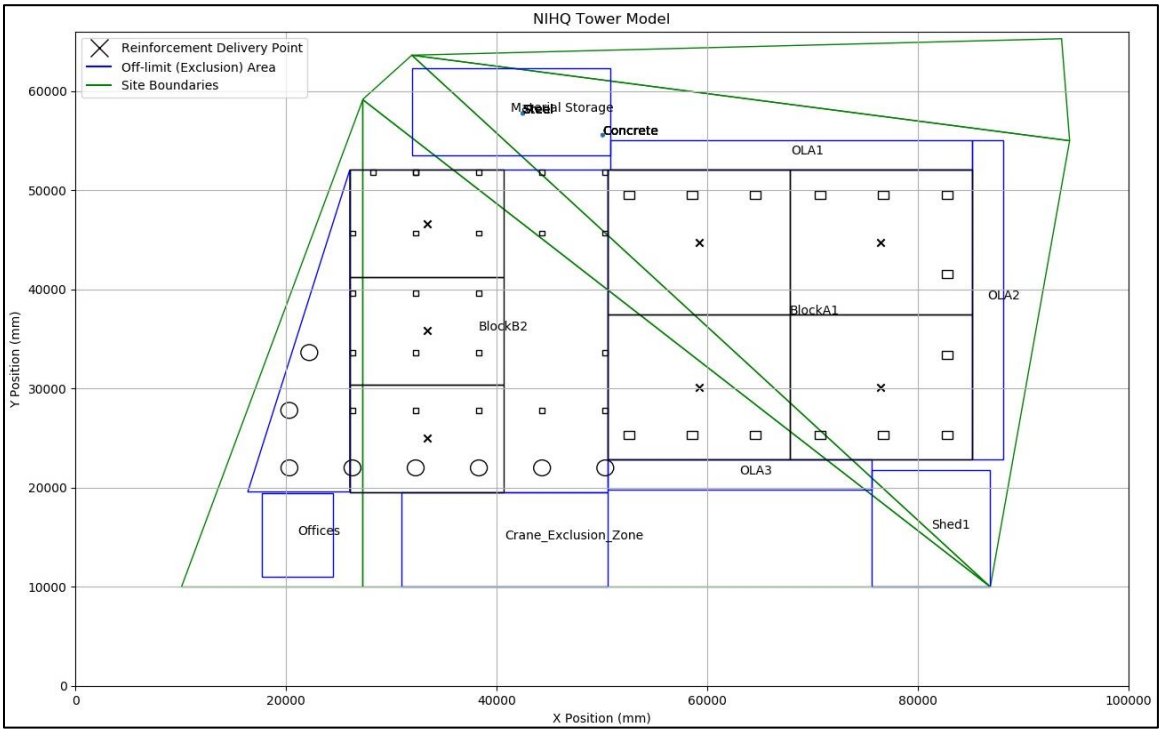

***Figure 28**: NI-HQP Site Model*

5.1.4 Optimization Results

The NI-HQP optimization is performed under the following scenarios:

- Scenario A: The Zoomlion crane is used for the entire duration of the project;
- Scenario B: The Zoomlion crane is used only for the construction of Block A; and
- Scenario C: The skylight in Block B is made available for the placement of the tower crane with both Block A and B constructed using the crane.

Since the Zoomlion tower crane was brought in after the completion of Block B, Scenario B is the one that most closely approximates the events on site. On the other hand, Scenario A assumes that the appropriate crane was brought in at the start of the project. Scenario C is purely theoretical and is performed because of the potential benefits that can be derived from placing the tower crane within the structure, especially for cramped sites.

The first crane that was brought in has been excluded in any of the modelling and optimization because it lacks the capacity to serve either block fully. The circles that correspond to the lifting radius of the crane has been omitted in the drawings to improve clarity. Instead the feasible regions are only shown.

The results are presented in the tables and figures on the following pages. Table 14 and Figure 29 present the results of Scenario A, Table 15 and Figure 30 present the results of Scenario B, and Table 16 and Figure 31 present the results of Scenario C.

Except for Run 1 under Scenario A and Run 8 under Scenario B, the results showed remarkable stability. In the case of Scenario B, the algorithm converged to the same optimal location on all runs except Run 8. Similarly, under Scenario C, the results showed remarkable stability, except under Runs 1 and 9, which a small change in the position led to an increase in the travel time. Again, this suggests the presence of nearby local minima that the algorithm converged to erroneously.

Figure 32 shows the optimal location on site, in addition to the constraints and supply points present.

***Table 14**: NIHQ Optimization Results, Scenario A*

RUN NO.	1	2	3	4	5	6	7	**8***	9	10	μ	σ	μ / σ (%)
X (mm)	52068.7	52061.7	52061.7	52061.5	52062.6	52061.6	52062.4	**52061.5**	52061.5	52061.5	52062.5	2.1111	4.055E-3
Y (mm)	18343.5	18343.6	18343.5	18343.6	18363.6	18343.6	18343.6	**18343.6**	18343.6	18343.6	18343.6	.0311	.167E-3
TIME (min)	33383.149	33383.118	33383.124	33383.119	33383.121	33383.121	33383.212	**33383.117**	33383.118	33383.118	33383.122	.0089	.027E-3

** Optimal Result*

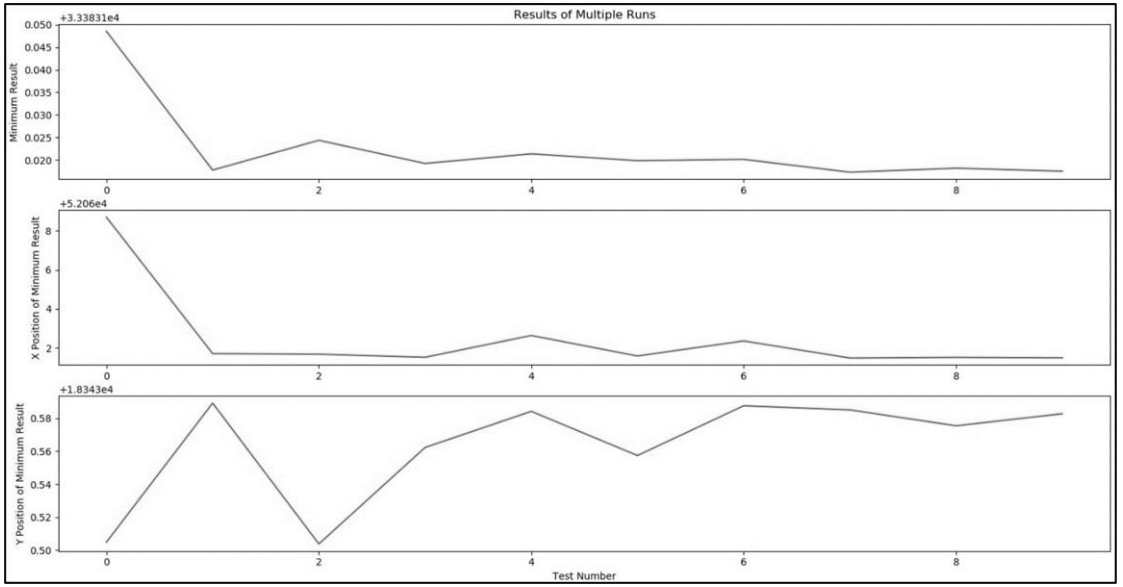

***Figure 29**: NIHQ Optimization Results, Scenario A*

***Table 15**: NIHQ Optimization Results, Scenario B*

RUN NO.	1	2	3	4	5	6	7	8*	9	10	μ	σ	μ / σ (%)
X (mm)	69879.9	69879.9	69879.9	69879.6	69879.8	69879.9	69879.9	70903.9	69879.9	69879.8	69879.8	.095581	.14E-3
Y (mm)	56563.6	56563.6	56563.6	56564.3	56563.6	56563.6	56563.6	58016.0	56563.6	56563.6	56563.7	.21999	.39E-3
TIME (min)	17101.398	17101.398	17101.398	17101.405	17101.399	17101.399	17101.398	17118.723	17101.398	17101.398	17101.399	.00216	.0126E-3

** Optimal Result*

** Run no. 8 has been omitted from further calculations because it is an anomaly compared to the other runs. All results other than Runs 4 & 8 are identical.*

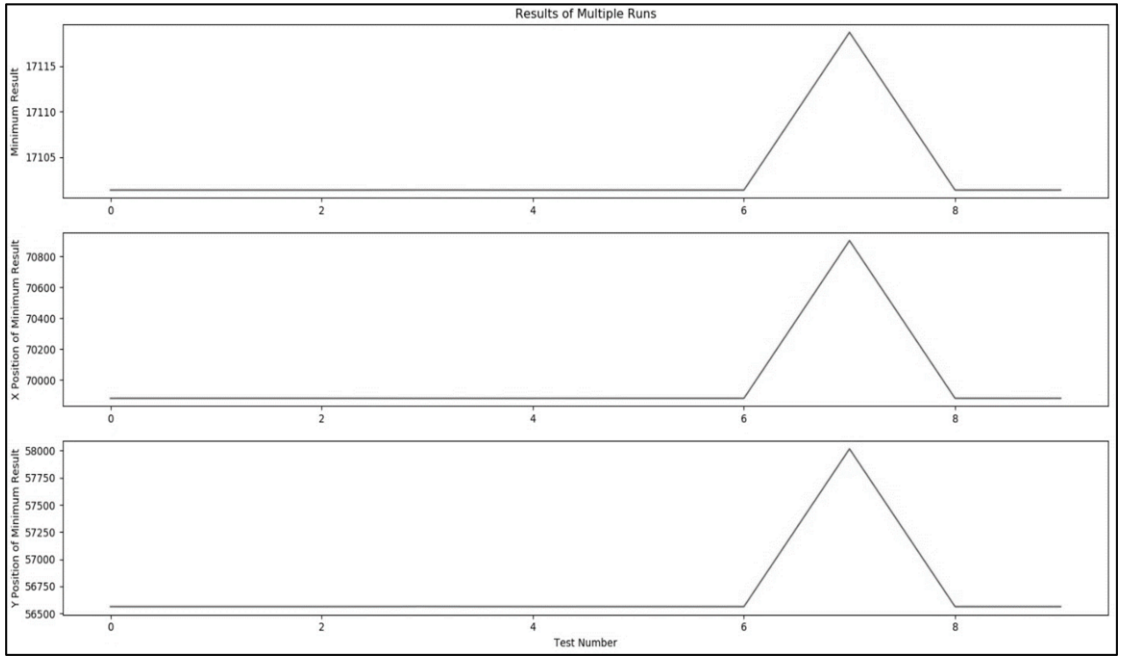

***Figure 30**: NIHQ Optimization Results, Scenario B*

***Table 16**: NIHQ Optimization Results, Scenario C*

RUN NO.	1	2	3	4	5	6	7	8*	9	10	μ	σ	μ / σ (%)
X (mm)	49057.5	49061.2	49061.2	49061.2	49061.2	49061.2	**49061.2**	49061.2	49058.2	49061.2	49060.5	1.3546	2.76E-3
Y (mm)	36659.7	36592.5	36505.5	36503.9	36638.0	36558.3	**36505.2**	36505.8	36515.5	36513.3	36549.6	56.9373	155.78E-3
TIME (min)	31949.595	31949.247	31949.189	31949.189	31949.272	31949.224	**31949.188**	31949.188	31949.369	31949.193	31949.265	.1226	.384E-3

** Optimal Result*

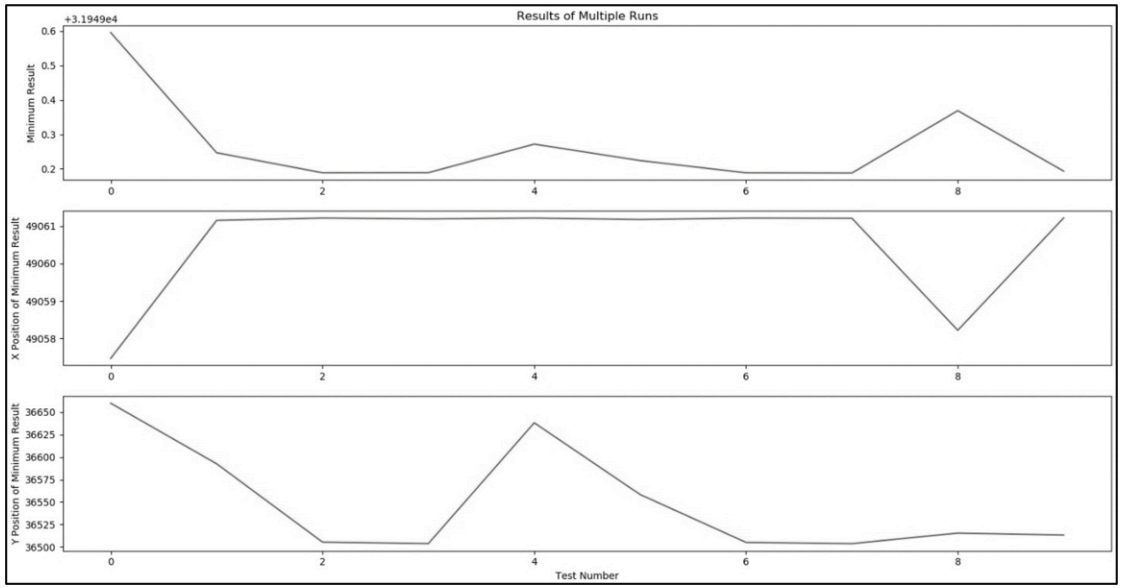

***Figure 31**: NIHQ Optimization Results, Scenario C*

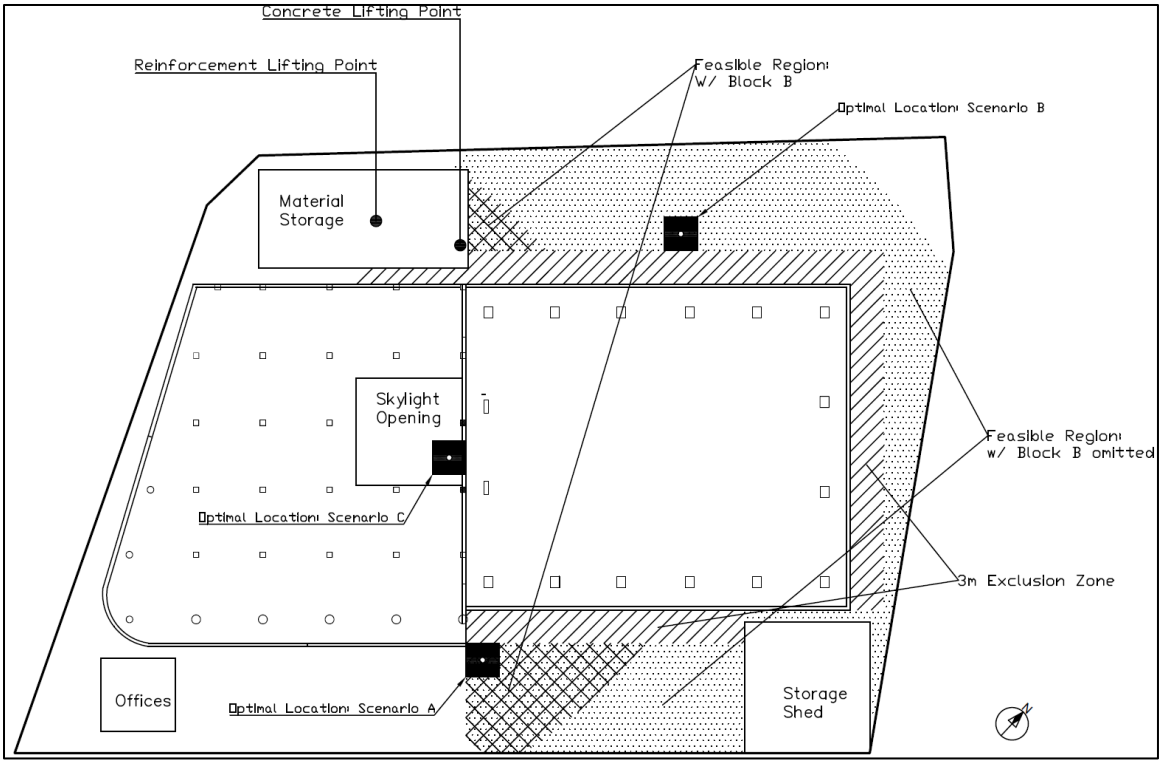

***Figure 32**: NI-HQP Optimization Results, Scenarios A, B and C*

The optimization resulted in remarkably accurate results, with most of the coefficients of variation in the order of a thousandth of a percent. This is especially true for the optimization done under Scenario B with all results except Run 8 having nearly identical results. Run 8 has been omitted from the calculations of the mean and standard deviation due to this fact.

The tuning of the parameters performed previously has allowed the algorithm to converge towards an optimum location on all the iterations with few outliers.

5.1.5 Discussion

Under Scenario B, which approximates the actual utilization of the crane most accurately, the results are very close to where the crane was located on the site. The contractor's choice to place the crane at the center of Block A is justified because it can have equal reach to all the demand points. The crane's jib length is more than enough to service Block A and can reach all the supply and demand points without getting to the end of the jib. Therefore, the 50-meter jib length configuration can be thought of as being excessive considering the site layout and desired use of the crane.

For Scenario A, where the crane is used to service both Block A and B, the optimal location is found to be at the center of the Eastern side of the building, near where Blocks A and B meet. This is a logical location to place the crane because it is equidistant from most demand points in both blocks.

The final case, where the opening for the skylight is a feasible location has further reduced the travel time compared to the second scenario. The minimum travel time was reduced by 1433.93 minutes when compared to scenario A. At this position, which is near the geometric center of the structures the distances from the crane to any of the demand and supply points becomes very similar. This reduces the number of cases whereby the item being lifted must be trolleyed to the end of the jib, where the crane's capacity is smaller**.** The potential benefits of placing the crane within the structure must be balanced against the costs associated with the decision, especially in terms of erection and dismantling costs.

Scenario B validates the decision by the contractor to place the Zoomlion crane at the chosen location. The actual location shifted slightly to the North-East so that the crane can be anchored to the columns. The omission of Block B from the optimization leads to a significant increase in the feasible area, as shown in Figure 30. While locations that are far from the structure are infeasible due to the anchoring requirements, there is still an increase in the feasible area.

The increase in the feasible region results from the removal of the columns located at the extreme ends of Block B that restrict the tower crane. According to the contractor, this location was chosen specifically because it was at the center of the building, allowing equal reach to all points. Since Block B wasn't under consideration, the selection procedure by the contractor focused solely on the requirements of Block A.

While it is possible to place the tower crane at the symmetrically opposite point, that area was occupied by the first tower crane at the time of erection for the Zoomlion crane. Like the CBE-HQP case, the increase in the feasible region increases the degree of freedom the contractor has in choosing a location.

The contractor's decision-making process for the selection of a location for the first crane was done in a haphazard manner. At the time of the installation of the first tower crane, the only crane available was the 30-meter crane, and the contractor decided to use it for the initial stages of the project despite knowing that it didn't have sufficient capacity to complete the project. The crane was also placed while the contractor was working on the foundation. This means that the contractor couldn't place the crane's base close to the structure. Therefore, the crane was placed too far from the building, rendering it unanchorable.

Two points of interest were discussed with the contractor during a brief follow up interview with engineers from Rama Construction. The first was the decision to not place the crane within the skylight. While the engineers understand that there are potential benefits to placing the crane within the building, they are reluctant to do so. Like many other local contractors, Rama Construction has never placed a crane within a building before and the lack of experience makes it harder to use the crane within the structure, and more importantly dismantle it after the completion of the project [28].

The second point of interest was the losses incurred by the contractor while it erected the Zoomlion crane and the reason behind the poor location of the first crane. While the actual costs haven't been quantified by the contractor or consultant, work was suspended for 15

days, during which the contractor assigned its daily laborers to tasks which weren't value generating such as site cleaning.

The contractor's experience illustrates the potential benefits that could be accrued had the selection of a crane been based upon the appropriate capacity and erection on the correct location. The contractor also confirmed that the most probable location for the Zoomlion crane had it been brought in at the start of the project would have been somewhere close to the location generated under Scenario A. The main reason behind the poor location of the first crane was that the crews assigned to the site for the mobilization and foundation work were responsible for the selection of the location of the crane. Their main priority at the time was to get the crane operational to assist with the construction of the foundations.

5.2 Zemen Bank Headquarters Project

The Zemen Bank Headquarters Project (ZB-HQP) is a G+32 building with a height of 130 meters, located in the Financial District of Addis Ababa City along with the other high-rise building that are to serve as the headquarters of other banks. The project has an estimated cost of 1.2 billion ETB and is being built by China Wu Yi Construction Co. Ltd. With JDAW Architects serving as the consultant.

The bank intends to use the building as its headquarters and to rent some of the available space to the public. The first 5 floors will be used as the Main Branch of Zemen Bank and parking space, with the 6^{th} floor used as a data center.

Like other projects in the Financial District, the ZB-HQP project suffers from an acute lack of open space. The plot has an area of 2304 m^2, of which 1900 m^2 is occupied by the structure. This means 82.5% of the total plot area was occupied by the building. The contractor was forced to lease 2400 m^2 of land from the Addis Ababa City Administration (AACA) to construct the temporary offices, residences and material storages. Zemen Bank plans to solve the lack of open space by building a parking structure on the adjacent plot currently occupied by the temporary facilities.

As with other high-rise buildings surveyed in this thesis, the tower crane is the main mode of vertical transport. The heaviest items lifted by the crane are the scaffoldings, reinforcement, plywood formworks and concrete for the vertical structures. However, the reinforcement and the concrete are the items transported most frequently. The remainder of the concrete was transported using a concrete pump.

As in the previous cases, the contractor was responsible for selecting a location for the tower crane. The consultant was then asked for approval. The contractor based its decision on the location by considering the ability of the crane to reach all of demand points for the project.

The crane used by the project is a Zoomlion TC6513, which has a maximum capacity of 6 tons and 1.3 tons at the tip of the jib [29]. The crane has a freestanding height of 25.2

meters, after which it is anchored every 25 meters. In a somewhat different anchoring procedure, the contractor anchored the crane to the beams rather than the columns. The base of the crane is connected to a concrete pad that was purpose cast for the crane.

The drawings and quantities presented below are courtesy of the Zemen Bank Client Representative's Office.

5.3.1 Background and Model Information

While there is a shortage of open space in all the projects located in the Financial District, with the exception of the CBE-HQP project, the problem was more pronounced at the ZB-HQP project. In addition to the space constraint, the contractor's decision to install a batching plant, and the presence of temporary offices that have since been moved to the leased land made the site planning and crane placement process complex.

The problem of site congestion and the proximity of the buildings on nearby sites is exemplified by the fact that the contractor had to coordinate the movements and the height of its crane with China Jiangsu, the contractor for the NIB-HQP. Since the sweep of the crane used by the NIB-HQP passes over the airspace above the ZB-HQP plot and vice-versa, the two contractors had to consult each other to avoid collisions. In fact, in some instances, the NBHQ crane was used to lift items for the NIB-HQP project [30]. The rear of the ZB-HQP plot also borders Artistic Printers, and the crane moves over their airspace as well.

The location of the crane was offset from the centerline of the building because the adjacent NIB-HQP building had already constructed the first 7 floors, which would have restricted the slewing movement of the crane. Similarly, the crane couldn't be positioned on the street side of the building because it would have to swing over Ras Abebe Aregay Street and the Addis Ababa University – School of Commerce (AAU-SOC). This is especially relevant when transporting concrete because the crane must avoid dropping material on adjacent

roads and buildings. By placing it on the rear side of the building, the crane was also made closer to the material storage area and the concrete batching plants.

The crane is positioned 4.2 meters away from the building, while the batching plant is located a further 5 meters away from the crane, providing the necessary space between the structure, the crane and the batching plant.

As Figure 33 shows, the building has a unique shape with the building tapering off as the height increases with the resource demand for each floor changing accordingly. For example, the total reinforcement requirement per floor decreases from 99023.6 kg on the ground floor to 15288.6 kg on the mechanical level. The figure also shows the constraints imposed by NIB-HQP building which is visible on the left.

The unique design also affects the feasible region because despite the building having a slimmer profile after the 7^{th} floor, the wider profile from the Ground to the 6^{th} floor determined the feasible region. The design also affects the layout of the columns. A set of columns are common to all the floors of the building, but some columns are needed from the basement up to the 6^{th} floor. However, since the crane was anchored to the beams, rather than the columns, it has no effect on the optimization process.

***Figure 33**: Side Profile of ZB-HQP Building*

Figure 34 shows the rear side of the ZB-HQP plot, with the batching plant (left) and tower crane (right) in the foreground. In the background, the temporary facilities are visible, however parts of the facility have been demolished. As the picture shows, the space available prior to the lease of the extra land is extremely limited.

***Figure 34**: Rear side of ZB-HQP Plot*

5.3.2 Crane Utilization

The crane was used in the transportation of reinforcement and concrete for the columns. As with the previous models, the concrete must be delivered to the exact point it's needed at while the reinforcement is delivered to one of the available reinforcement demand points which approximates the actual work methodology employed by the contractor. Since the crane was brought in after the completion of the sub-structural work, it played no part in the transportation of the material for that phase of the project. During the foundation construction, the contractor transported materials using a mobile crane and the concrete pump was sufficient to handle the transportation of all the required concrete.

Figure 35 shows the reinforcement requirement for the 32 floors of the ZB-HQP building. The reinforcement requirement for the first 7 floors is in excess of 80000 kg per floor, but the reinforcement requirement decreases drastically from the 8^{th} floor onwards, when the floor area and purpose of the building changes. The total quantity of steel and concrete to

be transported was extracted from the structural drawings and BOQ that were provided by the consultant.

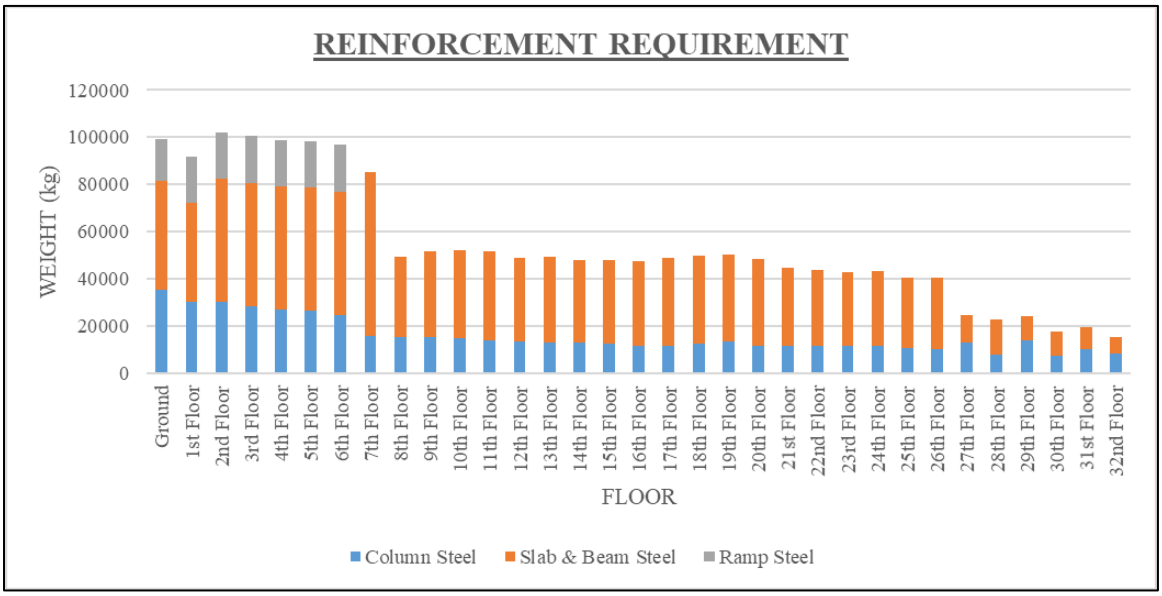

***Figure 35**: Reinforcement Requirement for 32 Floors of ZB-HQP*

5.3.3 Summary of Model

The model for the ZB-HQP optimization is made up of the same elements as previous models.

The coordinates for the delivery location of the steel are based on the advice of the project's staff in combination with observations on site. The steel required to construct one half of the slab is transported first, followed by the steel required for the second half. To replicate this process, the steel is delivered to one of four work zones on each floor except the mechanical floor, which only requires 2 locations due to its size.

The unique shape of the ZB-HQP increases the complexity of the demand points input. In previous models such as the NI-HQP and CBE-HQP, the fixed floor area and number of columns meant that the work information could be kept constant while changing the height based on the information from the Floor Heights file. For the ZB-HQP project, the constant

change meant that the 1035 tasks had to be listed individually in the CSV file containing the demand information. This step also made the use of the Floor Heights input file unnecessary since the Z locations are included with the work information.

There are only 3 excluded areas for the project: the base of the building and the batching plant. The off-limits area is modelled on the size of the Ground Floor of the building. The base of the building has the widest area and serves its purpose as an exclusion zone. Even though the batching plant was constructed prior to the positioning of the tower crane, it has been excluded in the model because there is enough space between the building and the plant to avoid any conflict. The temporary offices that were used by the consultant and contractor prior to the leasing of the plot behind the site have been included because it would have restricted the rotation of the crane during the initial stages of construction.

The site bounds in the model reflect the final site boundaries and are based on the site layout drawing provided by the Client Representative's Office. The extra plot of land that the contractor has leased from the AACA hasn't been included. As previously mentioned, this does not affect the results because the anchoring requirement automatically limits the distance that the crane can be from the building.

As with previous models, the tower crane's operating characteristics have been modelled using linear regression. Due to minor differences in the load capacity of the crane between the plate on the crane and documents from Zoomlion, the information displayed on the crane's plate has been used.

Table 17 summaries the inputs to the ZB-HQP model.

***Table 17**: Summary of ZB-HQP Model Inputs*

INFORMATION	PURPOSE	FILE NAME
Site Boundaries	Describes the boundaries of the construction site. The site is divided into 2 triangles.	Zemen_SITE_BOUNDS.csv
Off-limit Areas	Includes the location and size of areas which are infeasible as described previously.	OffLimitAreas_Zemen.csv
Demand Points	The x, y and z coordinates of the demand points along with the required loads	WorkInfo_Zemen.csv
Supply Location	The points on the ground from where the loads are lifted.	Supply.csv
Floor Heights	This file is unused, instead the Z positions have been included in the demand points file.	FloorHeights.csv

Figure 36 shows the demands points in isolation. In the previous models, a simple 2D figure would have sufficiently presented the locations but in this case the constant changes in the x and y coordinates as the building height increases necessitates a 3D figure.

Figure 37 shows the base of the building, which is the only off-limit area, and the boundaries of the site.

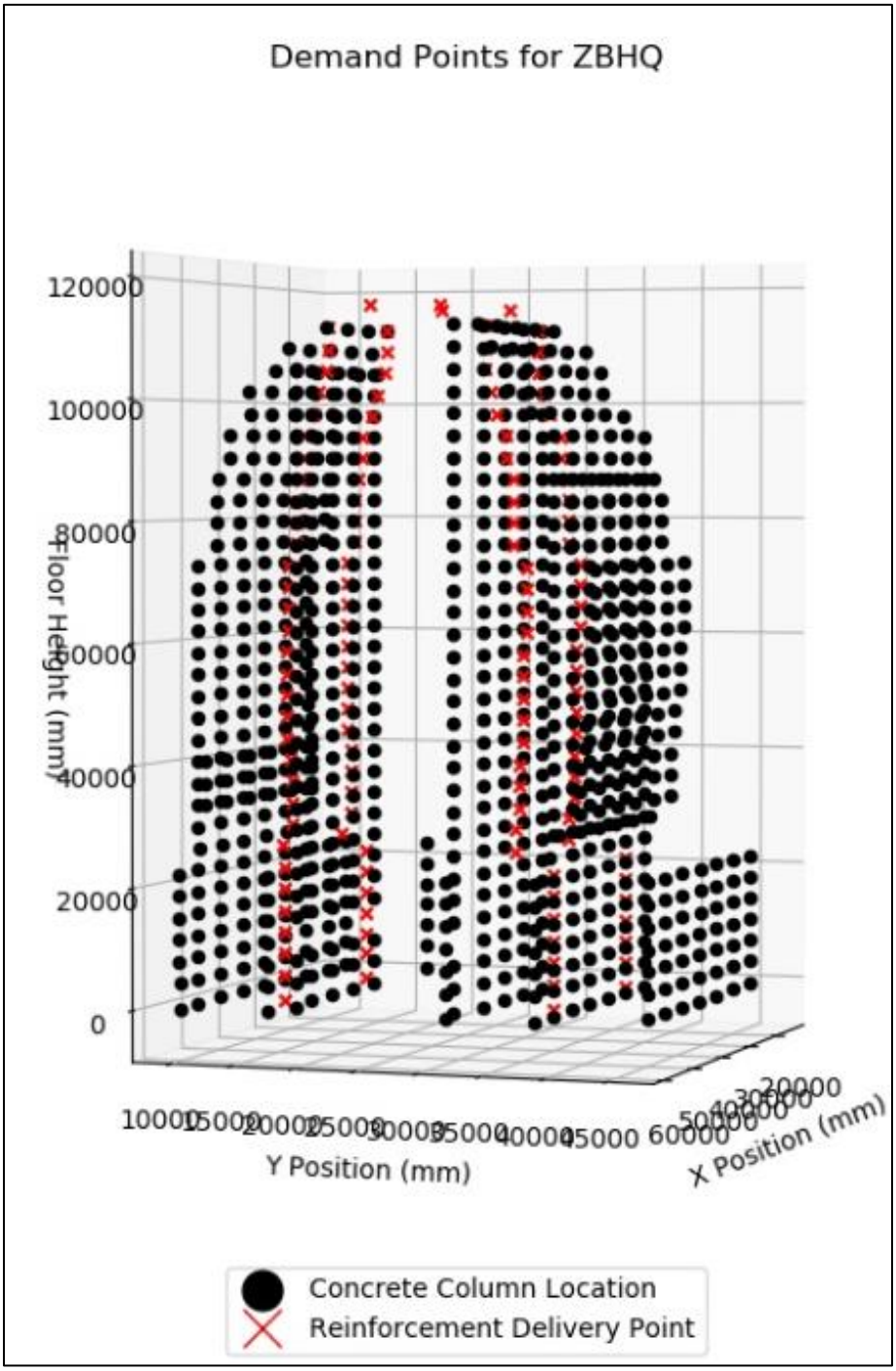

***Figure 36**: ZB-HQP Locations of Demand Points in 3D*

***Figure 37**: ZB-HQP Model, Demand Points Omitted*

5.3.4 Optimization Results

The optimization was performed under the following 2 conditions:

- Under Scenario A, the constraints described above have been included in the model.
- Under Scenario B, the crane's location is freely optimized, with the assumption that the initial temporary offices and NIB-HQP constraints are not present.

By comparing the results of the 2 cases, it is possible to investigate the effect of the presence of the temporary facilities. Table 18 and Figure 38 summarize the results of scenario A, while Table 19 and Figure 39 summarize the results of Scenario B.

***Table 18**: ZBHQ Optimization Results, Scenario A*

RUN NO.	1	2	3	**4***	5	6	**7***	8	9	10	μ	σ	σ/ μ (%)
X (mm)	30471.6	31818.6	30471.6	**31841.1**	31841.1	31957.6	31841.2	30471.7	31835.8	30471.8	31302.2	679.1	2.169
Y (mm)	51384.3	51393.3	51384.4	**51384.4**	51384.3	51384.4	51384.3	51384.3	51386.3	51384.5	51385.5	2.666	5.2E-3
TIME (min)	66247.415	66240.645	66247.459	**66230.318**	66230.324	66291.160	66230.283	66247.447	66232.693	66247.520	66244.526	17.24	.0260

* Optimal Result

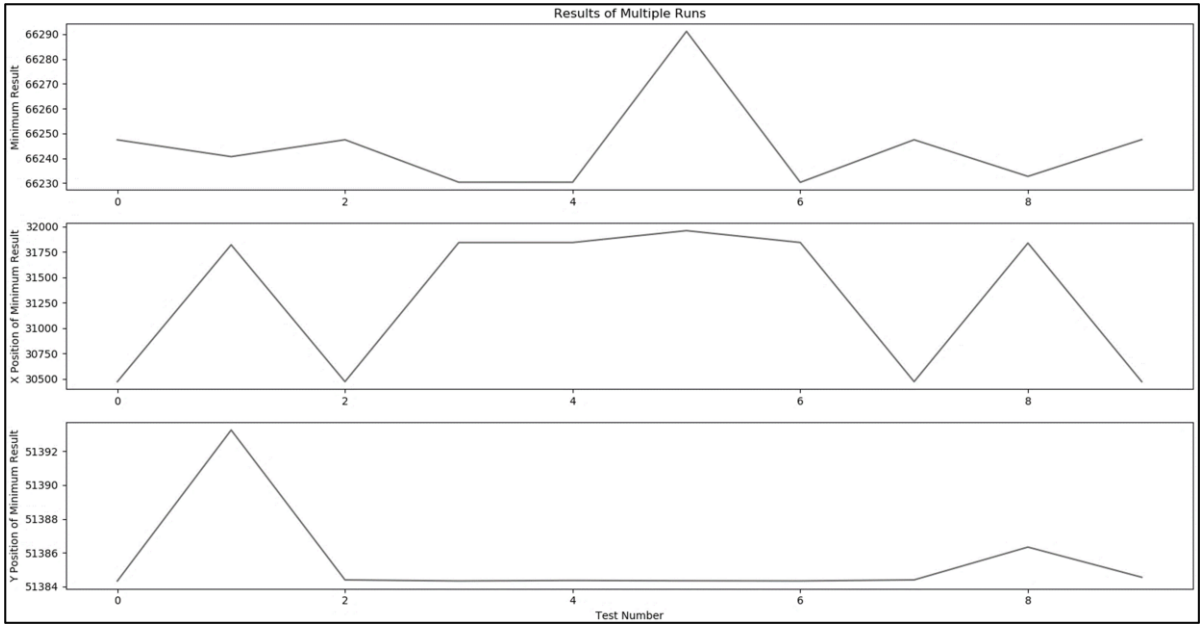

***Figure 38**: ZBHQ Optimization Results, Scenario A*

***Table 19**: ZB-HQP Optimization Results, Scenario B*

RUN NO.	1	2	**3***	4	5	6	**7**	8	**9***	10	μ	σ	σ /μ (%)
X (mm)	30471.6	30472.7	30471.6	31835.4	30471.6	30471.8	30471.6	30471.6	**31840.6**	30471.6	30744.9	546.516	1.779
Y (mm)	51384.3	51386.0	51384.3	51385.7	51384.3	51384.6	51384.3	51384.3	**51384.6**	51384.3	51384.7	.590	1.15E-3
TIME (min)	66247.419	66247.274	66247.422	66232.382	66247.416	66247.549	66247.415	66247.422	**66230.565**	66247.422	66244.329	6.445	9.73E-3

** Optimal Result*

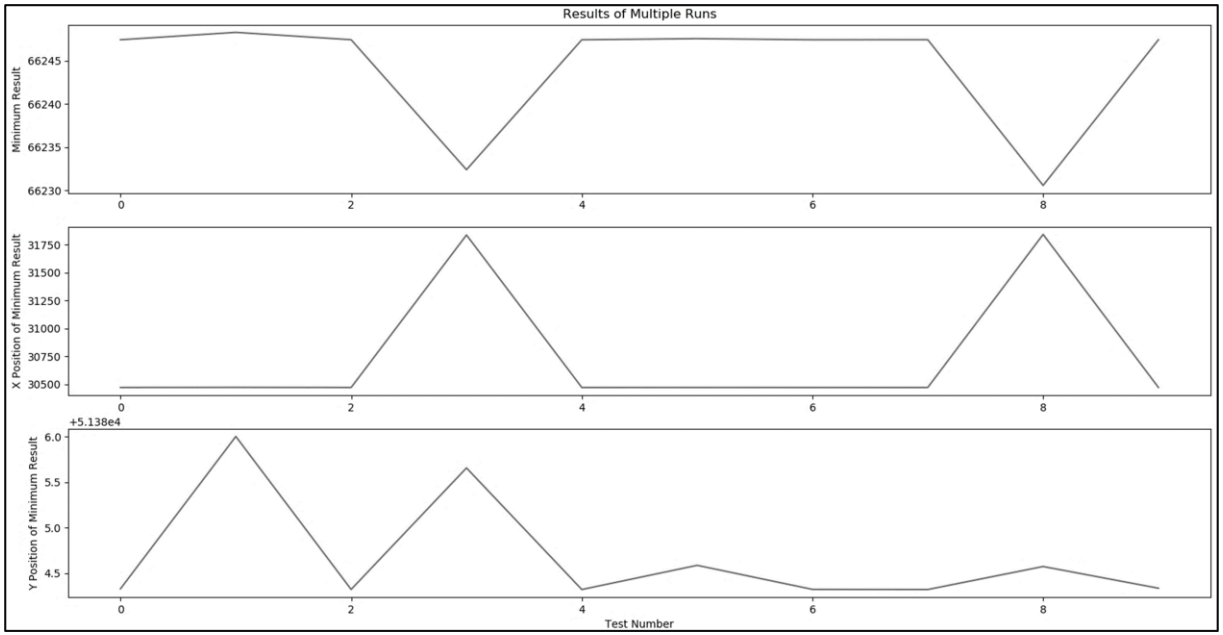

***Figure 39**: ZB-HQP Optimization Results, Scenario B*

The PSO algorithm's minimum output over 10 runs was the same for both scenarios, which indicates that the presence of temporary facilities has no effect on the optimal location. The results from Scenario B indicate the presence of a local minima. However, the algorithm has converged to a global minima in 2 cases, indicating the algorithm has functioned well.

Figure 40 presents the positions of the reinforcement and concrete supply points and the location of the tower crane as currently found as well as the optimal location generated.

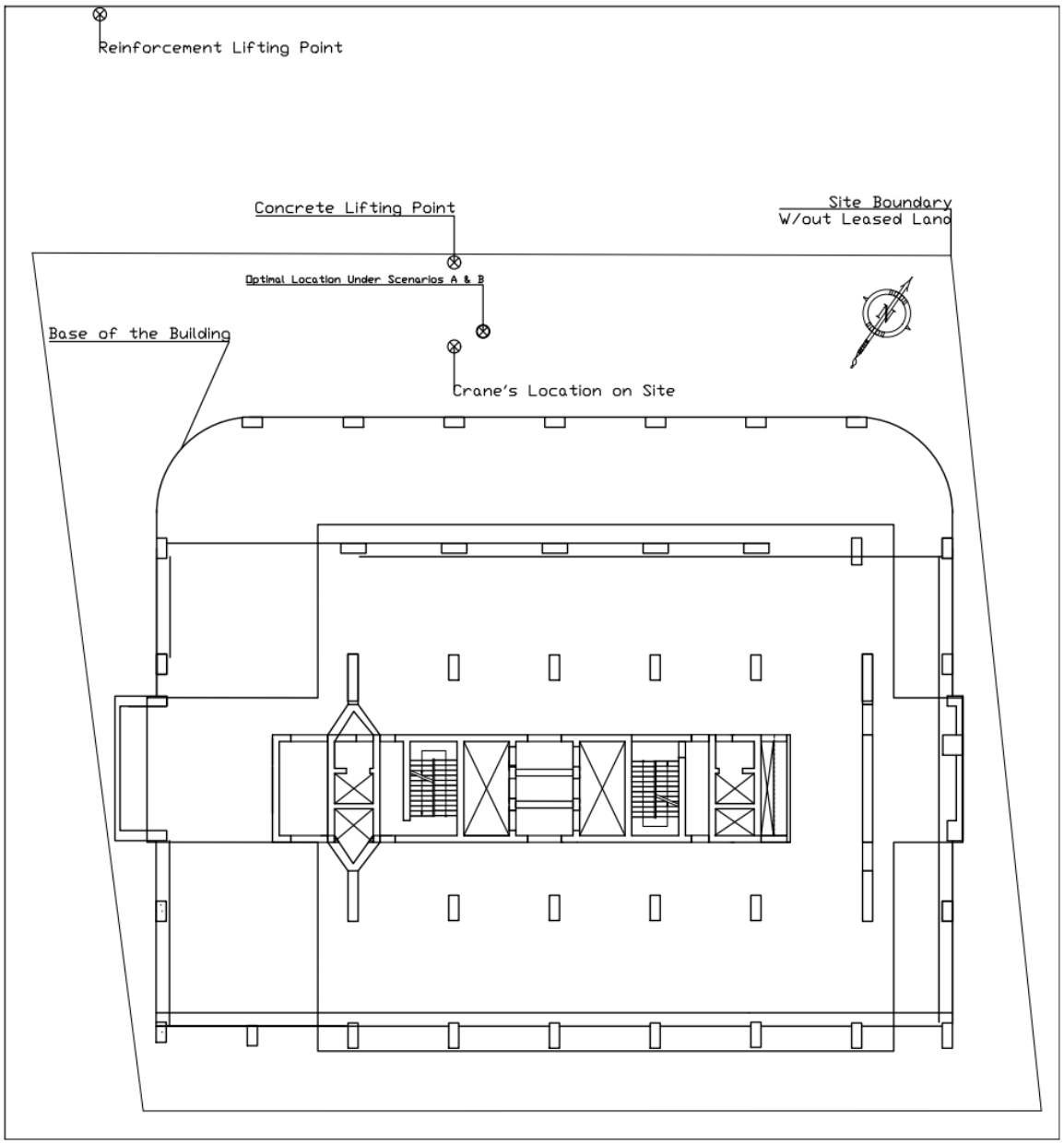

***Figure 40**: ZB-HQP Optimization Results, Scenarios A and B*

5.3.5 Discussion

In both scenarios, the results approximated the actual location of the tower crane. The location of the crane was only 1.94 meters away from the actual location. This is an interesting result because when allowed to optimize freely in previous cases, the optimal location was close to the centerline of the building. In this case, the reinforcement was lifted from a point that is far from the building and by moving the crane away from the centerline, the distance to the reinforcement is minimized.

It was previously discussed in the literature review that the minimum of the crane's capacity between the supply point and demand point is used to find the crane's capacity. Therefore, the crane's position would always attempt to find a location that is equidistant between the reinforcement lifting and demand points. Increasing the crane's capacity, thereby reducing the number of trips, the overall travel time is also reduced.

By anchoring the crane to the beams rather than the column, the contractor has given itself a greater degree of freedom in deciding the location of the crane. Taking the example of the CBE-HQP project (Fig. 24), the tower crane could be anchored to only one of 3 locations that were equidistant to the available columns. ZB-HQP's decision allows it to anchor the crane to any position with slight modifications to the design. Therefore, the location generated is acceptable despite not being equidistant from the columns.

Scenario B proved that the temporary offices and the NIB-HQP building didn't affect the optimal location. While the optimization validated the contractor's decision, it didn't validate the reasoning behind the decision-making process. The main reason the contractor offset the crane's location was to avoid NIB-HQP and Artistic Printers. In this case, the contractor could have easily made the mistake of placing the crane further to the South-West from the centerline, while the optimal location was found to be the North-East of its actual location.

Since the contractor could have easily made the mistake of moving the crane to the South-West of the centerline, which would have reduced its efficiency, it is important to apply rigorous mathematical techniques rather than intuition in order to avoid mistakes.

5.3 Nib International Bank Headquarters Project

The Nib International Bank Headquarters Project (NIB-HQP) project is a G+33 building with a height of 122.4 meters that is being constructed by China Jiangsu for 1.4 Billion ETB. The project is in the Financial District as well. The consultant for the project is ETG Consulting.

The crane used for the project was manufactured locally in the Jiangsu province of China, and its manufacturer and capacities are unknown. It has a jib length of 73 meters, and a free-standing height of 24 meters, after which it is anchored every 6 floors (21.6 meters). The crane is anchored using J-bolts that are cast into the slab. The base of the crane is placed on a pile cap, and the concrete surrounding the pile has an increased compressive strength of 60 MPa. Based upon the advice of the consultant, a comparable Zoomlion T7015-10E crane was used for the analysis.

During the design and bidding stage, the consultant and the client had planned on placing the crane outside the plot on the sidewalk of Ras Abebe Aregay Street. Instead, the contractor suggested that the crane be placed directly on the pile caps and that openings be made through 8 slabs.

In addition, the contractor preferred placing the crane on the street-side because it gave the operator a better view of the items being lifted by the crane. The consultant was heavily involved in the decision-making process due to the need to check the impacts the crane's placement would have on the foundation and the superstructure.

Placing the crane within the building means that the crane can dismantle itself using its own power only up to the 4^{th} floor, which makes the dismantling process more complicated. Another side effect of placing the crane on the street side of the plot was that there was a risk of striking nearby buildings during the early stages of construction. This risk was realized when the crane struck Bedilu Building which is found on the other side of Ras Abebe Aregay Street.

The 73-meter jib used by the contractor is the longest among the project's studied and raises a question regarding whether it was necessary to use such a long jib. It was possible to use a shorter jib length, but the contractor was anxious about being able to reach items that were placed on the rear side of the building. The analysis will be used to answer the question of whether such a long jib was needed for the project.

The drawings and quantities presented below are courtesy of the Nib International Bank Client Representative's Office.

5.3.1 Background and Model Information

Even compared to the other projects that were surveyed, the lack of open space is most pronounced in the NIB-HQP project, with almost all of the plot occupied by the building. Prior to the completion of the tower, the offices for the consultant and the contractor used cramped containers as offices.

The fact that the entire plot is occupied by the building affects the inputs for the NIB-HQP model. Since the entire plot is occupied by the building, there is no distinction between the building's base and the plot area. The building's base has been adopted as the plot limits of the site, and the off-limits area is composed of the main tower only.

Like Rama Construction and China Wu Yi, China Jiangsu chose to transport the concrete using a bucket to avoid the possibility of the concrete drying in the pipes due to the lack of sufficient volume. The concrete was mixed at the China Jiangsu batching plant located adjacent to the nearby UB-HQP building and transported using mixing trucks. The reinforcement is produced on the Ground Floor of the building and lifted from an access road.

The long jib was due to the contractor's fears that it wouldn't be able to reach the edges of the building, where it had stored materials. This concern will be tested by the optimization. The long jib also allows for the creation of a large feasible region and affects the convergence of the PSO algorithm since its forced to search through a large solution space compared to the other cases.

5.3.2 Crane Utilization

The crane was used to lift all the reinforcement for the superstructure and the concrete for the columns. The concrete was lifted with a 1.5 m^3 bucket, which weighs over 3600 kilograms when full.

According to the BOQ provided by the client representative, the total quantity of reinforcement used for the superstructure is 5,051,626.87 kg. The total reinforcement quantity is divided up among all the floor proportionally based on the floor area. Table 20 summarizes the division of reinforcement among the 33 floors based on their floor area.

The floor area changes considerably, however, there are 3 major changes in the floor area. The floors between Ground and the 4^{th} Floor; the 5^{th} Floor and the 20^{th} Floor; the 20^{th} Floor and the 31^{st} Floor; and the 32^{nd} up to the 33^{rd} floor have similar floor areas, and similar assignments of reinforcement.

***Table 20**: Reinforcement Distribution*

FLOORS	FLOOR AREA (m^2)	TOTAL AREA (m^2)	% OF TOTAL REBAR	WEIGHT OF REBAR (kg)	WEIGHT OF REBAR PER FLOOR
G → 4^{th}	3065.522	18393.13	42.5%	2,148,376	358062.6
5^{th} → 20^{th}	933.920	14008.8	32.4%	1,636,272	109084.8
21^{st} → 31^{st}	855.090	9405.99	21.7%	1,098,649	99877.2
32^{nd} → 33^{rd}	720.569	1441.138	3.3%	168,329.4	84164.72

The reinforcement that is assigned to each floor is then divided up among the demand points evenly. There are 9 demand points per floor from the Ground to the 4th floor, and there are 4 per floor for the remainder.

5.3.3 Summary of Model

The occupation of the entire site has made the model simpler. Unlike previous models, the inclusion of the plot limits is not necessary. Instead, 4 off-limits area objects have been added to the model that restrict the optimal location to a region that surrounds the building only. The objects also prevent the optimal location from being unanchorable. To satisfy the input requirements of the model, 1 plot area object has been added to the model.

The reinforcement delivery points are spread out throughout the floor area to mimic the delivery of reinforcement to multiple points on the slab. The concrete for the columns must be delivered exactly to the required location.

The elliptical tower is modelled using 18 triangles. This has allowed for a reasonable approximation of the elliptical shape. It is possible to increase the number of triangles, but it would cause an unnecessary increase in the computational load, with no effect on the results.

Table 21 summarizes the inputs for the NIB-HQP model.

***Table 21**: NIB-HQP Model Inputs*

INFORMATION	PURPOSE	FILE NAME
Site Boundaries	This input was unnecessary, 1 object has been included to satisfy the model requirements.	NIB-HQP_SITE_BOUNDS.csv
Off-limit Areas	Includes the location and size of areas which are infeasible as described previously. This includes 18 triangles and 3 rectangles for the tower of the building, as well as 4 artificial objects to enforce the anchoring requirement.	OffLimitAreas_NIB-HQP.csv
Demand Points	The x, y and z coordinates of the demand points along with the required loads.	WorkInfo_NIB.csv
Supply Location	The points on the ground from where the reinforcement and concrete are lifted.	Supply.csv
Floor Heights	This file is unused, instead the Z positions have been included in the demand points file.	FloorHeights.csv

Based on the information summarized in the table above, the model shown in Figure 41 has been generated in Python.

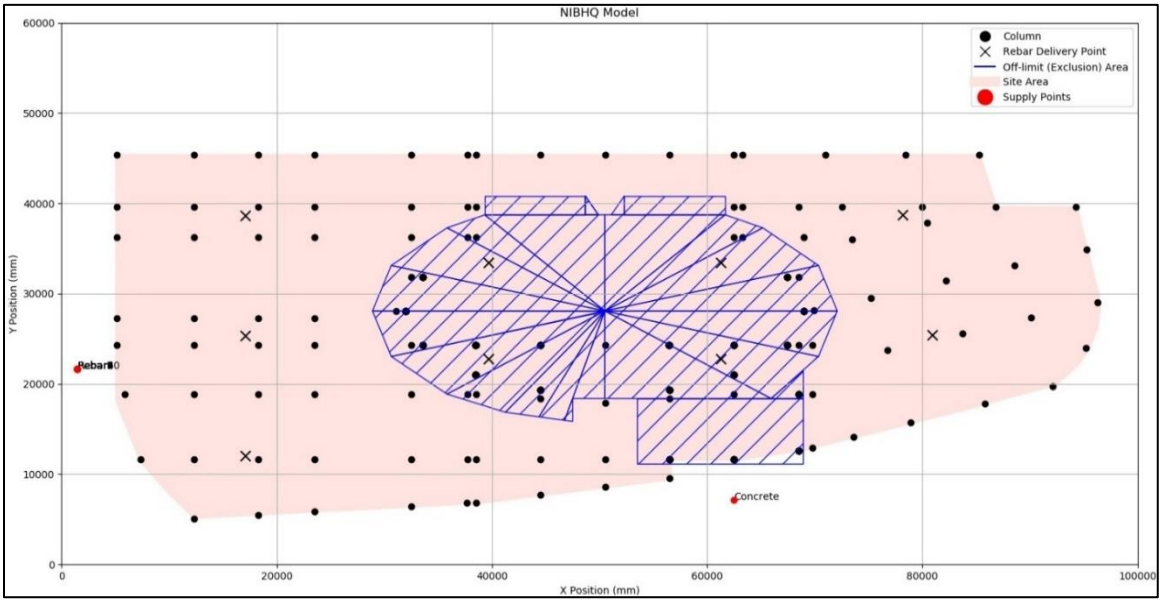

***Figure 41**: NIB-HQP Model*

5.3.4 Optimization Results

The optimization for the NIB-HQP was run using the inputs discussed previously. Due to the lack of information regarding the tower crane used on site, the Zoomlion T7015 crane was used with the approval of the consultant.

The results of the optimization are presented below. Table 22 and Figure 42 summarize the results of the 10 optimization runs that were performed, and Figure 43 shows the feasible region, supply points, and site boundaries. The large feasible region created by the choice of a 73-meter long jib can also be seen.

As with previous cases, the presence of nearby local minimal has pulled the particles away from the global minima. However, unlike previous cases, the particles managed to converge to a global minima in only one of the ten runs. The reasons for this instability are discussed further in Section 5.4.5. In addition, the 3D visualization of the solution space is presented in Appendix 7.

***Table 22**: NIBHQ Optimization Results*

RUN NO.	1	2	3	4	5	6	7	8	**9***	10	μ	σ	σ/μ (%)
X (mm)	34377.7	34437.0	34445.5	34404.0	34412.2	34339.2	34383.8	34492.1	**33792.9**	34276.7	34436.129	189.603	.552
Y (mm)	15876.7	16170.3	16287.4	16011.9	16039.7	15955.3	15864.7	16525.3	**16503.3**	17176.6	16241.106	384.847	2.370
TIME (min)	42289.666	42322.956	42301.987	42308.584	42312.524	42334.644	42288.111	42330.707	**42141.736**	42220.646	42220.646	56.828	.134

** Optimal Result*

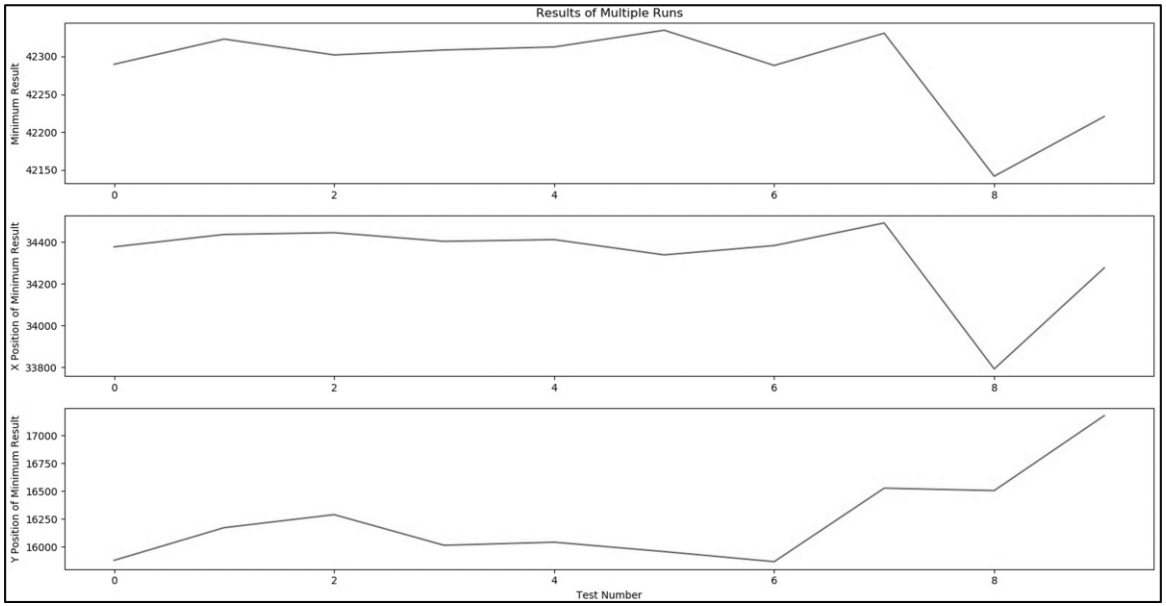

***Figure 42**: NIBHQ Optimization Results*

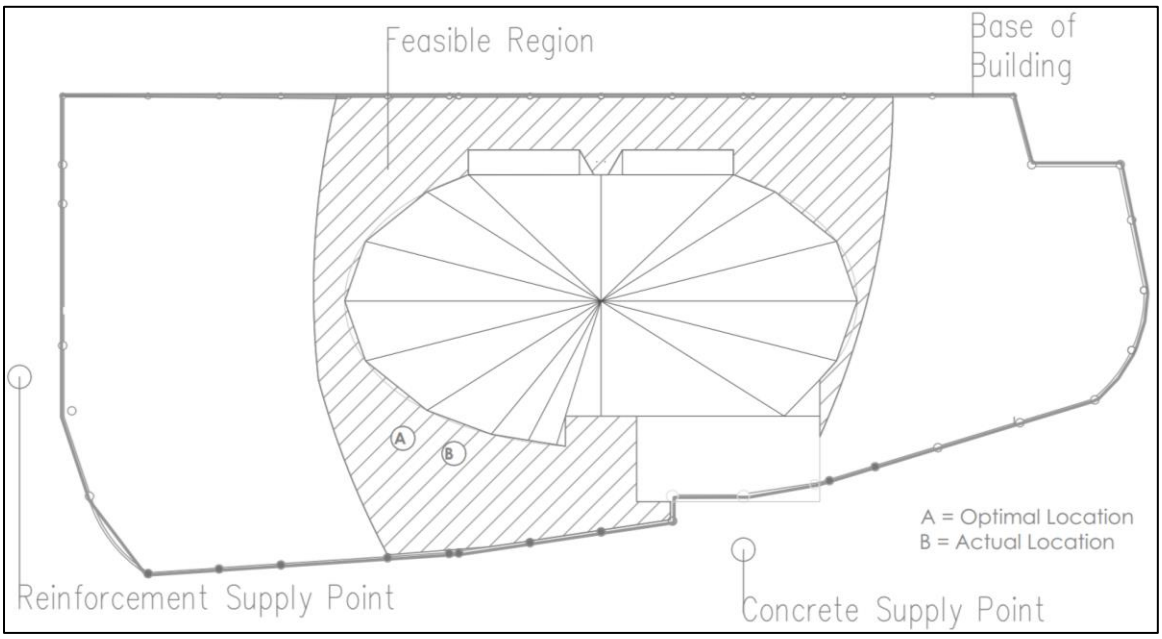

***Figure 43**: NIB-HQP Optimization Results, with Site Plan*

5.3.5 Discussion

The first point of interest regarding the results was its instability, as shown by the high coefficients of variation for both the position and the travel time. While the particles converged towards a solution on all runs, it was towards a sub-optimal point rather than the global minima. There are several reasons for this, including the abnormally large solution space, and the presence of multiple local minima that surround the global optima. Such local minima "pull" particles away from the global minimum, especially if they are large in number.

In order to confirm that the PSO algorithm was performing well, multiple runs of 10 were conducted, with changes in the parameters of the algorithm. In all cases, none of the results were beyond the minimum included in Section 5.4.4. The results show that since there were no results below the minimum indicated in the table above were found, the minimum found in Section 5.4.4 can be used in the following discussions.

Despite the large feasible region, the optimal location was in fact close to the actual location on site. It was surprising that despite the large feasible region, the optimum location was found to be close to the actual location.

Before discussing the results of the optimization, it is important to analyze the use of a 73-meter jib crane first. This choice increased the risk of collisions, both with nearby buildings and the ZB-HQP tower crane in the adjacent plot. Therefore, it's important to ask if it was a necessary choice. The results prove that a 73-meter long jib was unnecessary since a 70-meter jib crane could reach all edges. Therefore, the crane used has a capacity beyond what is needed for the project in terms of both jib length and lifting capacity.

In addition to the risk of collision with a nearby building, the use of a long jib has increased the size of the feasible region and its location. This in turn increases the contractor's placement options. Unfortunately, this increases the risk of placing the crane at a sub-optimal location due to the abundance of choices. This risk was realized and after striking a building across the street, the contractor was forced to repair the damages.

Compared to the optimal location, the actual position of the tower crane is closer to the street, and this is to improve the visibility of the supply points. However, both the optimal and actual locations are on the street-side of the building and the rear-side of the building is all sub-optimal despite being within the feasible region.

5.4 United Bank Headquarters Project

The final project to be analyzed is the Union Bank Headquarters Project (UB-HQP) project, which is also being built by China Jiangsu in the Financial District of Addis Ababa. The 1.9 Billion ETB project is a G+32 building with a total height of 133 meters. The consultant for the project is Eskender Architects. The project is made up of 3 blocks, with two G+5 blocks referred to as Blocks A and B, which will serve as a shopping center and banking hall respectively, and the office tower block (Block C).

The project is being built on 3300 m^2 plot of land, with the base of the building occupying 2700 m^2 of the available land. This represents 81.8% of the total available land. To minimize the space occupied by the crane, the contractor placed the crane on the pile caps and created an opening through the basement slabs for the tower of the crane. Figure 44 shows the crane which is anchored to the pile caps of the building.

The project uses a Zoomlion TC5013-B6 tower crane, similar to the one used on the NI-HQP project. The crane has a maximum capacity of 6 tons and 1.3 tons at the tip of the jib. The jib has a length of 50 meters. As shown in Figure 45, the crane is anchored to the slab of the office block every 5 floors (18 meters) once it exceeded its maximum freestanding height of 49 meters.

The drawings and quantities presented below are courtesy of Eskender Architects.

***Figure 44**: UB-HQP Tower Crane Base Anchored to a Pile Cap*

***Figure 45**: UB-HQP Crane Anchoring to Slab*

5.4.1 Background and Model Information

Like the ZB-HQP, NIB-HQP and NI-HQP projects, the space available at UB-HQP was limited, and the contractor was forced to rent space from the AACA to construct a concrete batching plant (which also services NIB-HQP) and the temporary offices for both the contractor and the consultant.

The contractor placed the crane on the street-side of the plot. This means that the crane swings over the AAU-SOC and Ras Abebe Aregay Street. Such a placement carries the risk of material being dropped on the road or AAU-SOC. The optimization will either prove the contractor correct in its decision to place the crane on the street side or find a more optimal location on the rear-side of the plot.

The site layout drawing shows the positions of the 3 blocks and the site boundaries. The Northern boundary is only 1.93 meters away from the building, while most of the space on the Ras Abebe Aregay side of the plot is occupied by the building.

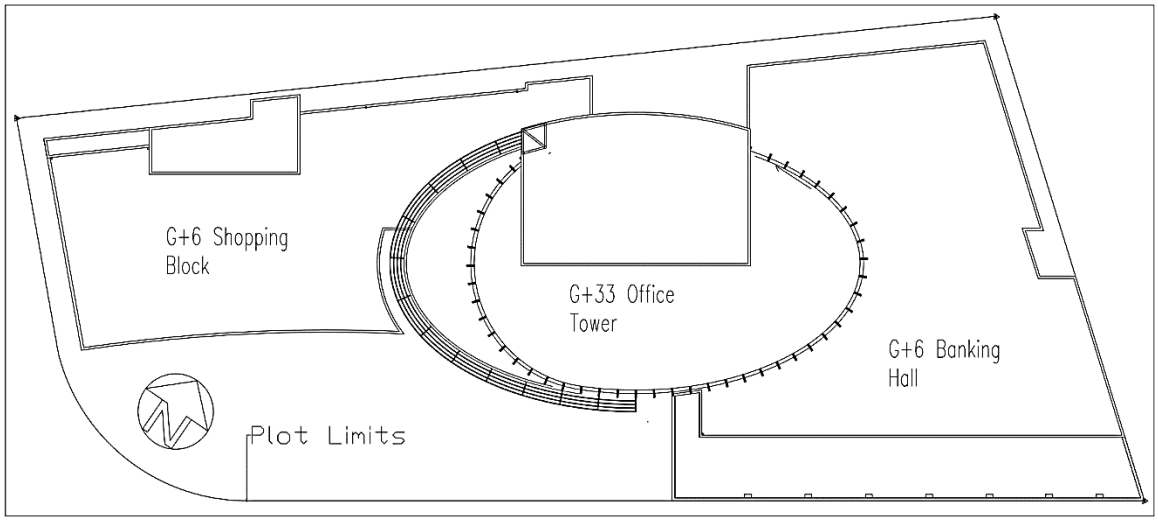

***Figure 46**: UB-HQP Site Layout*

5.4.2 Crane Utilization

Like the other high-rise projects that were studied, the crane is the main mode of vertical transportation for the UB-HQP project. The main materials transported for the project were reinforcement and concrete for the columns. The cooling towers required for the project were also transported using the tower crane. The reinforcement required for the project was extracted from the BOQ that was provided by Eskender Architects and the concrete volumes were calculated based on the structural drawings. The concrete used for the columns was C60, and the density was assumed to be 2400 $\frac{kg}{m^3}$.

Unlike the other projects surveyed, the cooling towers have already been installed, and their weights, lifting points and final locations are all known. This load is treated like the steel columns used by CBE-HQP since it's indivisible. According to the consultants, the cooling towers used for the project were Carrier 30-RA100 and Carrier 39-FX370. 6 Carrier 30-RA100 which each weigh 1183 kg were placed on the 5th floor roof, while 5 Carrier 39-FX370, which weigh 1300 kg are placed on the 33rd floor [31].

The steel quantities provided by the consultant was divided into 3: one for each of the blocks. This quantity of reinforcement is divided equally among the floors. There is minimal variation in the requirements among the floors, therefore this is an acceptable approximation. Table 23 summarizes the reinforcement requirement for each of the 3 blocks, and the reinforcement required per floor.

***Table 23**: Reinforcement Quantity for UB-HQP*

BLOCK	TOTAL QTY OF REINFORCEMENT (KG)	NO. OF FLOORS	REINFORCEMENT REQUIREMENT PER FLOOR (KG)
Block A	351607.78	6	58601.3
Block B	253198.05	6	42199.7
Block C	1279703.5	33	38778.9

5.4.3 Summary of Model

Compared to the other projects that were analyzed, the model for the UB-HQP project was more complex due to the shape of the buildings and the plot. For example, Block C has an elliptical shape, while Block A has a curved region. These shapes were approximated using triangles and an attempt was made to balance the accuracy of the model with the increase in computational powers needed with a more complex model.

Blocks A and B are too short to enable anchoring beyond the first 22.8 meters. Therefore, any crane position near Blocks A and B must be made infeasible. Several artificial off-limit areas were added to the model to prevent the optimal location being located near Blocks A and B.

During the mobilization stage and construction foundation, the contractor hadn't leased the extra land it currently occupies from the AACA. Therefore, this space hasn't been included in the model. The anchoring beams used for the crane have adjustable lengths, so that the crane can be anchored to any position on the slab.

Table 24 summarizes the model's inputs and the resulting visualization is shown in Figure 52.

***Table 24**: Summary of Model Inputs for UB-HQP*

INFORMATION	PURPOSE	FILE NAME
Site Boundaries	Describes the boundaries of the construction site. The site is divided into 4 triangles.	Union_SITE_BOUNDS.csv
Off-limit Areas	The base of the building and 4 areas that prevent render areas near Blocks A and B off-limits are included.	OffLimitAreas_UB-HQP.csv
Demand Points	The x, y and z coordinates of the demand points along with the required loads	WorkInfo_UB-HQP.csv
Supply Location	The points on the ground from where concrete, reinforcement and cooling towers are lifted from.	Supply.csv
Floor Heights	This file is unused, instead the Z positions have been included in the demand points file.	FloorHeights.csv

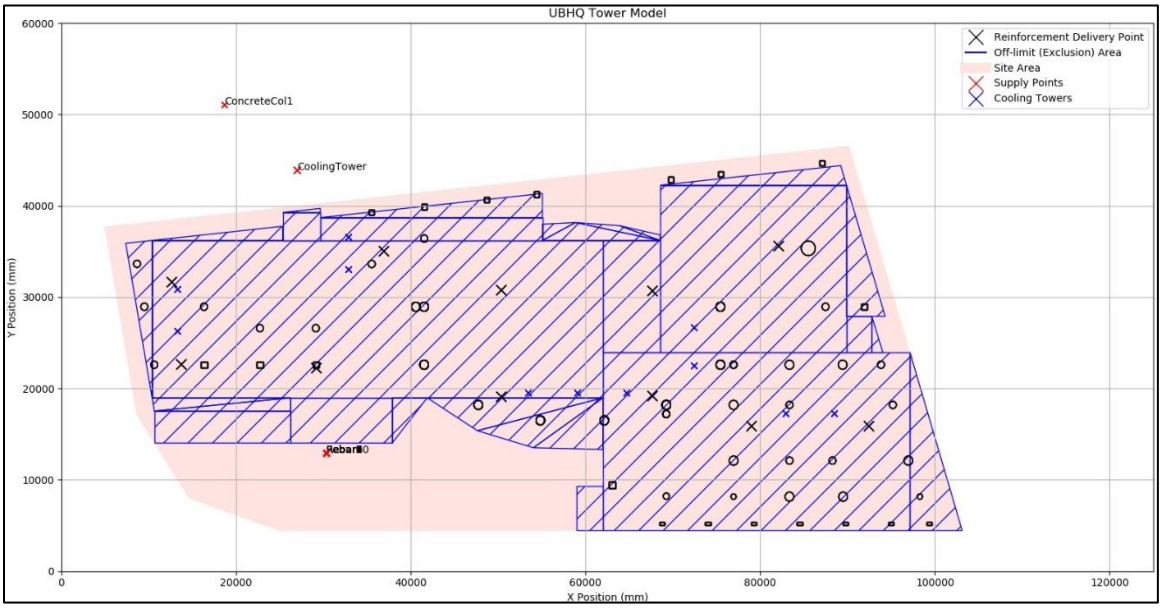

***Figure 47**: UB-HQP Site Model*

5.4.4 *Optimization Results*

The optimization for UB-HQP was performed under one scenario, with the assumption that all the concrete needed for the columns, cooling towers and reinforcement are transported using the tower crane.

Table 25 and Figure 48 summarize the results of the 10 optimization runs that were performed. The results are stable, with low coefficients of variation. The only exception was Run 2, which appears to have converged to a local minima instead.

Figure 49 shows the feasible region, supply points, site boundaries and the reach of a 50-meter crane. The use of crane with a short jib has led to two problems: the first is the inability of the crane to reach the edges of the plot and the second is the reduction of the size of the feasible region. These effects will be discussed further in the following section.

***Table 25**: UBHQ Optimization Results*

RUN NO.	1	2	**3***	4	**5***	**6***	**7***	**8***	**9****	10	μ	σ	σ/μ (%)
X (mm)	49843.2	49843.6	49843.1	49843.2	49843.1	49843.1	49843.1	49843.1	**49843.1**	49843.2	49843.197	.150	.300E-3
Y (mm)	13427.6	13427.5	13427.7	13427.6	13427.7	13427.7	13427.7	13427.7	**13427.7**	13427.7	13427.649	.050	.372E-3
TIME (min)	36366.324	36366.343	36366.317	36366.324	36366.317	36366.317	36366.317	36366.317	**36366.316**	36366.318	36366.321	7.83E-3	.0215E-3

** Identical optimal results were found of Runs 3,5,6,7 & 8; minimum results*

*** Differences during rounding have led to a 0.001-minute reduction without changes in the x & y positions*

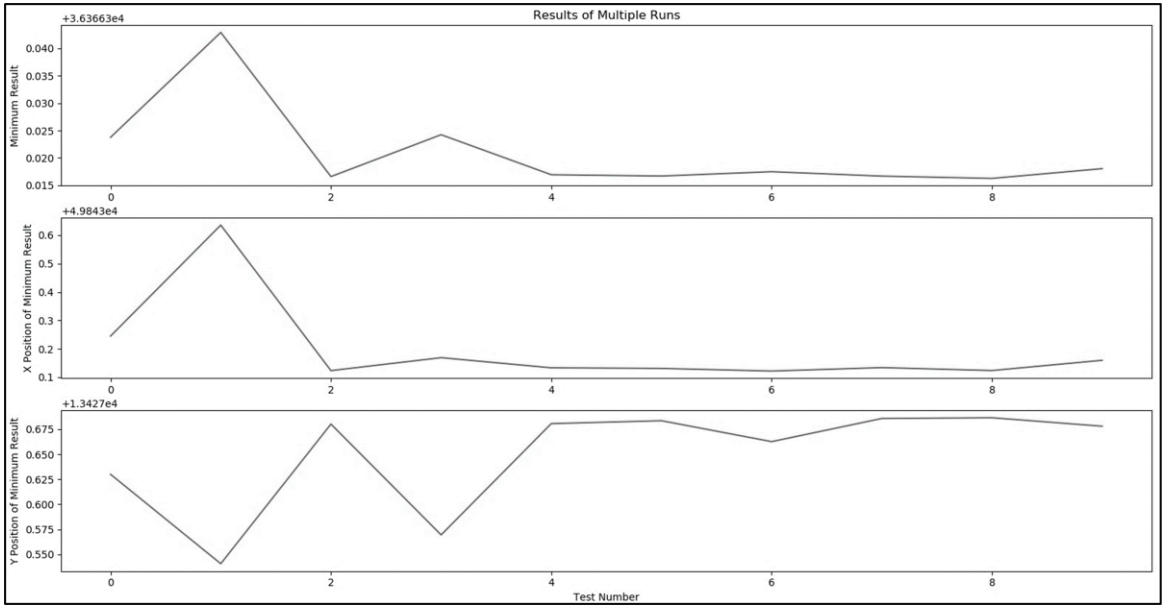

***Figure 48**: UBHQ Optimization Results*

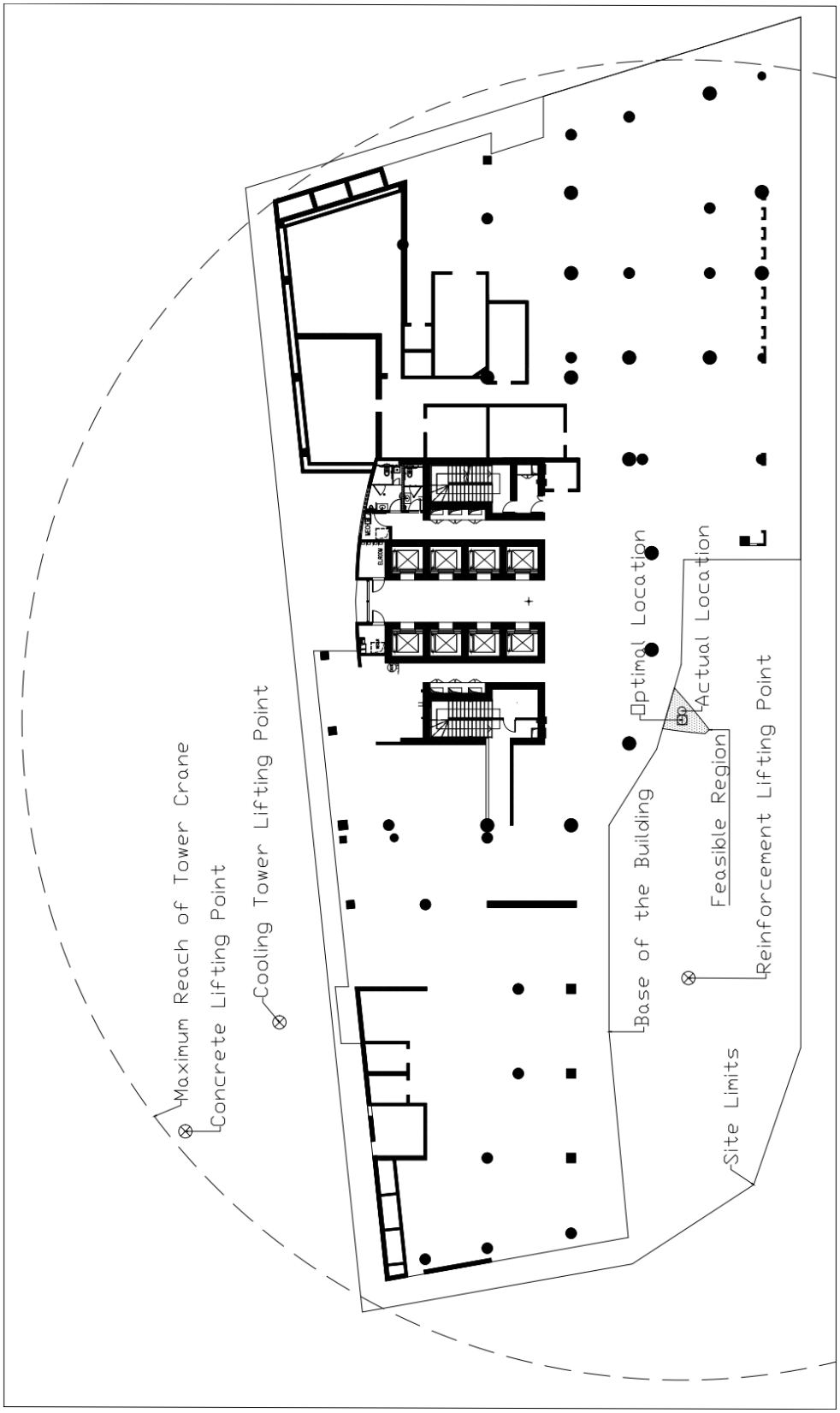

***Figure 49**: UB-HQP Optimization Results with Site Plan*

5.4.5 Discussion

On 6 occasions, the PSO algorithm was able to converge to the same solution. This supports the fact that the algorithm has managed to find a global minimum. The standard deviation, as well as the coefficient of variation of the travel time are 7.83E-3 and .0215E-3% respectively. This again indicates remarkable stability. The results can then be used to answer questions raised in the preceding sections.

Prior to performing the optimization, a visual inspection of the feasible region proved that the decision to place the crane on the street side of the plot was justified. As the output above shows, the only feasible area is located on the street-side, and the purpose of the optimization was to simply find the optimal point. The size of the feasible region has positively influenced the accuracy of the results. By making the search area very small, the algorithm is better able to explore and converge towards a solution.

The location picked by the contractor is also within the feasible region, and very close to the optimal location found. Therefore, the contractor was justified both in placing the crane on the street-side of the plot, and in selecting its exact position.

The second point of interest was the effect of the cooling towers on the results. Despite being an indivisible load, the cooling towers had no effect on the results because the crane's capacity at the edge of the jib was 1.3 tons, which is equal to the largest indivisible load. Therefore, the crane can utilize the full length of its jib to lift the cooling towers. This means that the cooling towers don't affect the feasible region like the steel columns used for the CBE-HQP did.

Instead, the restriction of the feasible region occurred because of the crane's jib length. Reducing the length of the crane's jib directly impacts the feasible area. Like the CBE-HQP model, the building is longer along one of its axes, and the crane couldn't be placed away from the center because this would prevent it from servicing areas on the extremes of the plot. Figure 50 illustrates the drastic change in the feasible region that occurs when the crane's jib length is assumed to have a length of 60 meters.

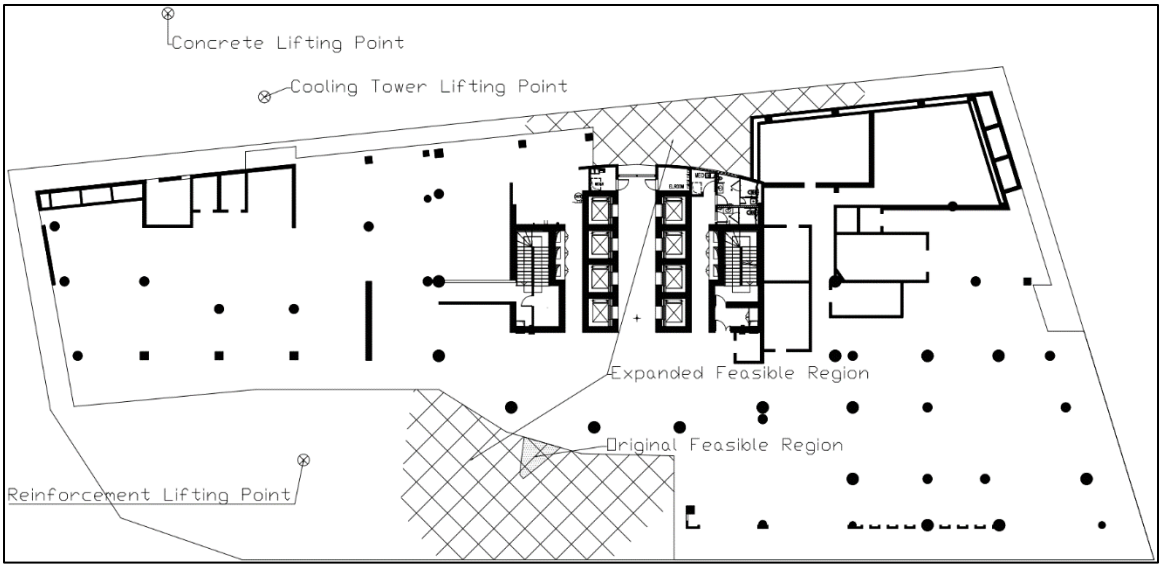

***Figure 50**: Expansion of Feasible Region with 60-Meter Jib*

It should be noted that large parts of the expanded feasible region are infeasible because they don't allow for anchoring of the crane. However, the new region allows for the crane to be placed on the rear-side of the building and away from the street, which would have prevented the jib from swinging over AAU-SOC.

6. ANALYSIS AND DISCUSSION OF RESULTS

The purpose of the analysis below is to collectively analyze the results of the optimization to tackle the question of whether the crane placement techniques used by the contractors are appropriate.

The projects presented in Chapters 4 and 5 have been analyzed individually in their respective sections. Table 26 summarizes data related to the 6 projects which are used in the analysis that follows.

***Table 26**: Summary of Results*

PROJECT	JIB LENGTH (m)	WEIGHT OF LARGEST INDIVISIBLE LOAD (kg)	JIB LENGTH FOR INDIVISIBLE LOAD (m)	FEASIBLE REGION'S AREA (m^2)	Δ DISTANCE (m)
CBE-HQP	60	6898	40.619	19.953	0
NI-HQP	50	0*	50	133.607	2.819
Marriott Hotel	60		60	11.752	3.200
ZB-HQP	60		60	181.150	1.943
NIB-HQP	73		73	688.274	4.486
UB-HQP	50	1300	50	6.222	0.677

** Only CBE-HQP and UB-HQP lifted indivisible loads using the tower crane.*

The areas of all the feasible regions don't include the effect of any other constraints such as anchoring requirements and other facilities that could have been present in the feasible area. Based on the information presented in the preceding chapters, and the interviews conducted with the various stakeholders in the projects after the optimization, the question of whether the techniques employed by the contractors being efficient can be answered.

6.1. Size of Feasible Region and Impact on Results

All the projects managed to place their crane within the feasible region. However, without a mathematical optimization technique, projects with larger feasible regions were prone to placing the tower crane at a sub-optimal location. Except for CBE-HQP, a larger feasible region corresponded to a larger difference in distance from the optimal location that was generated to the actual position of the tower crane. Therefore, the traditional crane location selection techniques are prone to errors, especially when the feasible region is large since this provides the contractor with more options.

Since traditional techniques are prone to errors, it is important to verify the results scientifically. The technique used in this research has been shown to be effective, and in the future, it can be used to either find the mathematically optimal location or to ensure that the position found using traditional techniques accurate. CBE-HQP is an outlier because the location of the region left only 2 columns available for the anchoring requirement. Therefore, there was no other logical position for the crane. This was the result of the effective jib length imposed by the steel columns which will be discussed in Section 6.2.

The analysis performed in this study is based on the available tower crane and site conditions. In some cases, the crane's capacity approaches the limits of the project's needs. For example, UB-HQP used a 50-meter crane, and CBE-HQP lifted steel columns that nearly exceeded the crane's capacity for the far side of the buildings. This restricts the ability of the contractors to freely utilize their tower cranes and can increase the risks of the crane exceeding its operating limits and endangering and safety of people on site.

6.2. Crane Placement Techniques

The questions of who selected the crane's position, and how they reached that decision was an important factor. Of the 5 contractors and 6 projects analyzed, CSCEC which is constructing the CBE-HQP project is the only contractor that employed a scientific technique in deciding upon a location for their tower crane. An initial mechanical team was

responsible for the selection of the tower crane and its position prior to the construction of the foundations. This team considered the effect that the crane would have on the piles it rested on and made sure that the crane could lift the steel columns.

In part, this attention to detail can be attributed to the size and experience of the contractor, and the prestige associated with the construction of a landmark building in Addis Ababa. The use of structural steel columns for the first 30 floors of the building also made the placement a critical issue, forcing the contractor to think critically about the placement of the crane. If the crane was unable to lift the columns and deliver them to the desired location, the contractor would have been forced to take expensive remedial measures such as having to cut the columns into smaller pieces.

By comparison, NI-HQP's crane's position was determined by an inexperienced mobilization team, and the contractor used the only available crane at the time instead of one that was appropriate for the project.

Another component of crane placement technique is the decision of whether to anchor the crane to the slab or to the beam. Only CBE-HQP and NI-HQP anchored their crane to the columns, and in both cases the class of concrete was already high enough to support the anchoring. In the other 4 cases where the crane was anchored to the slab, the contractor was forced to increase the class of concrete in the area that surrounds the anchoring plates.

This has a second effect on the results as well: if the crane is to be anchored to a pair of columns, the feasible region is automatically limited to a discrete set of locations which must be equidistant to a pair of columns, and within the feasible region. For example, the CBE-HQP crane could only be placed at one specific location, as shown in Chapter 4. If a tower crane is anchored to the slab instead, it increases the number of feasible locations, because as the UB-HQP case has shown, symmetrical positions of the anchoring arms isn't even a necessity.

6.3. Physical Jib Length

Among the projects surveyed, 60-meter cranes were the most common. However, UB-HQP and NI-HQP both used a Zoomlion 5013-B6 crane, with a 50-meter jib. For the NI-HQP project, the shape and size of the building allowed the feasible region to be large enough to allow the contractor to choose a location freely. However, in the UB-HQP project, the feasible region was severely restricted and had an area of 6.22 m^2. If a 60-meter jib had been used, a 336.2 m^2 feasible region would have been available. Even with large areas rendered off-limits by the anchoring requirement, it still marks a significant expansion. The main benefit of a larger feasible region was that it made the rear of the building feasible, placing the crane away from the street and adjacent buildings.

This effect was observed on the Marriott Hotel case study as well. With a 60-meter jib, the only feasible region was on the rear-side of the building, and if the contractor had placed the crane on the street-side as originally intended, it would have been unable to reach the demand points located on the extremes of the rear-side of the building.

While the crane used by the contractor for the UB-HQP project wasn't long enough, the crane used by the same contractor for the NIB-HQP project was too long. As discussed previously, a 73-meter jib was used by the contractor, which was shown to be too long for the site and managed to strike a nearby building, forcing the contractor to repair the building.

While a selection of a tower crane is beyond the scope of this thesis, it has great bearing on the outcomes of the analysis.

6.4. Effective Jib Length

The effects of the physical length of the cranes jib were discussed in the preceding section, however, the optimizations have shown that the effective jib length has as much effect on the optimization results as the capacity of the crane. This effect is of great concern for heavy indivisible loads such as the steel columns used in the CBE-HQP project.

While not explicitly coded into the algorithms, the following function affects the result:

$$Effective\ Jib\ Length\ (EQ.21) = \min(Actual\ Jib\ Length, Maximum\ Jib\ Length\ Determined\ by\ Load\ Radius\ Curve)$$

Taking the case of the CBE-HQP, the crane's actual jib length was 60 meters. However, the steel columns could only be carried to 40.619 meters from the tower. Therefore, the crane's effective jib length is reduced by 32.3%.

The effective jib length also affects divisible loads, but in a subtler manner. To illustrate this effect, the cases of ZB-HQP and Marriott Hotel will be considered:

ZB-HQP transported the concrete for the columns using a 1 m^3 bucket, which weighs 2500 kg, but the crane's capacity at the tip was 1540 kg. In fact, a full bucket could only be transported up to 42.05 meters along the jib. By comparison, for the Marriott Hotel project, a 0.5 m^3 bucket, which weighs 1300 kg when full was used. The crane has a capacity of 1500 kg at the tip, meaning the crane can transport the full bucket along the entire jib.

For divisible loads, a reduced effective jib length leads to increased travel time because the crane would need to make a larger number of trips with smaller loads. However, for an indivisible load, a reduced effective jib length limits the feasible region.

6.5. Suitability of Optimization Technique

The PSO algorithm performed admirably well and produced stable results. However, the results were made unstable in certain cases because the models were built using millimeters as units. With such a high degree of accuracy in measurement, a small change in the position of the crane can lead to large variations in the travel time. Practically speaking, the positions of objects on construction sites are rarely measured to such a high degree of accuracy.

Despite the variations in the results that occurred, the particles never "exploded" and the optimal locations that was generated was always within the expected area. This was in part due to the restriction imposed on the first generation of particles. By ensuring the initial particles were within the feasible region, it was possible to save computational power and time as well as avoid the explosion of particles.

Another factor which influenced the variation of the results was the size of the feasible region. For sites with small feasible regions, the results were remarkably stable compared to those with larger feasible regions. If the PSO algorithm is made to search a larger area, it finds it difficult to converge towards the same solution.

The optimization problem is analogous to the real-life swarms which inspired the algorithm, with the best food source for a swarm corresponding to the optimal crane location. Intuitively, searching a larger space for the best food source is a harder problem, and this was reflected in the performance of the PSO algorithm.

7. CONCLUSIONS AND RECOMMENDATIONS

7.1. Summary

The interviews, observations on construction sites and the optimization performed for the 6 case studies have been used to define the research questions put forward at the outset. The results for the 3 research questions/objectives raised in Chapter 1 of the thesis are as follows:

1. The first aim of this thesis was to find the tower crane location planning practices among high-rise building construction projects.

   It was found that the tools and techniques used varied greatly among the contractors. Of the 5 contractors engaged on the 6 projects studied, only CSCEC used a scientific method in selecting a location. While the other 4 used some rule of thumb or semi-scientific technique in selecting the position for their tower crane. The contract type for the CBE-HQP project also affects the contractor's decision-making process. Since the contractor in DB projects is responsible for both the design and construction of the building, it can decide on the placement of temporary facilities, including tower cranes ahead of the construction. By comparison, in a Design-Bid-Build (DBB) project, the contractor must make decisions regarding tower crane placements under the constraints imposed by the designs which are made by an external party.
2. The second aim of this thesis was to find the mathematically optimal location for a selected group of projects. In total, 5 construction projects undertaken by 4 different contractors were studied, and it was possible to generate a mathematically optimal location for all 5. One additional case study located away from the Financial District was used to check the external validity of the algorithms.
3. The final aim was to compare the mathematically optimal location with the actual location on site to see what lessons could be learnt. The mathematically optimal location was found for all 6 cases which were close to the actual location on the construction site and no drastically different results observed.

The best results were observed for the CBE-HQP project, for which the optimal and actual results were essentially identical. The worst result was recorded for the NI-HQP project's first tower crane, which had to be dismantled and replaced because it couldn't meet the project's needs in terms lifting radius and anchoring requirements.

Based on the interviews conducted with both contractors, the technical knowhow of the team that determined the location was a determinant factor. CBE-HQP's advance mechanical team confirmed the suitability of the location prior to the commencement of the construction. They worked with the crane's manufacturers and the buildings designers in determining the location. On the other hand, NI-HQP's crane position was determined by the mobilization team which lacked the required experience.

Beyond the research objectives, the following findings are also summarized:

1. Among the projects studied, the location selection for tower crane locations appears to be more scientific among foreign contractors. Sunshine Construction's first choice for the tower crane would have left the crane unable to service the edges of the building, and Rama Construction placed the crane at an unanchorable location, forcing a change in tower cranes midway through the project.
2. The effective jib length, and the actual jib length affected the size and position of the feasible region directly. In turn, this affected the optimal location.
3. Unless a crane's location is chosen well, a contractor can incur needless costs in dismantling and erecting a second crane or relocating the first crane.
4. Crowded sites restrict the contractor's ability to move around facilities and to freely choose a location for the tower crane. As shown in the ZB-HQP example, the neighboring UB-HQP plot forced China Wu Yi to offset its crane to minimize any interference and collision between their respective cranes.
5. The PSO algorithm has performed well for the task at hand. Reducing the accuracy of the model by using meters instead of millimeters would increase the stability while leaving the accuracy of the results unaffected.

7.2. Recommendations

The analysis of the 6 case-studies has shown that, contractors employ a range of techniques for determining the location of their tower cranes. Apart from CSCEC, the contractors didn't use a scientific technique in determining the tower crane's location.

Based on the results of the case studies and interviews with the contractors and consultants, the primary recommendation is that all the contractors should use a scientific optimization technique like that of CSCEC in selecting a location for their tower cranes.

Other recommendations are as follows:

1. Contractors should consider placing the tower crane within the building. This can increase the complexity of the dismantling process but could potentially lead to savings in travel time as shown in the NI-HQP case study.
2. Decisions regarding tower crane locations should be made by engineers with knowledge of the project including the site locations rather than by the mobilization team.
3. Site congestion should be reduced by moving unnecessary facilities such as material storage, offices, and concrete batching plants off-site. This can increase the potential number of tower crane locations and affords the contractor greater latitude in choosing supply points.

   Contractors can make use of tools such as prefabrication of structural elements and Just-In-Time (JIT) construction to maximize the amount of free space available on site. Both techniques allow materials to be brought to construction sites only when needed, reducing the space taken up by material storage facilities.
4. The physical length of the crane's jib determines the feasible region and the optimal location. Contractors should confirm that the jib length is appropriate for the project's demands.
5. Contractors which need to transport heavy indivisible loads, such as the steel columns used in the CBE-HQP project must confirm that the crane can lift and deliver these items safely.

6. Contractors should consider anchoring their tower cranes to beams and slabs instead of columns. This will increase the number of possible anchoring locations, as discussed in the CBE-HQP case study.
7. Beyond the projects surveyed, several private and public companies such as Ethiopian Electric Utility Company, Abay Bank, Bunna Bank are now building new headquarters throughout the city. The contractors for these projects and others can adopt the optimization techniques used in this research to either select a position for their tower crane or to verify a chosen location.

7.2.1. Areas of Further Research

The field of Construction Site Layout Optimization encompasses a wide range of problems. Additionally, there are a variety of optimization techniques that can be used.

The recommended areas of further research are:

1. Find solutions to a CSL problem, considering the position of supply points, offices and other temporary facilities in addition to the tower cranes. In this thesis, the locations of temporary facilities and supply points have been taken as constraints rather than decision variables. Optimizing their location can lead to more efficient construction.
2. Application of other optimization techniques, such as those discussed in the literature review to find the optimal location for the tower crane.
3. Simulation based analysis of concrete transportation using a tower crane compared to a concrete pump.
4. Optimization of the selection and assignment of tower cranes to specific projects. This can help contractors assign the appropriate crane to projects they are involved in based on the demands of the project and available tower cranes.
   This can solve problems such as the extreme length of the jib used in the NIB-HQP and the short jib used by the same contractor for the UB-HQP.
5. Expansion to multi-crane optimization problems.

6. Since the tools and techniques used in this thesis have been shown to be functional, it can be used to find the optimal location for a project prior to its placement instead of being used as a confirmatory tool.

REFERENCES

[1] I. Tommelein, R. Levitt and B. Hayes-Roth, "Site-Layout Modelling: How Artificial Intelligence Can Help?," *Journal of Construction Engineering & Management,* vol. 118, no. 3, pp. 594-611, 1992.

[2] Emporis GMBH, "High-Rise Building," Emporis GMBH, [Online]. Available: https://www.emporis.com/building/standard/3/high-rise-building. [Accessed 13 OCT 2018].

[3] A. W. Leung and C. Tam, "Models for Assessing Hoisting Times of Tower Cranes," *Journal of Construction Engineering & Management,* vol. 125, no. 6, pp. 385-391, 1999.

[4] M. A. Abdelmegid, K. M. Shawki and H. Abdel-Khalek, "GA Optimization Model for Solving Tower Crane Location Problem in Construction Sites," *Alexandria Engineering Journal,* pp. 519-526, 2015.

[5] A. Kaveh and Y. Vazirinia, "Tower Cranes and Supply Points Locating Problem Using CBO, ECBO, & VPS," *International Journal of Optimization in Civil Engineerings,* pp. 393-411, 2017.

[6] S. Hasan, A. Bouferguene, M. Al-Hussien, P. Gillis and A. Telyas, "Productivity & CO2 Emission Analysis for Tower Crane Utilization on High-Rise Building Projects," *Automation in Construction,* pp. 255-264, 2013.

[7] R. L. Peurifoy, C. J. Schexnayder and A. Shapira, Construction Planning, Equipment, and Methods, New York: McGraw-Hill, 2006.

[8] A. Shapira, G. Lucko and C. J. Schexnayder, "Cranes for Building Construction Projects," *Journal of Construction Engineering & Management* , pp. 690-700, 2007.

[9] H. Li and P. E. Love, "Site-Level Facilities Layout Using Genetic Algorithms," *Journal of Computing in Civil Engineering,* vol. 12, no. 4, pp. 227-231, 1998.

[10] L. Lien and M. Cheng, "Particle Bee Algorithm for Tower Cranes Layout with Materials Quantity Supply and Demand Optimization," *Automation in Construction,* pp. 25-32, 2014.

[11] S. RazaviAlavi and S. AbouRizk, "Site Layout and Construction Plan Optimization Using Integrated Genetic Algorithm Simulation Framework," *Journal of Computing in Civil Engineering,* 2017.

[12] K. Alkriz and J.-C. Mangin, "A New Model for Optimizing the Location of Cranes and Construction Facilities Using Genetic Algorithms," in *21st Annual ARCOM Conference*, London, 2005.

[13] P. Zhang, F. Harris, P. Olomolaiye and G. Holt, "Location Optimization for a Group of Tower Cranes," *Journal of Construction Engineering & Management,* pp. 115-122, 1999.

[14] C. Huang, C. Wong and C. Tam, "Optimization of Tower Crane and Material Supply Locations in a High Rise Building Site by Mixed-Integer Linear Programming," *Automation in Construction,* pp. 571-580, 2011.

[15] Liebherr-Werk , "630 EC-H 40 Litronic," Liebherr, Biberach an Der Riss, 2016.

[16] National Commission for the Certification of Crane Operators (NCCCO), "Tower Crane Reference Manual," NCCCO, Fairfax, 2014.

[17] Y. Shi, "Particle Swarm Optimization," *IEEE Neural Networks Society, Feature Article,* pp. 8-13, 2004.

[18] A. Hazem and J. Glasgow, "Swarm Intelligence: Concepts, Models & Applications," Queen's University, Ontario, 2012.

[19] J. Kennedy and R. Eberhart, "Particle Swarm Optimization," in *IEEE International Conference on Neural Networks*, Perth, 1995.

[20] Z. S. Nadoushani, A. W. Hammad and A. Akbarnezhad, "Location Optimization of Tower Crane and Allocation of Material Supply Points in a Construction Site Considering Operating and Rental Costs," *Journal of Construction Engineering & Management,* vol. 143, no. 1, 2017.

[21] China State Construction and Engineering Corporation, "Site Layout Drawings," CSCEC, Addis Ababa, 2018.

[22] T. Molla, Interviewee, *Interview with AAiT Client Representative Office, Deputy Resident Engineer*. [Interview]. Various.

[23] Engineering News Record, "Top 250 International Contractors," ENR, [Online]. Available: https://www.enr.com/toplists/2016-Top-250-International-Contractors1. [Accessed 28 DEC 2018].

[24] W. Bin, Interviewee, *Interview with CBEHQ Design Manager for CSCEC.* [Interview]. 03 Jan 2019.

[25] Shenyang Sanyo Building Machinery Co. Ltd., "Tower Crane (R75/25)," Shenyang Sanyo Building Machinery Co. Ltd., Shenyang.

[26] Occupational Safety and Health Branch, Labor Dept, "Code of Practice for Safe Use of Tower Cranes," HK Labor Department, Hong Kong, 2011.

[27] Wossen Architects PLC., "Tender Document Bill of Quantities: HQ Building for Nile Insurance Share Company," Wossen Architects PLC., Addis Ababa, 2015.

[28] A. Eshetu, Interviewee, *Follow Up Interview.* [Interview]. 6 Feb 2019.

[29] Zoomlion Heavy Industry Science & Technology Co. Ltd., "Zoomlion TC6513," Zoomlion, Hunan, 2017.

[30] E. Mereye, Interviewee, *Interview With ZBHQ Client Representative.* [Interview]. 27 Feb 2019.

[31] D. Abebe, Interviewee, *Interview with Office Engineer, Eskender Architects.* [Interview]. 18 Mar 2019.

[32] M. S. Kiran, "Particle Swarm Optimization With a New Update Mechanism," *Applied Soft Computing,* vol. 60, pp. 670-678, 2017.

[33] China State Construction and Engineering Corporation, "20th Floor Structural Drawings," CSCEC, Addis Ababa, 2018.

[34] Soima, "SGT5015TL," Soima, Senhorim.

[35] S. a. J. P. Seabold, "Statsmodels: Econometric and Statistical Modeling With Python," in *Proceedings of the 9th Python in Science Conference*, 2010.

[36] W. A. PLC, "Drawings: Site Layout, Second Floor Block B, Block A Typical," Wossen Architects PLC, Addis Ababa, 2015.

[37] Zoomlion Heavy Industry Science and Technology Co., Ltd., "Zoomlion TC5013B-6," Zoomlion, Changsha.

[38] Portland Cement Association (PCA), "Chapter 11, Batching, Mixing, Transporting & Handling Concrete," in *Design & Control of Concrete Mixtures, 14th Ed.*, Skokie, PCA, 2003, pp. 179-189.

[39] JDAW Consulting Architects & Engineers, "Zemen Bank HQ Office Building Architectural Working Drawings," JDAW Consulting Architects & Engineers, Addis Ababa, 2018.

[40] JDAW Architects & Engineers, "Zemen Bank HQ Building Project Specification and Bill of Quantity," JDAW Architects & Engineers, Addis Ababa, 2017.

[41] Nib International Bank, Client Representative's Office, "Structural Drawings: Ground, 20, 31," NIB, Addis Ababa, 2019.

[42] JDAW Consulting Engineers & Architects, "Marriott Hotel Structural Drawings," JDAW, Addis Ababa, 2019.

[43] Eskender Architects, "Union Bank HQ Structural Drawings," Eskender Architects, Addis Ababa, 2019.

APPENDIX 1: PROOF OF OVERLAP CONSTRAINT EQUATIONS

Proof of the overlap equations

$$Assume\ m = distance\ between\ the\ two\ objects\ in\ the\ x\ direction$$

$$m \in [-\infty, \infty]$$

$$Then\ c_2 = \frac{w_2}{2} + m + c_1 + \frac{w_1}{2}$$

$$dX_{12} = c_2 - c_1 = \frac{1}{2} * (w_2 + w_1) + m$$

$$\left(dX_{ij} - \frac{W_j + W_i}{2}\right) \times \left(dX_{ij} + \frac{W_j + W_i}{2}\right) becomes:$$

$$\left(\frac{1}{2}(w_1 + w_2) + m - \frac{1}{2}(w_1 + w_2)\right) * \left(\frac{1}{2}(w_1 + w_2) + m + \frac{1}{2}(w_1 + w_2)\right)$$

$$= (m) * (w_1 + w_2 + m) \quad [22]$$

$$if\ m < 0 \rightarrow [EQ\ 22] < 0$$

$$if\ m = 0 \rightarrow [EQ\ 22] = 0$$

$$if\ m > 0 \rightarrow [EQ\ 22] > 0$$

∴ The equation can check for overlaps in the *x* direction. Since the calculations are identical in the *y* direction, the proof can be extended in the *y* dimension as well.

APPENDIX 2: INTERVIEW QUESTIONS

Project Name	Contractor	Location	Total Cost	Floor Number	Building Height	# Tower Crane	Rental/Owned

Would you be willing to participate in the future and provide input for the thesis?

What is/was your crane location selection procedure?

- Who had input?
- Is there a procedure you follow to find a location? If so, what is it?

Information regarding the crane(s):

1. Crane Manufacturer and Model:
2. Maximum freestanding height and maximum height of the building under construction
3. Procedure to anchor to the structure
4. Maximum load that has been lifted by the crane
5. Jib length
6. Picture of load-radius curves
7. Procedure to anchor to the ground
8. Rental or sales prices
9. Operational costs
10. Cost to erect and dismantle the crane

APPENDIX 3: CREATION OF LOAD-RADIUS CURVES FOR CRANES

In order to replicate the load-radius curves, linear regression was used, with the load as the dependent variable and the length as the independent variable. The necessary data points are extracted from the crane's operating manual.

The regression with the highest R^2 value is selected, which in the selected example was 1.

OLS Regression Results

Dep. Variable:	Load	R-squared:	1.000
Model:	OLS	Adj. R-squared:	1.000
Method:	Least Squares	F-statistic:	1.444e+07
Date:	Thu, 08 Nov 2018	Prob (F-statistic):	0.000193
Time:	20:48:19	Log-Likelihood:	-8.1572
No. Observations:	5	AIC:	24.31
Df Residuals:	1	BIC:	22.75
Df Model:	3		
Covariance Type:	nonrobust		

	coef	std err	t	P>|t|	[0.025	0.975]
Intercept	1.347e+05	168.400	799.838	0.001	1.33e+05	1.37e+05
np.power(Radius, 1)	-8775.5587	19.808	-443.028	0.001	-9027.245	-8523.872
np.power(Radius, 2)	236.8096	0.752	314.958	0.002	227.256	246.363
np.power(Radius, 3)	-2.3079	0.009	-249.926	0.003	-2.425	-2.191

Omnibus:	nan	Durbin-Watson:	3.493
Prob(Omnibus):	nan	Jarque-Bera (JB):	0.414
Skew:	-0.254	Prob(JB):	0.813
Kurtosis:	1.685	Cond. No.	3.50e+06

***Figure 51**: Linear Regression Results*

According to the summary of the results, the formula for the line of best fit was:

$$Load = 134700 - 2.3079(Radius^3) + 236.81(Radius^2) - 8775.55(Radius)$$

Figure 9, in Chapter 3 includes the line of best fit and the points extracted from the crane's operating manual that visually proves the fit.

Note: The regression was performed using the statsmodels 0.9.0 package in Python 3.6

APPENDIX 4: CBE-HQP PROJECT MAIN TOWER BILL OF QUANTITY

All the quantities are calculated based on the drawings provided by the AAiT Client Representative's office.

The steel columns used for the first 30 floors of the structure are made of steel with a density of 8050 kg/m^3. Each column spans 3 floors, which means they each have a length of 11.4 meters. The cross-sectional area of the columns is 0.075166176 m^2. Therefore, each column weighs 6898 kg.

The formworks have a weight of 125 kg/m^2. Again, with a typical floor to floor height of 3.8 meters, the weights can be calculated by multiplying the length of each piece by 475 kg/m. The heaviest piece weight 3864.13 kg. Based upon the advice of the project's design manager, the weights of the formworks used for the columns, beams and slabs are not included in the optimization process because they are made of plastic of wood, making them significantly lighter when compared against the steel formworks.

APPENDIX 5: SHENYANG-SANYO R75/25 REGRESSION RESULTS

The following regression results were produced in the statsmodels 0.9.0 package of Python 3.6.

The following regression is for the Load-Hoisting Speed curve.

OLS Regression Results

Dep. Variable:	Speed	R-squared:	1.000
Model:	OLS	Adj. R-squared:	1.000
Method:	Least Squares	F-statistic:	2.476e+29
Date:	Wed, 24 Apr 2019	Prob (F-statistic):	1.28e-15
Time:	11:21:08	Log-Likelihood:	90.966
No. Observations:	3	AIC:	-177.9
Df Residuals:	1	BIC:	-179.7
Df Model:	1		
Covariance Type:	nonrobust		

	coef	std err	t	P>|t|	[0.025	0.975]
Intercept	161.3571	2.65e-13	6.1e+14	0.000	161.357	161.357
np.log(Load5)	-14.4270	2.9e-14	-4.98e+14	0.000	-14.427	-14.427

Omnibus:	nan	Durbin-Watson:	1.000
Prob(Omnibus):	nan	Jarque-Bera (JB):	0.531
Skew:	0.707	Prob(JB):	0.767
Kurtosis:	1.500	Cond. No.	149.

***Figure 52**: OLS Regression Results, Load-Hoisting Curve*

The following regressions are for the Load-Radius curves.

OLS Regression Results

Dep. Variable:	Load1	R-squared:	1.000
Model:	OLS	Adj. R-squared:	nan
Method:	Least Squares	F-statistic:	0.000
Date:	Wed, 24 Apr 2019	Prob (F-statistic):	nan
Time:	11:07:45	Log-Likelihood:	39.189
No. Observations:	3	AIC:	-72.38
Df Residuals:	0	BIC:	-75.08
Df Model:	2		
Covariance Type:	nonrobust		

	coef	std err	t	P>|t|	[0.025	0.975]
Intercept	0.0007	inf	0	nan	nan	nan
Radius1	4.8557	inf	0	nan	nan	nan
np.power(Radius1, 2)	-0.0003	inf	-0	nan	nan	nan
np.power(Radius1, 3)	5.92e-09	inf	0	nan	nan	nan

Omnibus:	nan	Durbin-Watson:	0.260
Prob(Omnibus):	nan	Jarque-Bera (JB):	0.339
Skew:	0.339	Prob(JB):	0.844
Kurtosis:	1.500	Cond. No.	3.54e+10

***Figure 53**: OLS Regression Result, Load-Radius, No. 1*

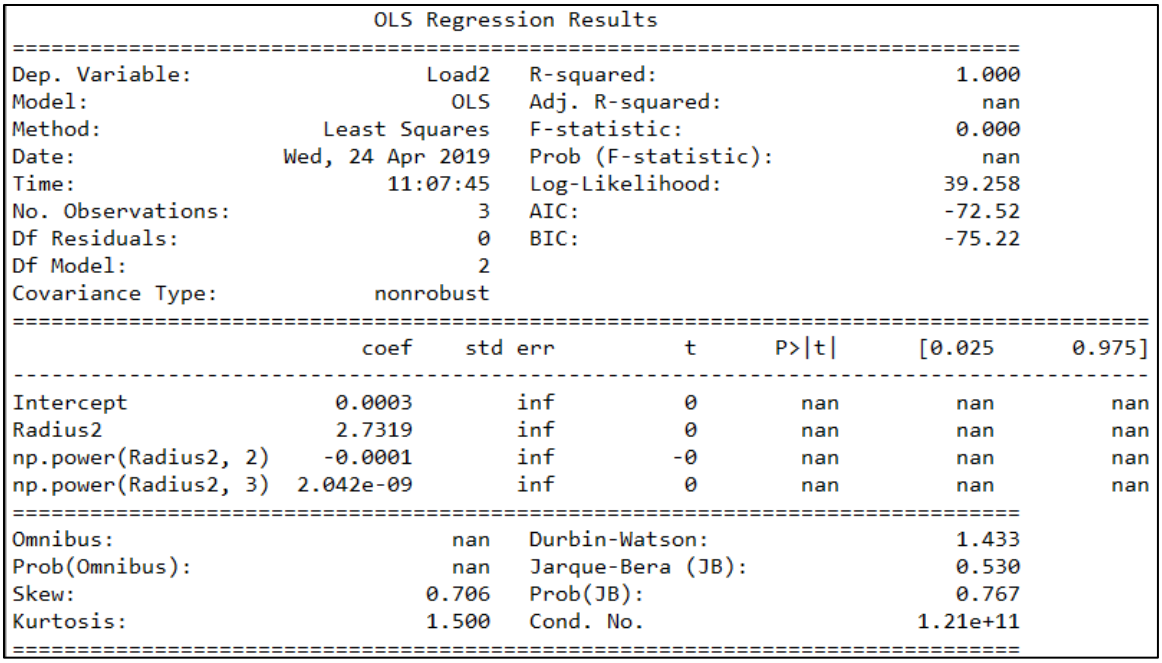

OLS Regression Results

Dep. Variable:	Load2	R-squared:	1.000
Model:	OLS	Adj. R-squared:	nan
Method:	Least Squares	F-statistic:	0.000
Date:	Wed, 24 Apr 2019	Prob (F-statistic):	nan
Time:	11:07:45	Log-Likelihood:	39.258
No. Observations:	3	AIC:	-72.52
Df Residuals:	0	BIC:	-75.22
Df Model:	2		
Covariance Type:	nonrobust		

	coef	std err	t	P>|t|	[0.025	0.975]
Intercept	0.0003	inf	0	nan	nan	nan
Radius2	2.7319	inf	0	nan	nan	nan
np.power(Radius2, 2)	-0.0001	inf	-0	nan	nan	nan
np.power(Radius2, 3)	2.042e-09	inf	0	nan	nan	nan

Omnibus:	nan	Durbin-Watson:	1.433
Prob(Omnibus):	nan	Jarque-Bera (JB):	0.530
Skew:	0.706	Prob(JB):	0.767
Kurtosis:	1.500	Cond. No.	1.21e+11

***Figure 54**: OLS Regression Result, Load-Radius, No. 2*

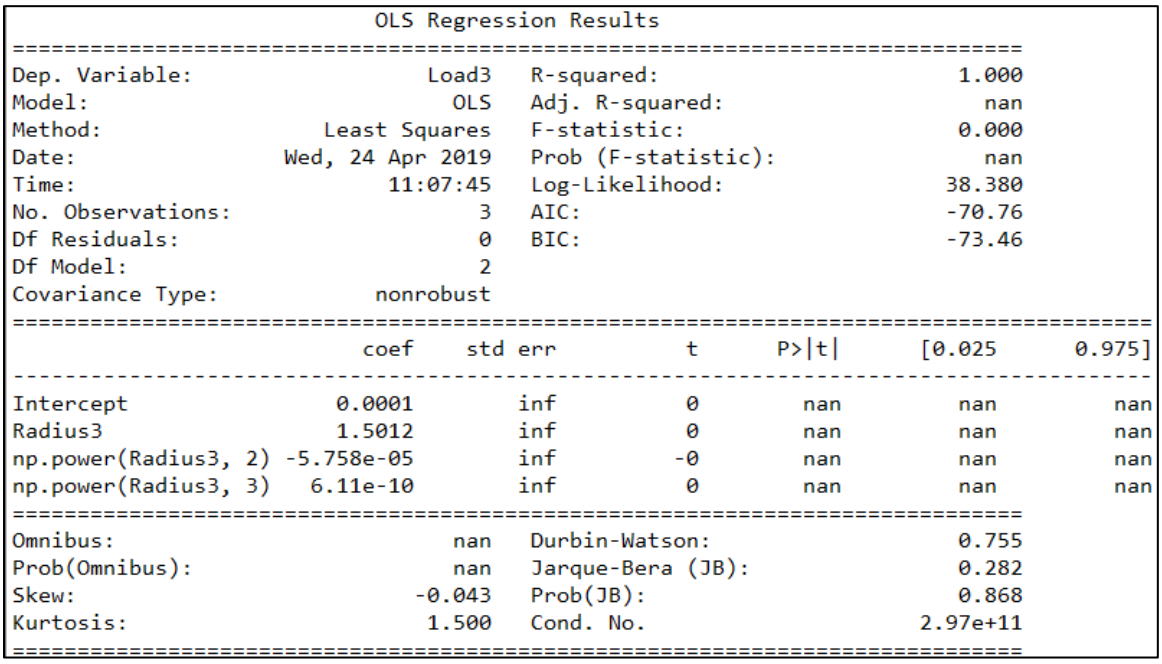

OLS Regression Results

Dep. Variable:	Load3	R-squared:	1.000
Model:	OLS	Adj. R-squared:	nan
Method:	Least Squares	F-statistic:	0.000
Date:	Wed, 24 Apr 2019	Prob (F-statistic):	nan
Time:	11:07:45	Log-Likelihood:	38.380
No. Observations:	3	AIC:	-70.76
Df Residuals:	0	BIC:	-73.46
Df Model:	2		
Covariance Type:	nonrobust		

	coef	std err	t	P>|t|	[0.025	0.975]
Intercept	0.0001	inf	0	nan	nan	nan
Radius3	1.5012	inf	0	nan	nan	nan
np.power(Radius3, 2)	-5.758e-05	inf	-0	nan	nan	nan
np.power(Radius3, 3)	6.11e-10	inf	0	nan	nan	nan

Omnibus:	nan	Durbin-Watson:	0.755
Prob(Omnibus):	nan	Jarque-Bera (JB):	0.282
Skew:	-0.043	Prob(JB):	0.868
Kurtosis:	1.500	Cond. No.	2.97e+11

***Figure 55**: OLS Regression Result, Load-Radius, No. 2*

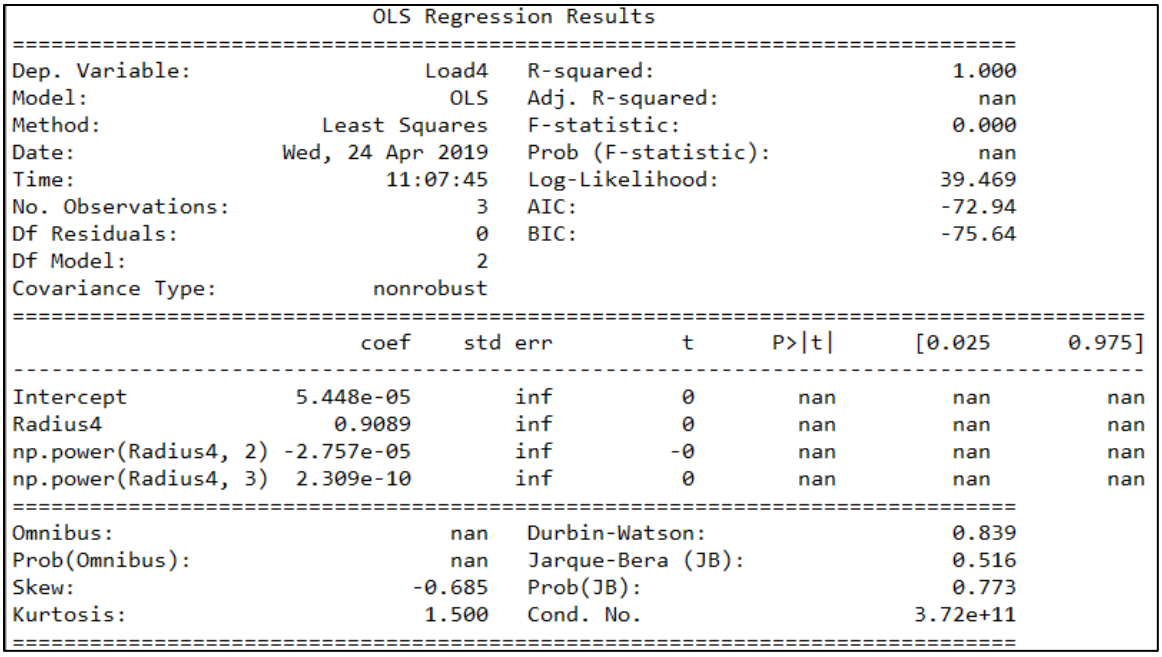

OLS Regression Results

Dep. Variable:	Load4	R-squared:	1.000
Model:	OLS	Adj. R-squared:	nan
Method:	Least Squares	F-statistic:	0.000
Date:	Wed, 24 Apr 2019	Prob (F-statistic):	nan
Time:	11:07:45	Log-Likelihood:	39.469
No. Observations:	3	AIC:	-72.94
Df Residuals:	0	BIC:	-75.64
Df Model:	2		
Covariance Type:	nonrobust		

	coef	std err	t	P>|t|	[0.025	0.975]
Intercept	5.448e-05	inf	0	nan	nan	nan
Radius4	0.9089	inf	0	nan	nan	nan
np.power(Radius4, 2)	-2.757e-05	inf	-0	nan	nan	nan
np.power(Radius4, 3)	2.309e-10	inf	0	nan	nan	nan

Omnibus:	nan	Durbin-Watson:	0.839
Prob(Omnibus):	nan	Jarque-Bera (JB):	0.516
Skew:	-0.685	Prob(JB):	0.773
Kurtosis:	1.500	Cond. No.	3.72e+11

***Figure 56**: OLS Regression Result, Load-Radius, No. 3*

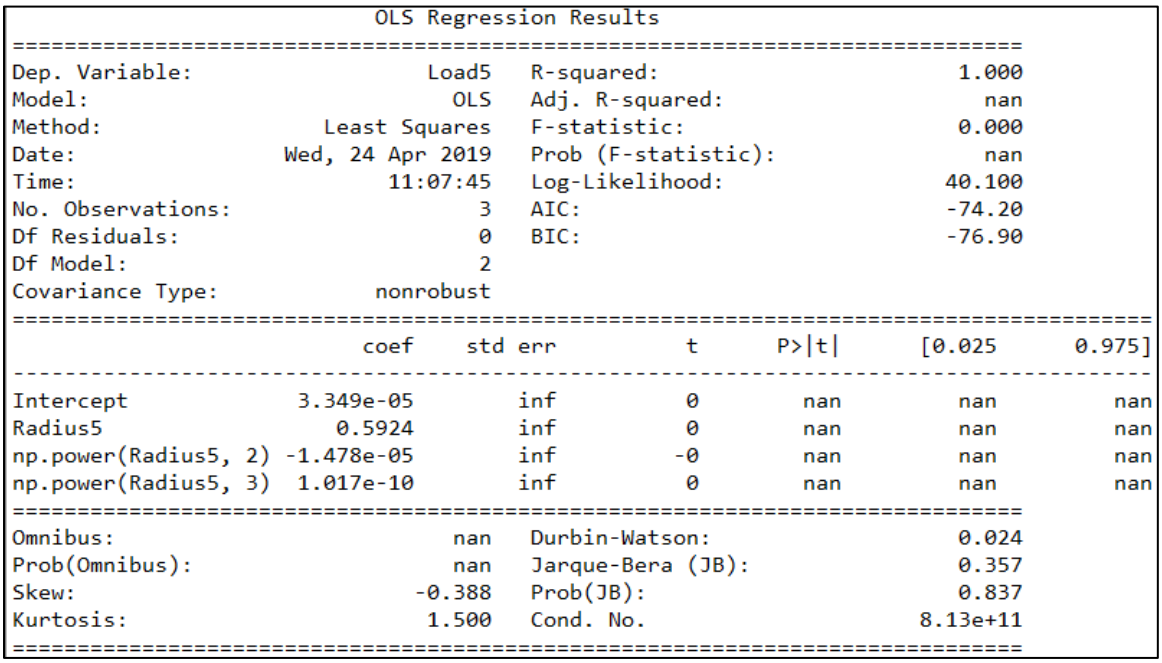

OLS Regression Results

Dep. Variable:	Load5	R-squared:	1.000
Model:	OLS	Adj. R-squared:	nan
Method:	Least Squares	F-statistic:	0.000
Date:	Wed, 24 Apr 2019	Prob (F-statistic):	nan
Time:	11:07:45	Log-Likelihood:	40.100
No. Observations:	3	AIC:	-74.20
Df Residuals:	0	BIC:	-76.90
Df Model:	2		
Covariance Type:	nonrobust		

	coef	std err	t	P>|t|	[0.025	0.975]
Intercept	3.349e-05	inf	0	nan	nan	nan
Radius5	0.5924	inf	0	nan	nan	nan
np.power(Radius5, 2)	-1.478e-05	inf	-0	nan	nan	nan
np.power(Radius5, 3)	1.017e-10	inf	0	nan	nan	nan

Omnibus:	nan	Durbin-Watson:	0.024
Prob(Omnibus):	nan	Jarque-Bera (JB):	0.357
Skew:	-0.388	Prob(JB):	0.837
Kurtosis:	1.500	Cond. No.	8.13e+11

***Figure 57**: OLS Regression Result, Load-Radius, No. 4*

The following regressions are for the Radius-Load curves.

OLS Regression Results

Dep. Variable:	Radius1	R-squared:	1.000
Model:	OLS	Adj. R-squared:	nan
Method:	Least Squares	F-statistic:	0.000
Date:	Wed, 24 Apr 2019	Prob (F-statistic):	nan
Time:	11:16:11	Log-Likelihood:	44.128
No. Observations:	3	AIC:	-82.26
Df Residuals:	0	BIC:	-84.96
Df Model:	2		
Covariance Type:	nonrobust		

	coef	std err	t	P>|t|	[0.025	0.975]
Intercept	5.462e+04	inf	0	nan	nan	nan
Load1	-3.4361	inf	-0	nan	nan	nan
np.power(Load1, 2)	7.493e-05	inf	0	nan	nan	nan

Omnibus:	nan	Durbin-Watson:	0.025
Prob(Omnibus):	nan	Jarque-Bera (JB):	0.519
Skew:	0.690	Prob(JB):	0.771
Kurtosis:	1.500	Cond. No.	1.03e+10

***Figure 58**: OLS Regression Result, Radius-Load, No. 1*

OLS Regression Results

Dep. Variable:	Radius2	R-squared:	1.000
Model:	OLS	Adj. R-squared:	nan
Method:	Least Squares	F-statistic:	0.000
Date:	Wed, 24 Apr 2019	Prob (F-statistic):	nan
Time:	11:16:11	Log-Likelihood:	39.335
No. Observations:	3	AIC:	-72.67
Df Residuals:	0	BIC:	-75.37
Df Model:	2		
Covariance Type:	nonrobust		

	coef	std err	t	P>|t|	[0.025	0.975]
Intercept	1.439e+05	inf	0	nan	nan	nan
Load2	-19.8231	inf	-0	nan	nan	nan
np.power(Load2, 2)	0.0008	inf	0	nan	nan	nan

Omnibus:	nan	Durbin-Watson:	0.002
Prob(Omnibus):	nan	Jarque-Bera (JB):	0.295
Skew:	-0.165	Prob(JB):	0.863
Kurtosis:	1.500	Cond. No.	1.59e+10

***Figure 59**: OLS Regression Result, Radius-Load, No. 2*

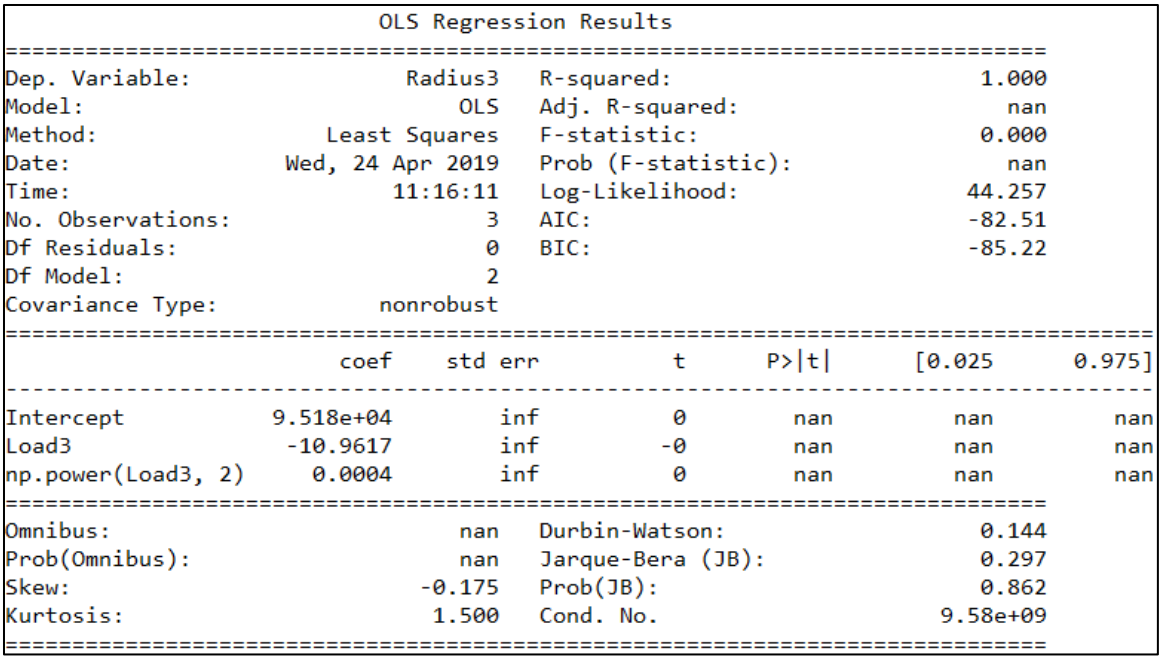

OLS Regression Results

Dep. Variable:	Radius3	R-squared:	1.000
Model:	OLS	Adj. R-squared:	nan
Method:	Least Squares	F-statistic:	0.000
Date:	Wed, 24 Apr 2019	Prob (F-statistic):	nan
Time:	11:16:11	Log-Likelihood:	44.257
No. Observations:	3	AIC:	-82.51
Df Residuals:	0	BIC:	-85.22
Df Model:	2		
Covariance Type:	nonrobust		

	coef	std err	t	P>|t|	[0.025	0.975]
Intercept	9.518e+04	inf	0	nan	nan	nan
Load3	-10.9617	inf	-0	nan	nan	nan
np.power(Load3, 2)	0.0004	inf	0	nan	nan	nan

Omnibus:	nan	Durbin-Watson:	0.144
Prob(Omnibus):	nan	Jarque-Bera (JB):	0.297
Skew:	-0.175	Prob(JB):	0.862
Kurtosis:	1.500	Cond. No.	9.58e+09

***Figure 60**: OLS Regression Result, Radius-Load, No. 3*

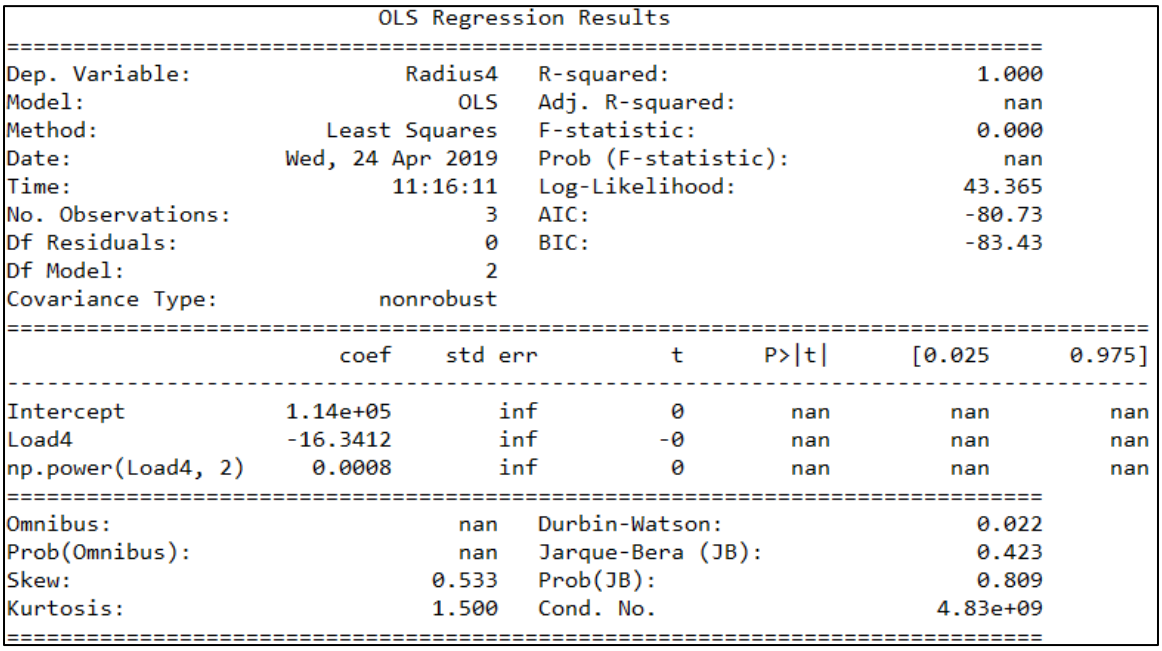

OLS Regression Results

Dep. Variable:	Radius4	R-squared:	1.000
Model:	OLS	Adj. R-squared:	nan
Method:	Least Squares	F-statistic:	0.000
Date:	Wed, 24 Apr 2019	Prob (F-statistic):	nan
Time:	11:16:11	Log-Likelihood:	43.365
No. Observations:	3	AIC:	-80.73
Df Residuals:	0	BIC:	-83.43
Df Model:	2		
Covariance Type:	nonrobust		

	coef	std err	t	P>|t|	[0.025	0.975]
Intercept	1.14e+05	inf	0	nan	nan	nan
Load4	-16.3412	inf	-0	nan	nan	nan
np.power(Load4, 2)	0.0008	inf	0	nan	nan	nan

Omnibus:	nan	Durbin-Watson:	0.022
Prob(Omnibus):	nan	Jarque-Bera (JB):	0.423
Skew:	0.533	Prob(JB):	0.809
Kurtosis:	1.500	Cond. No.	4.83e+09

***Figure 61**: OLS Regression Result, Radius-Load, No. 4*

OLS Regression Results

Dep. Variable:	Radius5	R-squared:	1.000
Model:	OLS	Adj. R-squared:	nan
Method:	Least Squares	F-statistic:	0.000
Date:	Wed, 24 Apr 2019	Prob (F-statistic):	nan
Time:	11:16:11	Log-Likelihood:	43.272
No. Observations:	3	AIC:	-80.54
Df Residuals:	0	BIC:	-83.25
Df Model:	2		
Covariance Type:	nonrobust		

	coef	std err	t	P>|t|	[0.025	0.975]
Intercept	1.369e+05	inf	0	nan	nan	nan
Load5	-24.7608	inf	-0	nan	nan	nan
np.power(Load5, 2)	0.0016	inf	0	nan	nan	nan

Omnibus:	nan	Durbin-Watson:	0.001
Prob(Omnibus):	nan	Jarque-Bera (JB):	0.372
Skew:	-0.426	Prob(JB):	0.830
Kurtosis:	1.500	Cond. No.	4.09e+09

***Figure 62**: OLS Regression Result, Radius-Load, No. 5*

APPENDIX 6: MARRIOTT HOTEL ADDIS ABABA PROJECT

Marriott Hotel is a 5-star hotel project, which is being built by Sunshine Construction PLC. in the Bole Medhanialem Area of Bole Sub-City. The project has an approximate cost of 3 billion ETB (108 Million USD). The G+11 building has a height of 67.55 meters that uses 1 tower crane: a Soima 6015TL, with a 60-meter-long jib that has a maximum capacity of 4 tons close to the tower, and 1.5 tons at the tip. Several local and foreign consultants participated in the design of the project, with JDAW Consulting Architects & Engineers serving as the main design consultant. This case study is located away from Financial District, and the results are used to test the external validity of the model.

The drawings and quantities presented below are courtesy of Sunshine Construction PLC.

Background and Model Information

The Marriott Hotel project has 2 unique features, which makes it an interesting project to analyze. The first is the shape of the building, which changes after the 3rd floor and becomes slimmer, while the second is the reliance of the crane to transport all the concrete used in the project.

The building's slimmer profile after the 3rd floor limits the feasible region because if the crane is placed on the rear-side (South-West), it is too far to allow for anchoring. However, the crane was placed on the rear side of the building, far away from the taller side of the building because the front side of the building had a cave-in during excavation and the crane couldn't be placed on the front side at the time. The anchoring beams provided by the crane's manufacturer cannot be used due to the extreme length from the crane to the building. Figure 63 shows the wires and custom-built steel anchoring pieces used to anchor the crane to the slimmer part of the building. Additionally, the crane is anchored on the 3rd floor using the manufacturer's anchoring. In both cases, the crane has been anchored to the slab.

***Figure 63**: Anchoring of Marriott Hotel Tower Crane Using Wires*

The results of the optimization will be used to check if it is possible to place the crane under the current site layout, and what effects moving the supply points closer to the building has on the results. If a better location is found on the street-side of the building, it would confirm the initial choice of the contractor.

Crane Utilization

The tower crane was mainly used to transport the reinforcement and concrete needed for the building. Additionally, the crane was sporadically used to transport pieces of formwork. The project is unique among those studied in this thesis because in the absence of a concrete pump, all the concrete used in the project was transported using a bucket with a capacity of 0.5 m^3. This included C50 columns of varying dimensions, and a C40 slab which is 27 cm thick. The challenges in modelling the transportation of a large volume of concrete using a bucket, and the modelling techniques applied are discussed in Section 5.2.3.

Tables 17 and 18 summarize the total quantities of reinforcement and concrete used throughout the project. The quantities of reinforcement and concrete were provided by the contractor.

***Table 27**: Marriott Hotel Reinforcement Requirement*

BAR DIAMETER (mm)	QUANTITY (kg)
ϕ 8	46,271.48
ϕ 10	228148.48
ϕ 12	850,214.22
ϕ 14	893,703.72
ϕ 16	1,449,988.52
ϕ 20	193,434.78
ϕ 24	259,457.74
ϕ 32	112,528.95
TOTAL	4,033,748.28

***Table 28**: Marriott Hotel Concrete Requirement*

FLOOR	CONCRETE QUANTITY (m^3)
Mezzanine	670.47
1	929.24
2	577.61
Mech	795.42
3	777.21
4	563.8
5→Roof	3,488.0

Following the approach employed for the NI-HQP model, the total steel quantity is divided among the floors based on the proportions of the floor area.

Transportation of Large Volumes of Concrete with a Crane

Transporting small quantities of concrete using a crane is common practice despite its inefficiency. However, as the volume of concrete that needs to be transported increases, it becomes a more challenging task that requires significant planning and coordination.

In the absence of a concrete pump, Sunshine Construction transports all the concrete for its Marriott Hotel project using the tower crane. This practice is unique among the projects surveyed where most of the concrete used is transported using a pump except for columns.

Unlike the NI-HQP project, the number of demand points for the concrete is significantly larger because the concrete required for the slab must be transported using the crane. The building is also longer along one of its axes, and some of the demand points are located on the far edges of the structure, making them far from the crane. According to the contractor, there were only 2 points that could be considered for the placement of the crane: both of which are along the center line.

Two types of demand points are used to model the transportation of concrete using a tower crane. The concrete for columns must be transported exactly to the required location as done in the previous model for NI-HQP. The concrete for the slabs must be distributed across the slab to mimic the functioning of the crane. However, there is no known exact location to which the concrete can be delivered to and the location to which the concrete is delivered is dependent on the foreman and the crane operators.

To approximate the delivery of concrete for the casting of the slab, each floor is divided into a grid, with each cell in the grid receiving a corresponding volume of concrete based on its area. Clearly, increasing the number of cells would increase the accuracy of the model, but such an approach would lead to a dramatic increase in the computational time and power expended. The combination of the crane's capacity at the tip of the jib and the use of a 0.5 m^3 bucket allows the crane to utilize its entire jib length with a full bucket. However, the use of a small bucket meant that a larger number of trips was required to complete the casting. According to the contractor, a typical slab took 7-10 days to complete.

Summary of Model

As discussed in the previous section, the concrete for the slab must be transported to cells that are spread out throughout the slab. The concrete for the columns is transported directly to the required locations. As a means of reducing the complexity of the model, the reinforcement used is also be directed to the cells, rather than to other demand points. As with the NI-HQP model, the concrete for the vertical elements is transported to the precise location at which it is needed.

Unlike the previous models, the complex shape of the building and the plot meant that in order to accurately represent the conditions, a larger number of rectangular and triangular objects had to be used. Additionally, the slab concrete grid introduced a large number of demand points. Several steps have been taken to mitigate their effect within the model.

The temporary offices for the contractor are in an area outside the feasible region and can have no impact on the results of the optimization. Therefore, they have been omitted from the model to reduce its complexity. The off-limits areas are made complicated for this project by the presence of multiple corners which must be broken up into a group of triangles and rectangles. An attempt was made to reduce the number of triangular and rectangular objects, again to reduce the complexity of the model.

The grid shown on the following page represents a breakdown of the floors with the largest floor area. Of the 11 floors, only the 3rd floor slab has no openings. In the other cases, there is a change in the floor area such as the 4th to the 11th floors, or there are several openings in the slab to suit the architectural needs of the projects. In cases where there is an opening in the slab, the cells which correspond to the opening are omitted, meaning no concrete is sent to that point. The building adopts a typical layout beyond the 4th floor, as all the space is dedicated to guest rooms. The model for this area is identical, except for changes in the vertical position.

Figure 64 shows a drawing of the building, including the slab concrete delivery cells and the columns.

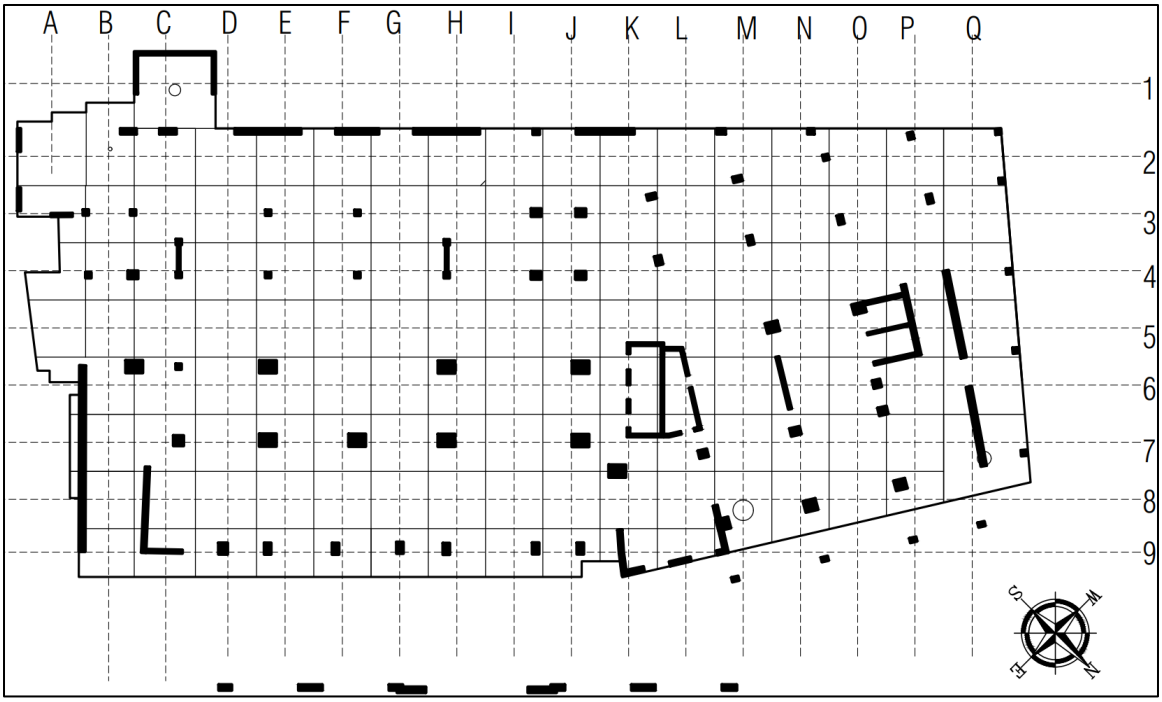

***Figure 64**: Marriot Hotel Columns and Slab Grid*

The table below summarizes the inputs for the Marriott Hotel optimization model.

***Table 29**: Marriott Hotel Model Inputs*

INFORMATION	PURPOSE	FILE NAME
Site Boundaries	The boundaries of the hotel have no impact on the results due to the positioning of the building. However, they have been included for reference.	NI-HQP_SITE_BOUNDS.csv
Off-limit Areas	No off-limit areas have been included based on site conditions. However, an artificial off-limits area object is used to render the rear-side of the building artificially infeasible to test Scenario B.	OffLimitAreas_MH.csv OffLimitAreas_MH_ScenarioB.csv
Demand Points	The x and y coordinates of the demand points along with the required loads. The concrete is transported to the positions of the columns or the slab grid. This file includes the z-positions of all the demand points as well.	WorkInfo_Marriott.csv
Supply Location	The points on the ground from where the loads are lifted.	Supply.csv
Floor Heights	This file is unused as all the z-positions are included directly in the Demand Points.	FloorHeights.csv

Based on the information presented in the previous sections, a model for the optimization algorithm that was generated in Python is presented in Figure 65.

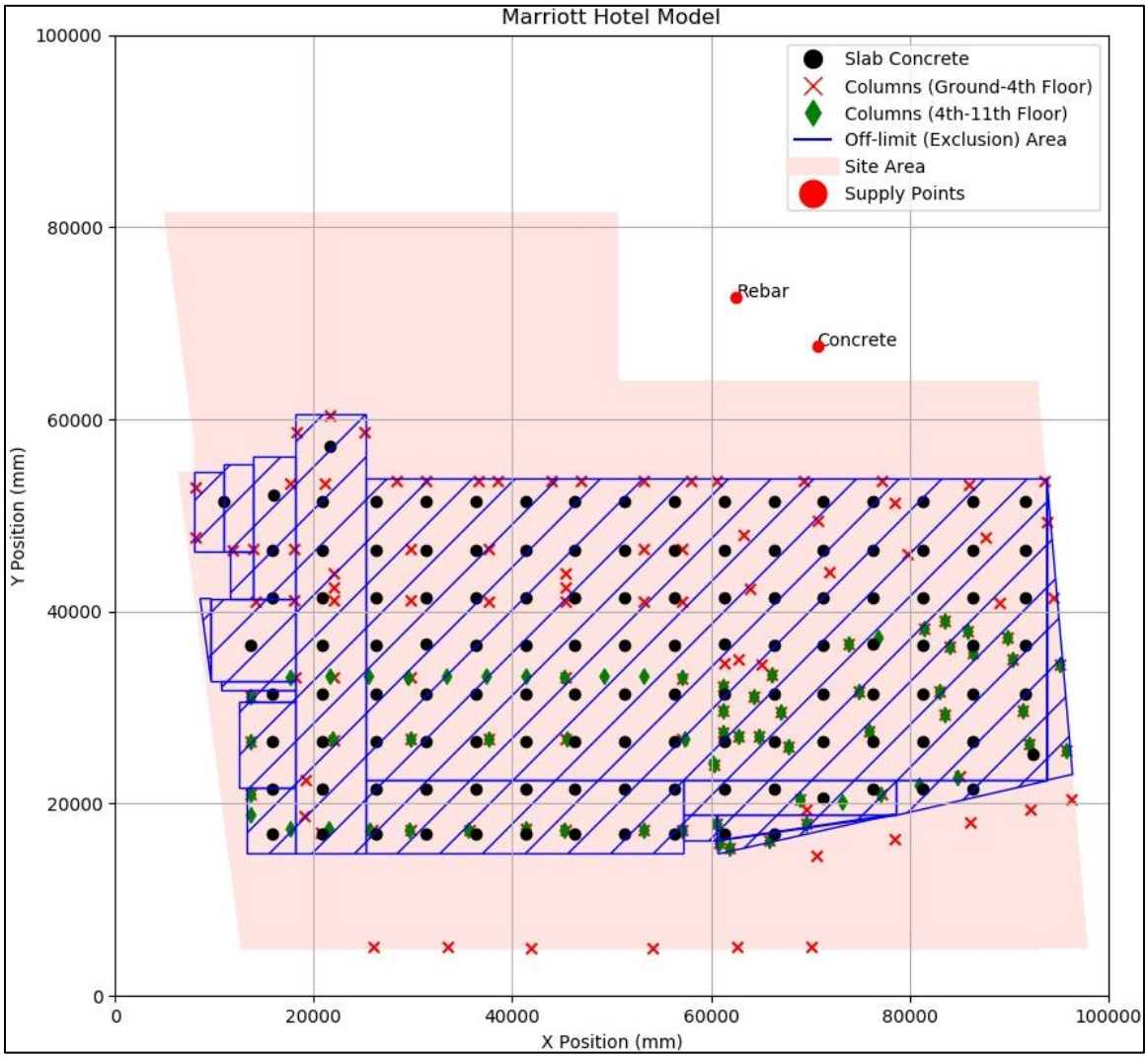

***Figure 65**: Marriott Hotel Site Model*

Optimization Results

The optimization is run under 2 scenarios:

- Scenario A: In the base scenario, the optimization is run with conditions found on the construction site and;
- Scenario B: The concrete and reinforcement lifting points are brought closer to the building, allowing the feasible region on the street-side of the building to become larger. The area on the rear side of the plot is rendered artificially infeasible as well.

The benefit of using a crane and bucket to transport concrete allows for the trucks to be parked at any location which is convenient for the contractor. Similarly, the reinforcement can be moved closer to the building because it is transported to the actual supply point using trucks and there is space available closer to the building. The alternative locations are based on the advice of the contractor. This hypothetical scenario is modelled using Scenario B.

Under Scenario B, the result would allow the crane to be anchored to the taller side of the building using the anchoring equipment provided by the contractor.

The results of the optimization are presented in Table 30 and Figure 66.

***Table 30**: Marriott Hotel Optimization Results, Scenario A*

RUN NO.	1	2	3	**4**	5	**6**	**7**	8	9	10	μ	σ	μ / σ (%)
X (mm)	49259.1	49259.7	49259.1	49259.1	49259.1	**49259.1**	49259.1	49259.1	49259.1	49259.1	49259.2	.16995	.345E-3
Y (mm)	57724.9	57725.0	57724.9	57724.9	57724.9	**57724.9**	57724.9	57724.9	57724.9	57724.9	57724.9	.0290	.050E-3
TIME (min)	284114.123	284115.162	284114.160	284114.203	284114.290	**284114.106**	284114.170	284114.239	284114.414	284114.158	284114.302	.2980	.105E-3

** Optimal Result*

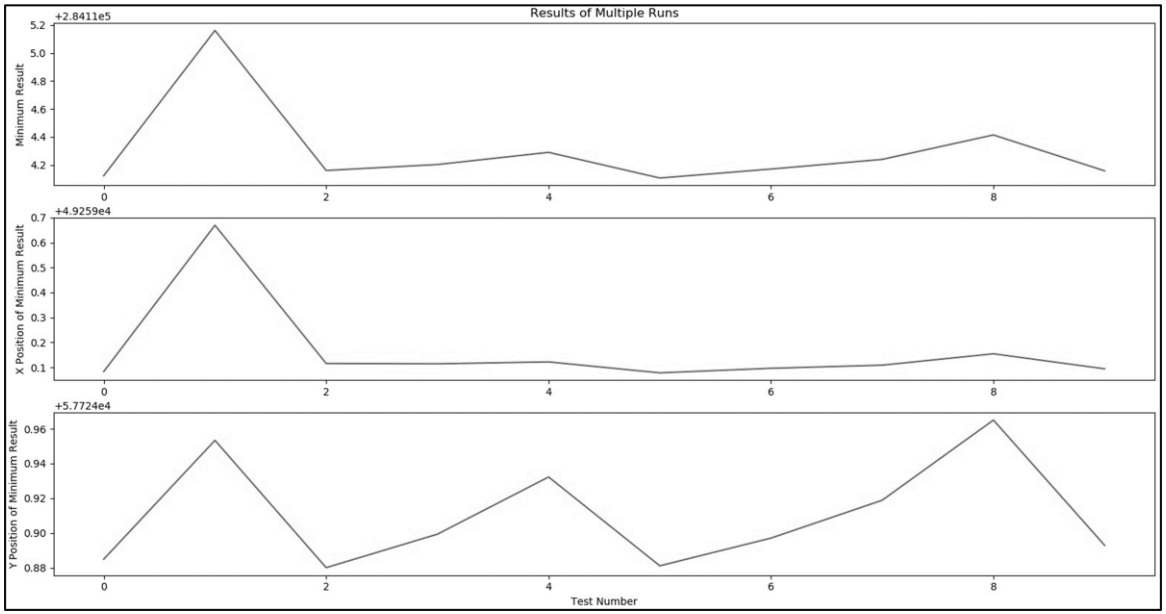

***Figure 66**: Marriott Hotel Optimization Results, Scenario A*

Figure 67 shows the optimal location on the rear-side of the building, with no feasible region on the North-East side of the building.

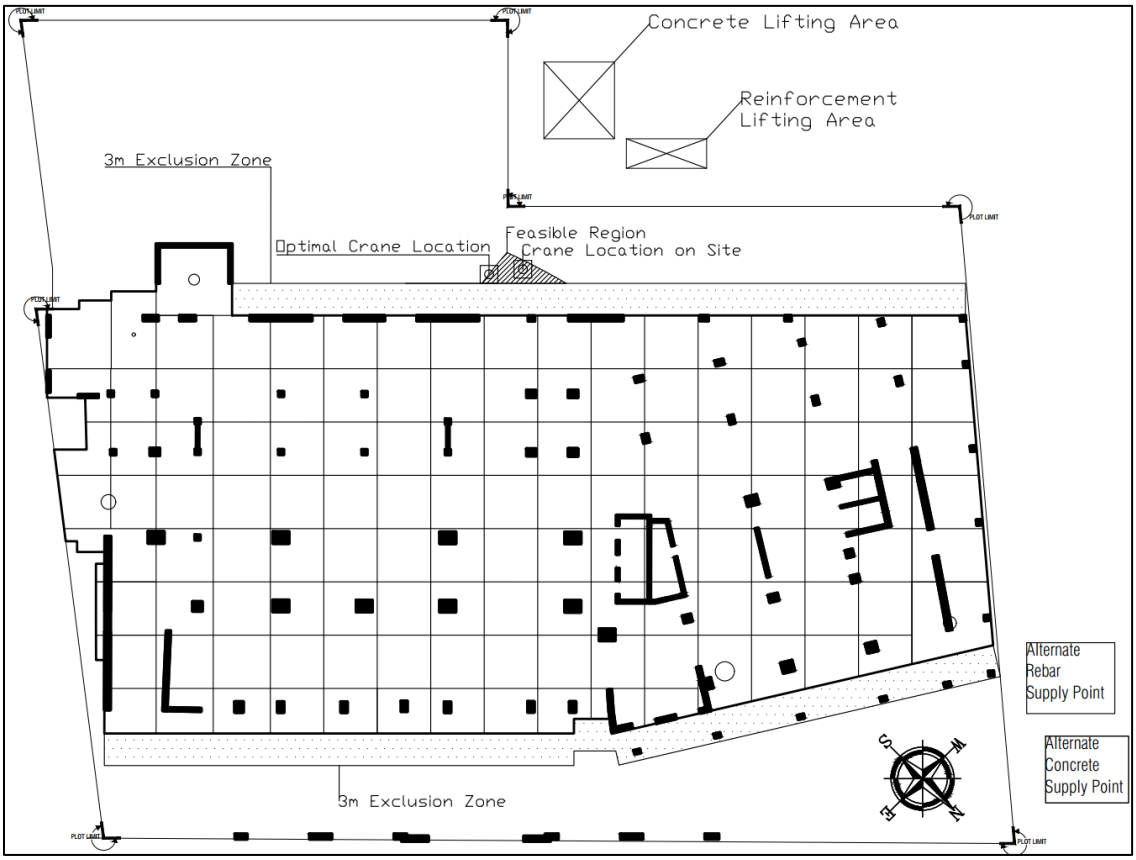

***Figure 67**: Marriott Hotel Optimization Results*

Under Scenario B, there was no feasible region under the actual site conditions. An attempt was made to create a feasible region by moving the supply points to alternate locations on the North-West side of the plot as suggested by the contractor. Even under this scenario, it was impossible to generate a feasible region, therefore, it is impossible to place the crane on the street-side of the building.

Discussion

The results for Scenario A confirm that the crane has been placed on the correct position, despite the difficulties that were encountered during anchoring. The results also show that the only optimal location for the crane would be near the middle of the longer axis. If the crane was placed away from the center, it would be unable to reach the columns at the edges of the building.

While there is a feasible region on the street-side of the building, it is impossible to place the crane on the street-side of the building because any position on that side would place the base of the crane closer to the building than permitted. This hypothesis was tested by making the rear-side of the building artificially infeasible and the algorithm was unable to generate feasible locations, proving it correct. The effects of the increased distance between the street-side of the building and supply points can be visualized using the size of the feasible region

The lack of a feasible region under Scenario B invalidates the contractor's initial decision to place the crane on the North-East side of the building. Even with the supply points moved, a feasible region couldn't be created. Had the contractor placed the crane on the street-side, it would have been unable to serve the extremes of the building.

APPENDIX 7: NIB-HQP OPTIMIZATION VISUALIZATIONS

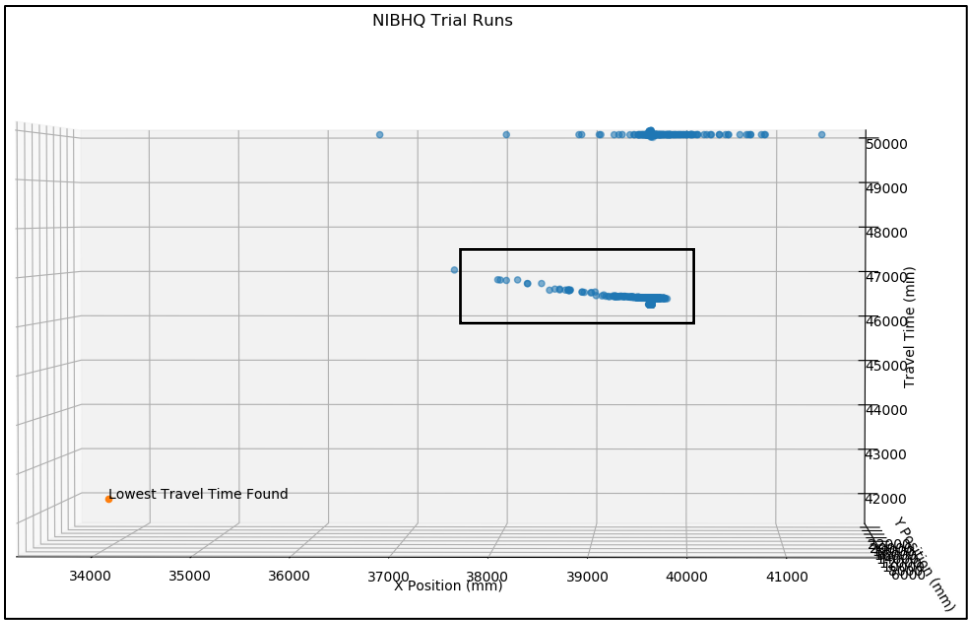

***Figure 68**: NIB-HQP, Trial Run 1*

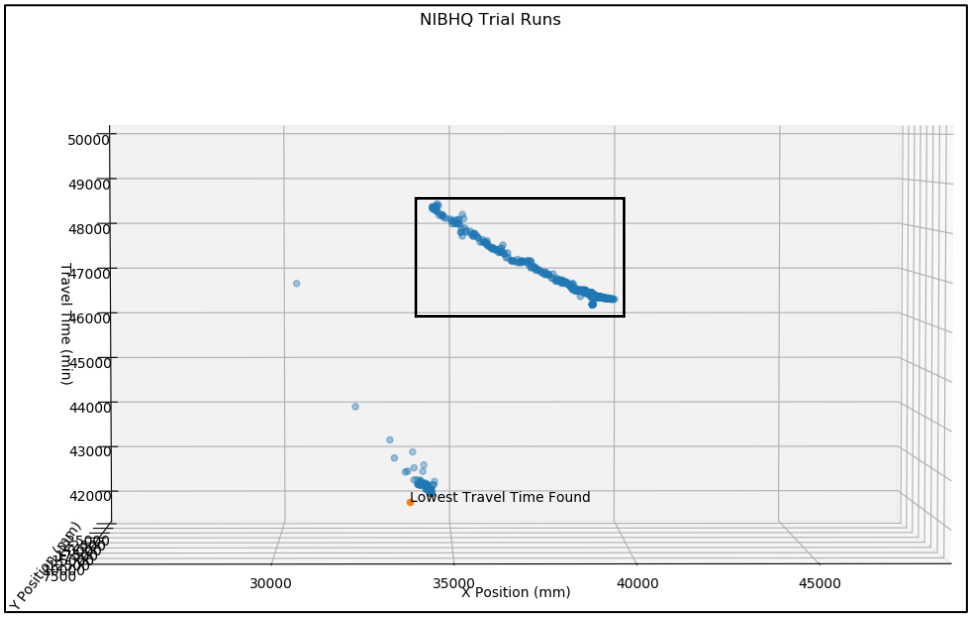

***Figure 69**: NIB-HQP, Trial Run 2*

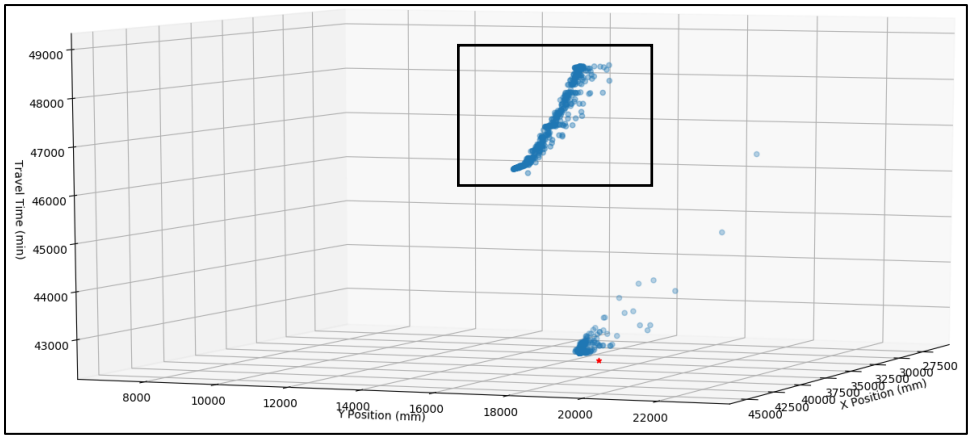

***Figure 70**: NIB-HQP, Trial Run 3*

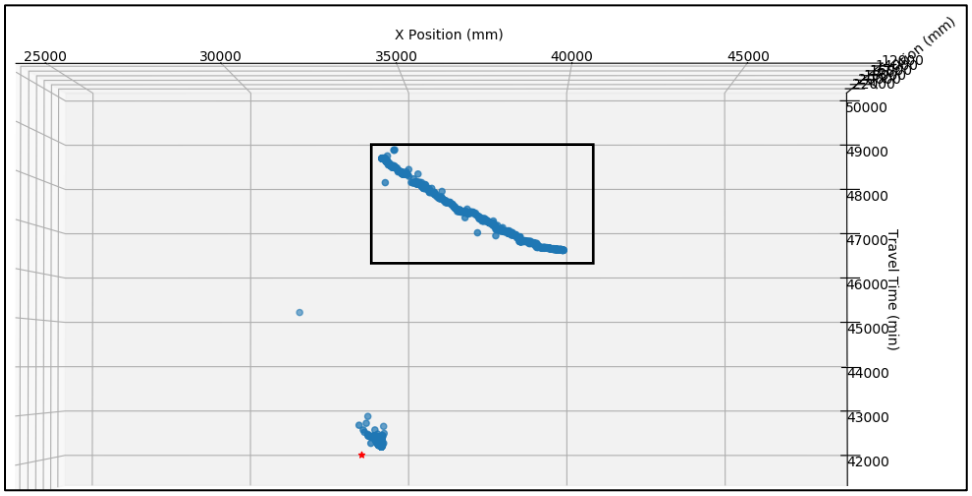

***Figure 71**: NIB-HQP, Trial Run 4*

The global minima are shown in all the diagrams as the red dot. In all the runs, it is found to be lower than all other points. Therefore, it can be concluded with reasonable confidence that the result presented in Section 5.4 is the global minima.

As hypothesized previously, the reason for the instability of the results was the presence of a local minima. The area containing the local minima is shown within rectangular boxes. The presence of local minima is visually confirmed, which explains the variation in the results as the particles are pulled towards the local rather than the global minima.

APPENDIX 8: SUMMARY OF PYTHON CODE

```
13 def MainFn(SiteBounds, OffLimitAreas, DemandPoints, SupplyPoints, FloorHeights,ParticleNum,\
14           CraneJibLength, CraneBaseHeight,CraneBaseLen,ALPHA, BETA,LocalWeight,\
15           GlobalWeight,MaximumIterations, MaxVelocity, XMIN, XMAX, YMIN, YMAX, Omega):
```

MainFn calls the PSO module, the data input files and returns the optimal location. There are 20 variables which can be used to control various aspects of the optimization process. MainFn function also calls the ParticleSwarm function, which calls the TotalTimeCalc function. This function is based on the equations developed by Zhang et al. (1999) and is the objective function to be optimized.

```
146 def inclusionExclusionChk (PlotArea,Area,WorkInfo,SupplyPts,crane_x,\
147                           crane_y,crane_width,crane_height,jib_len):
```

inclusionExlusionChk is a function which checks if any location that is passed to it satisfies all the physical constraints imposed such as the site perimeter, inclusion zones, exclusion zones and the load-radius curves. The function relies upon 2 other functions which check for inclusion/exclusion from a triangle or a rectangle.

An optional constraint is introduced when the crane needs to be anchored. This consists of requirement that the location be equidistant from the anchoring structure (ex. Column) and at a certain range the edge of the structure, based on the maximum anchoring distance as stipulated by the crane's manufacturer.

SupportFn is a module that contains several functions which provide inputs to one of the other functions. This includes:

- Importing Function which loads the .csv files which contain the various information into Python. They rely on the Pandas module in Python.
- DistCalc which calculates the distance between a pair of (x,y) coordinates.
- TripNum which calculates the number of trips required to deliver a load based on the capacity of the crane at a certain distance.

- CraneReachCheck: A function which checks if a proposed location for the tower crane can reach all the demand and supply points based on its capacity and the distances from the crane to all the supply and demand points.
- 3 functions which calculate the time taken for the hoisting, slewing and trolleying travel times.
- A visualization function which produces a figure of the results produced by the MainFn.

A module also contains the functions which are based on the outputs of the OLS regression. There are 3 functions:

- A function which takes a distance, in milimeters and returns the capacity of the crane at that distance.
- A function which takes a weight, in kilograms and calculates the maximum capacity of the crane for that weight.
- A function which takes a weight in kilograms and returns the hoisting speed of the crane in mm/min.

In addition, a set of CSV files were used to input all the necessary information into the model. These files had the following purposes:

- Supply points were included in a file called Supply.csv, which were the locations on the site from where the loads were to be lifted;
- WorkZones.csv is a file which contained the x and y locations of all the demand points along with the weight, in kilograms of each load to be transported.
- OffLimitsAreas contain the coordinate of the spaces on the construction site which are off-limits such as offices, residential blocks and exclusion zones that surround the building.
- Floor Heights is a file that contains the z locations of each floor.

APPENDIX 9: MATHEMATICAL OPTIMIZATION PROBLEM

The optimization problem aims to minimize the total travel time of the crane's hook block. The objective function is based on the equations developed by Zhang et al. (1999) in "Location Optimization for a Group of Tower Cranes". The equations have been discussed in Section 2.3.2, Crane Travel Time Calculation. The decision variable of the objective function represents the *(x,y)* position of the tower crane. In all cases, the crane's z-position is assumed to be at *z=0*.

The formulation of the mathematical optimization problem is as follows:

$$\textbf{\textit{Minimize}} \quad Hook\ Block\ Travel\ Time\ as\ Defined\ by\ Zhang\ et\ al.\ (1999)$$

where:

$$(x, y) = tower\ crane\ coordinates$$
$$P = set\ of\ all\ coordinates\ within\ the\ site\ plot$$
$$E = set\ of\ exclusion\ (off - limit)\ coordinates\ on\ site$$
$$E \subseteq P$$

$$dist\ ((x_1, y_1), (x_2, y_2)) = Eucledian\ distance\ from\ any\ 2\ points$$
$$= \sqrt{(x_1 - x_2)^2 + (y_1 - y_2)^2}$$
$$S = set\ of\ (x, y)\ coordinates\ representing\ the\ location\ of\ all\ supply\ points$$
$$Ex., \quad S_i = (x_{s,i}, y_{s,i}) = position\ of\ i^{th}\ supply\ point.$$
$$D = set\ of\ (x, y)\ coordinates\ representing\ the\ location\ of\ all\ demand\ points$$
$$Ex., \quad D_j = (x_{d,j}, y_{d,j}) = position\ of\ j^{th} demand\ point$$

$$liftingRadius = lifting\ radius\ determined\ by\ radius - load\ curve\ for\ a\ given\ load$$
$$load_k = weight\ of\ k^{th}\ indivisible\ item\ lifted;$$

subject to:

$$(x, y) \in P\ \textbf{\textit{and}}\ (x, y) \notin E \ ;$$
$$dist\ ((x, y), S_i) < Jib\ Length, \quad \forall\ i$$
$$dist\ ((x, y), D_j) < Jib\ Length, \quad \forall\ j$$
$$liftingRadius\ (load) < dist((x, y), S), \quad \forall\ k$$
$$liftingRadius\ (load) < dist((x, y), D), \quad \forall\ k$$
$$x, y \geq 0$$
$$S, D \geq 0$$